

Smart Polymer Microspheres: Preparation, Microstructures, Stimuli-Responsive Properties, and Applications

Tao Guo,[▽] Lan Luo,[▽] Linlin Wang, Fenghua Zhang,* Yanju Liu, and Jinsong Leng*

Cite This: <https://doi.org/10.1021/acsnano.5c00998>

Read Online

ACCESS |

Metrics & More

Article Recommendations

ABSTRACT: Smart polymer microspheres (SPMs) are a class of stimulus-responsive materials that undergo physical, chemical, or property changes in response to external stimuli, such as temperature, pH, light, and magnetic fields. In recent years, their diverse responsiveness and tunable structures have enabled broad applications in biomedicine, environmental protection, information encryption, and other fields. This study provides a detailed review of recent preparation methods of SPMs, focusing on physical methods such as emulsification-solvent evaporation, microfluidics, and electrostatic spraying as well as chemical approaches such as emulsion and precipitation polymerization. Meanwhile, different types of stimulus-responsive behaviors, such as temperature-, pH-, light-, and magnetic-responsiveness, are thoroughly examined. This study also explores the applications of SPMs in drug delivery, tissue engineering, and environmental monitoring, while discussing future technological challenges and development directions in this field.

KEYWORDS: Smart Materials, Microspheres, Preparation, Microstructure, Physical Stimulus, Chemical Stimulus, Biological Stimulus, Stimuli-Responsive Properties, Applications



This study also explores the applications of SPMs in drug delivery, tissue engineering, and environmental monitoring, while discussing future technological challenges and development directions in this field.

1. INTRODUCTION

Polymer materials are now integral to daily life, from spacecraft exploring the universe¹ to submarines navigating ocean depths² and artificial organs in biomedical applications.³ Stimulus-responsive polymers are a type of smart material capable of receiving external signals (e.g., temperature, pH, magnetic field, and light) and converting them into changes in the structure, properties, or behavior of materials, enabling functional adaptability.^{4–8} They can modify wettability and adhesion of different substances by adjusting the mobility of ions and molecules, and even transduce chemical and biological signals into optical, electronic, thermal, or mechanical responses.^{9–11} Their intelligent responsiveness has enabled diverse applications, including disease diagnosis,¹² tissue engineering,¹³ soft robots,¹⁴ environmental management,¹⁵ mechanical engineering,¹⁶ and food engineering.¹⁷

Polymer microspheres are polymer particles with micrometer- or nanometer-scale dimensions and a spherical morphology.^{18,19} Their common structures include solid,²⁰ hollow,²¹ core-shell,²² and multilayer²³ morphologies. These diverse architectures confer unique properties such as tunable

physicochemical properties, internal cavities for molecular loading, and asymmetric surface properties.^{24–26} To address application-specific performance demands, polymer microspheres are engineered with multifunctional attributes. Key strategies involve doping with responsive nanoparticles²⁷ and targeted surface modification,²⁸ synergistically enabling programmable stimuli-responsiveness while maintaining structural integrity.

Smart microspheres integrate smart materials with microtechnology and nanotechnology, enabling them to generate feedback in response to changes in the external environment while retaining the unique properties of nanomaterials.²⁹ Their stimuli-responsive properties are usually achieved in two ways:

Received: January 16, 2025

Revised: April 23, 2025

Accepted: April 23, 2025

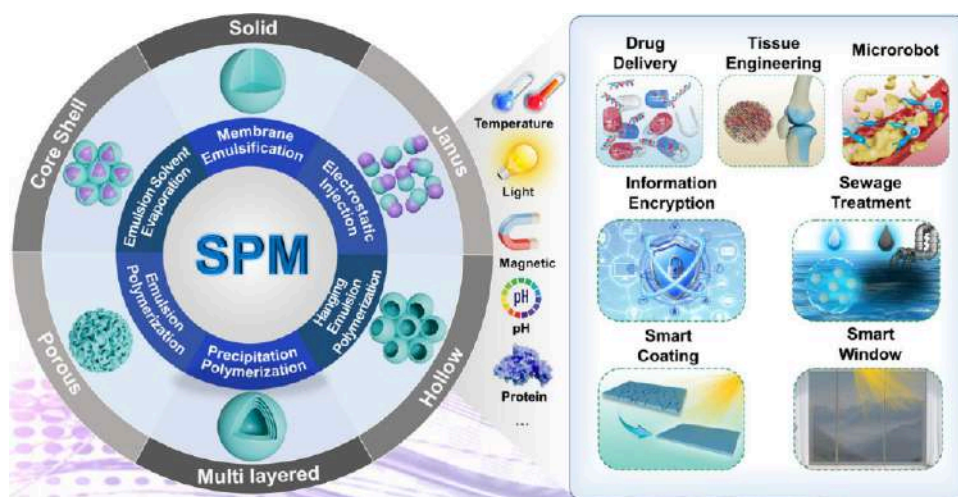


Figure 1. Preparation methods, microstructures, stimulus-response types, and applications of stimulus-responsive polymer microspheres.

by directly using stimuli-responsive materials to prepare microspheres^{30,31} or by embedding or grafting functional components into polymer chains, inducing transformations in physical and chemical properties under external stimuli to meet the application requirements of specific environments.^{32,33} By combining the advantages of both smart materials and micromaterials and nanomaterials, stimulus-responsive microspheres hold promise for applications in life sciences, environmental protection, and information technology.^{34–36} Based on the above background, this study reviews recent advancements in stimulus-responsive microspheres, examining their preparation, structure, excitation modes, and applications while offering insights into future development (Figure 1).

2. SYNTHESIS OF MICROSPHERES AND THEIR STRUCTURE

Polymer microspheres can be synthesized by using physical or chemical methods. Physical methods, such as emulsification-solvent evaporation, spray drying, microfluidics, electro-spraying, and membrane emulsification, primarily utilize natural or synthetic polymers. While straightforward and convenient, these methods often produce microspheres with uneven size distributions, limiting their applicability. By contrast, chemical methods involve the polymerization of small-molecule monomers through processes, such as emulsion polymerization, soapless emulsion polymerization, microemulsion polymerization, fine emulsion polymerization, and seed swelling polymerization. Chemical approaches offer superior control over microsphere structure and properties, making them advantageous for applications requiring high precision.

2.1. Physical Synthesis of Microspheres. 2.1.1. Emulsification-Solvent Evaporation Method. The emulsification-solvent evaporation method, depicted in Figure 2a, is widely used for microsphere synthesis and is classified into single-emulsion and complex-emulsion systems based on the dispersed and continuous phases.³⁷ Microsphere properties are influenced by several factors, including the oil phase, polymer carrier, emulsifier, aqueous phase composition, droplet dispersion method, and solvent evaporation rate.

The single-emulsion method is categorized based on the emulsion system employed, with oil-in-water (O/W) and oil-in-oil (O/O) being the most common. In the O/W system, a polymer dissolves in a volatile, water-immiscible organic

solvent and is gradually introduced into an aqueous emulsifier solution under stirring. The emulsifier stabilizes the emulsion, preventing droplet coalescence. As the mixing continues, the organic solvent diffuses into water and evaporates, precipitating the polymer to form microspheres. Deliormanli et al.³⁸ prepared poly epsilon-caprolactone (PCL) microspheres with different structures using the O/W emulsion-solvent evaporation method and investigated the effect of various oils on the surface state and size of PCL microspheres. Wu et al.³⁹ also prepared PCL microspheres via this method, demonstrating that the microsphere morphology is influenced by parameters such as the type and concentration of alkane porogenic agents, polymer concentration, and reaction temperature. Additionally, incorporating lipophilic compounds or drugs into the oil phase during O/W emulsion-solvent evaporation enables the efficient encapsulation of these agents. Li et al.⁴⁰ prepared ropivacaine-loaded microspheres via O/W emulsion-solvent evaporation, incorporating oil-soluble ropivacaine to achieve a narrow particle size distribution and high drug-loading efficiency. Xu et al.⁴¹ fabricated polylactide (PLA) porous microspheres via O/W emulsion-solvent evaporation, achieving bupivacaine encapsulation efficiency exceeding 70%. However, hydrophilic compounds tend to diffuse into the aqueous phase during solvent evaporation, reducing active ingredient retention and limiting embedding efficiency.⁴² Consequently, the preparation of microspheres coated with water-soluble compounds is effectively achieved through O/O emulsion-solvent evaporation. Mei et al.⁴³ employed this method to encapsulate a microwater-soluble drug, such as rifampicin, in PCL microspheres.

The compound emulsion method, an advancement of the single-emulsion technique, is categorized into O/W/O and W/O/W systems. It involves forming a primary O/W or W/O emulsion, which is subsequently dispersed into water or volatile solvents to create a compound emulsion. Polymer microspheres are obtained by removing solvents from the dispersed droplets via ultrasonication or heating, resulting in solidified particles. Ji et al.⁴⁴ demonstrated this method to synthesize porous polyimide hollow microspheres using the O/W/O system, demonstrating that emulsifier content influences microsphere size and morphology. Commonly applied in drug delivery, this method enables the encapsulation of peptides, proteins, and enzymes into the microspheres. For instance, Lin

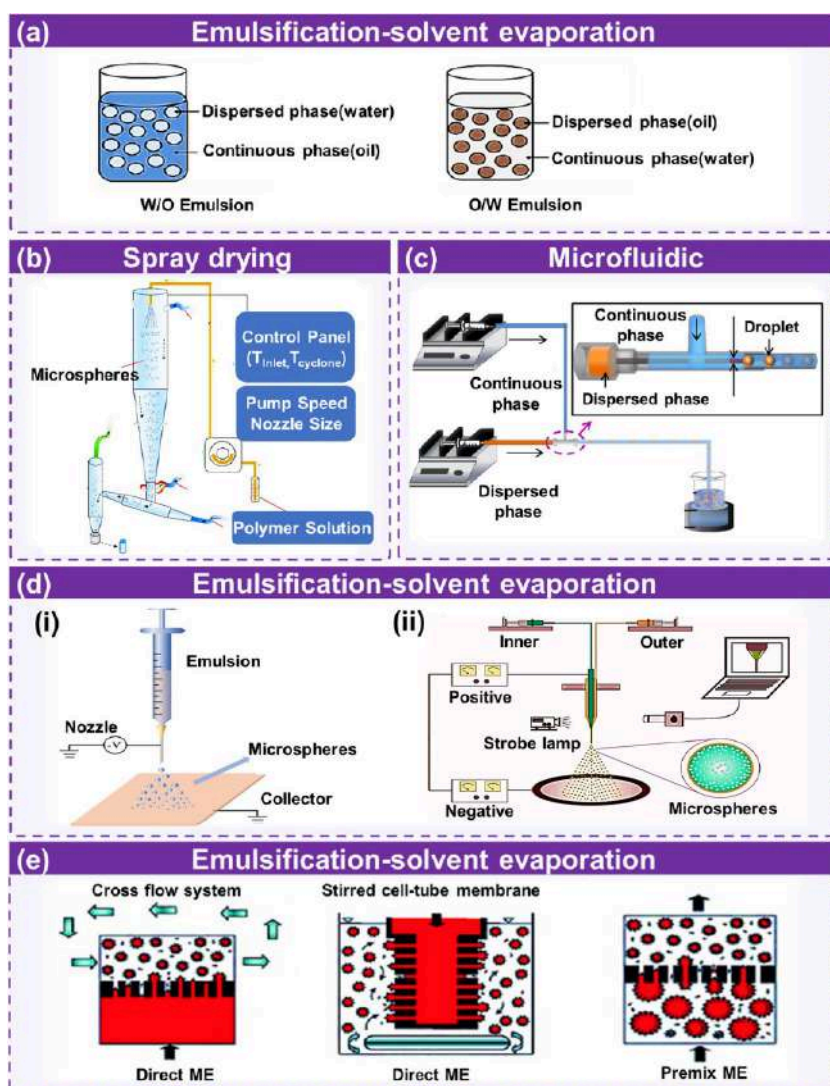


Figure 2. Preparation of polymer microspheres via physical methods. (a) Schematic of the emulsification-solvent evaporation method. Reprinted with permission from ref 37. Available under a CC-BY 4.0. Copyright 2021, Springer Nature. (b) Schematic of the spray-drying method. Reprinted with permission from ref 51. Copyright 2020, Elsevier. (c) schematic of the microfluidic method. Reprinted with permission from ref 58. Copyright 2019, Elsevier. (d) (i) Schematic of the electrostatic spraying method. Reprinted with permission from ref 66. Copyright 2022, Elsevier. (ii) schematic of the coaxial electrohydrodynamic nebulization method. Reprinted with permission from ref 71. Available under a CC-BY 4.0. Copyright 2019, Taylor & Francis. (e) Schematic of the membrane emulsification method. Reprinted with permission from ref 74. Copyright 2012, Springer Nature.

et al.⁴⁵ used W/O/W solvent evaporation to encapsulate TGF- β 3 and growth factor-releasing peptides within polyethylene glycol (PEG)/PLA microspheres, achieving sustained drug release. Park et al.⁴⁶ prepared poly(lactic-co-glycolic acid) (PLGA) microspheres loaded with xenatide using the W/O/W emulsion-solvent evaporation method. Despite its effectiveness in encapsulating active macromolecules, the complex-emulsion method exposes proteins and drugs to organic reagents during fabrication, potentially compromising their biological activity.⁴⁷ Furthermore, this method often leads to hydrophilic drugs diffusing into the external aqueous phase and weakly associating with the microsphere surface, causing an initial burst release that elevates risks and diminishes therapeutic and economic value.⁴⁸ To address these challenges, Marquette et al.⁴⁹ developed the solid-in-oil-in-water (S/O/W) emulsification method, replacing the aqueous drug phase with immunoglobulin powder. In this approach, solid protein particles are dispersed in a polymer solution to form an S/O

emulsion, which is then emulsified in an aqueous surfactant solution to create an O/W system, encapsulating solid particles. Microspheres are obtained through organic solvent evaporation. By maintaining the drug in a solid state throughout the preparation process, this method minimizes protein conformational changes caused by solvent exposure, thereby preserving the biological activity of the encapsulated proteins and reducing the initial burst release of the drug. Chen et al.⁵⁰ addressed the initial burst release of PLGA microspheres prepared via the W/O/W method using the S/O/W technique. Composite microspheres were formed by embedding anhydrous anticellulose lecithin nanoparticles loaded with bovine serum proteins within a PLGA matrix, which markedly reduced the initial burst release of the drug.

2.1.2. Spray-Drying Method. The spray-drying method, among the earliest and most direct techniques for industrial microsphere production, involves preparing a solution or emulsion of raw materials, which is atomized into fine droplets

by using a high-pressure nozzle (Figure 2b). Hot air rapidly evaporates the solvent, which dries the droplets into microspheres with ultrafine particle sizes.⁵¹ Microsphere properties are influenced by factors such as material composition, carrier concentration, feed rate, and inlet/outlet temperatures.⁵² Zhang et al.⁵³ utilized spray-drying to prepare drug-loaded microspheres with chitosan as a carrier, systematically analyzing the effects of chitosan concentration, drug-to-chitosan ratio, inlet air temperature, and injection rate. The optimized process yielded sustained-release microspheres with smooth surfaces and a high drug-loading efficiency.

The spray-drying technique offers several advantages, including operational simplicity, one-step particle formation, precise particle size control, high active ingredient utilization, and scalability for industrial production. By selecting suitable encapsulating materials, it enables effective drug delivery and controlled release.⁵⁴ Wei et al.⁵⁵ utilized *N*-maleoylalanine and succinic acid amide-modified starch to fabricate anticancer drug-loaded microspheres via spray-drying, achieving sustained-release properties. However, a major limitation is the high drying temperatures required, which can compromise the stability of temperature-sensitive compounds.⁵⁶

2.1.3. Microfluidic Method. Microfluidics, an innovative technology combining physics, materials science, and micro-machining, enables precise control of fluid volumes at the microscale.⁵⁷ As depicted in Figure 2c, this method generates droplets within microfluidic channels using volumetric or pressure-driven forces to manage continuous and dispersed phase flows. The continuous phase compresses the dispersed phase, destabilizing the interface and forming spherical droplets, which are solidified into microspheres via solvent evaporation.⁵⁸ Su et al.⁵⁹ employed a microfluidic technique to fabricate smooth, sustained-release bicalutamide-loaded microspheres. The properties of these microspheres are influenced by the material choice, fluid dynamics, and chip design. By fine-tuning these factors, diverse microsphere structures can be achieved, including core-shell,⁶⁰ multilayered,⁶¹ multi-nucleated,⁶² and multicomponent⁶³ configurations.

Microfluidic methods for microsphere fabrication offer key advantages, such as tunable size and morphology, high reproducibility, scalability, reduced risk of air-induced drug degradation, and ease of aseptic manufacturing. However, limitations include low throughput,⁶⁴ difficulty modifying prefabricated chips, additional costs for new chip designs, and susceptibility to channel blockages during production owing to small channel sizes.⁶⁵

2.1.4. Electrostatic Spraying Method. Electrostatic injection or electrohydrodynamic atomization has gained traction for preparing drug-loaded microspheres. As illustrated in Figure 2d(i), the setup comprises an electric field, a syringe pump, and a collection device. A high-intensity electric field and electrohydrodynamic forces drive the process, with the syringe pump ensuring uniform electrolyte flow through a high-potential needle. This generates a Taylor cone at the needle tip, from which the liquid jet disintegrates into droplets under the competing effects of surface tension, electric field stress, gravitational force, and viscous shear. The space-charge effect disperses these droplets, and solvent evaporation reduces their size as they move toward the collection device, where they solidify into microspheres.⁶⁶ Lu et al.⁶⁷ established a sequential process integrating electrostatic jetting with freeze-drying to synthesize biodegradable chitosan microspheres. A primary electrostatic jetting step first generated monodisperse

microspheres with tailored surface morphology through the precise control of voltage and flow rate. This is followed by a programmed freeze-drying protocol that manipulates ice crystal formation via freezing temperature, followed by hierarchical pore engineering during primary and secondary drying stages. This two-step methodology achieves precise structural control of the microspheres, yielding uniform particle diameters and adjustable porosities in the resultant chitosan microspheres. The performance of microspheres produced through this method depends on factors such as voltage intensity, electrode gap, needle size, flow rate, polymer concentration, and solvent type.^{68,69} Li et al.⁷⁰ utilized electrostatic spraying to fabricate polycarbonate microspheres, analyzing how solution concentration, temperature, nozzle aperture, and voltage affected their shape, uniformity, size, and settling velocity. While effective for producing small micro-carriers, this method often results in microspheres with suboptimal monodispersity. Furthermore, drug-loaded microspheres generated via this technique frequently exhibit issues such as abrupt drug release, limiting their suitability for applications demanding precise and controlled drug release profiles.

The coaxial electrohydrodynamic nebulization method, illustrated in Figure 2d(ii), enhances conventional electrospray by separating the drug and polymer solutions, which are ejected through inner and outer coaxial capillary tubes under a high-voltage field. This setup forms a drug core and polymer shell simultaneously.⁷¹ Liang et al.⁷² utilized this technique to produce gelatin methacryloyl-alginate core-shell microspheres encapsulating human dental pulp stem cells and human umbilical vein endothelial cells. This method effectively minimizes premature drug release during production and reduces drug degradation by limiting the drug-solvent interactions.

2.1.5. Membrane Emulsification. Membrane emulsification, renowned for its cost-efficiency, scalability, and reproducibility, has gained immense attention. It is broadly classified into direct and premixed methods, differentiated by their emulsion formation mechanisms. Advances in this technique enabled the production of granular emulsions with controlled particle sizes.

As illustrated in Figure 2e, direct membrane emulsification for microsphere fabrication⁷³ involves passing the dispersed phase through a microporous membrane, where droplets form at the pore openings owing to surface tension. These droplets grow to a critical size and detach, producing uniform particles. A continuous-phase flow or surfactant stabilizes the droplets, preventing agglomeration. The emulsion is then cured to form microspheres, typically 3–4 times the membrane pore size.

Premixed membrane emulsification⁷⁴ applies external pressure to force a pre-emulsion, initially with droplet sizes larger than the membrane pore size, through a microporous membrane. This process generates small, uniform droplets with repeated cycles achieving highly homogeneous particle sizes. Solidification of these droplets forms microspheres, which are notably smaller than the membrane pore size. The porous membrane surface must be wetted by the dispersed phase of the premix to prevent phase inversion during membrane emulsification.⁷⁵ Mi et al.⁷⁶ utilized both direct and premixed membrane emulsification to produce agarose and calcium alginate microspheres with uniform size distributions. The properties of microspheres prepared via membrane emulsification depend on factors such as pore size, porosity, temperature, emulsifier type, and transmembrane pres-

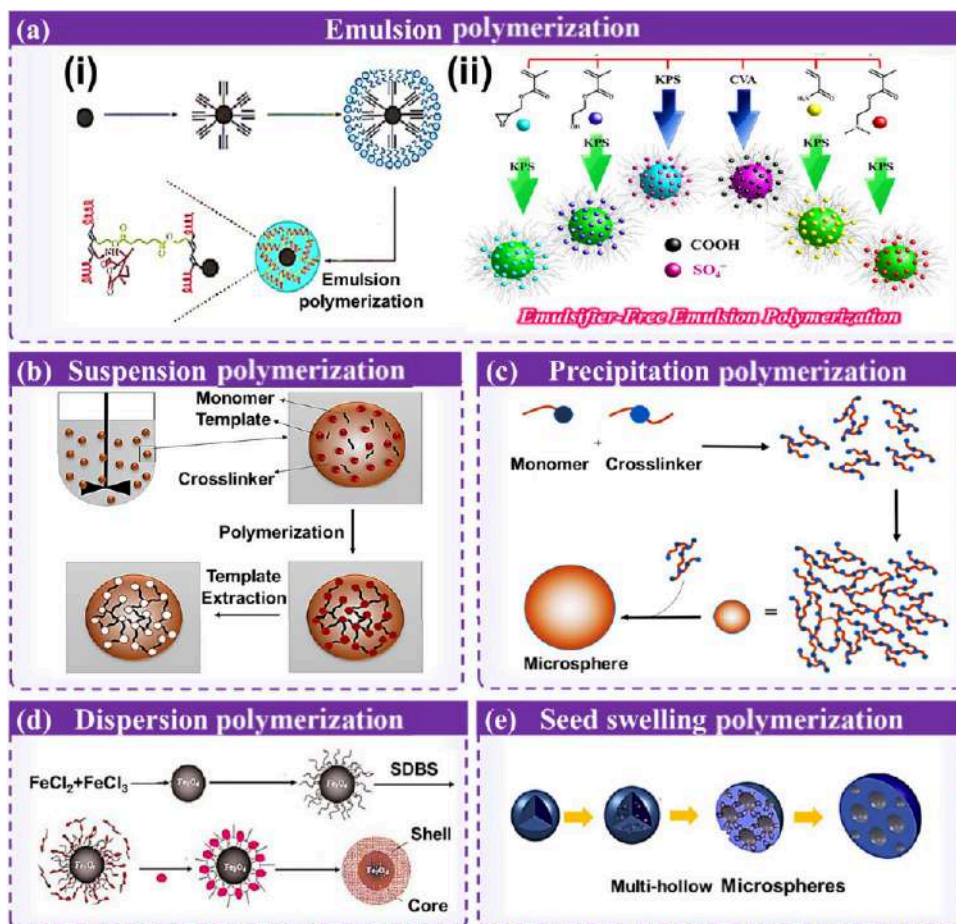


Figure 3. Preparation of polymer microspheres via chemical methods. (a) (i) Schematic illustration of core–shell $\text{Fe}_3\text{O}_4/\text{PA}$ composite microspheres prepared via emulsion polymerization. Reprinted with permission from ref 82. Copyright 2016, Royal Society of Chemistry. (ii) Schematic of functionalized latex nanoparticles synthesized via soapless emulsion polymerization. Reprinted with permission from ref 85. Copyright 2020, Elsevier. (b) Schematic of suspension polymerization. Reprinted with permission from ref 90. Available under a CC-BY 4.0. Copyright 2020, Molecular Diversity Preservation. (c) Schematic of precipitation polymerization. Reprinted with permission from ref 90. Available under a CC-BY 4.0. Copyright 2020, Molecular Diversity Preservation. (d) Schematic of $\text{P}(\text{MAH-MAA})/\text{Fe}_3\text{O}_4$ composite microspheres prepared through dispersion polymerization. Reprinted with permission from ref 98. Copyright 2002, John Wiley and Sons. (e) Schematic of microspheres prepared via seed swelling polymerization. Reprinted with permission from ref 109. Copyright 2016, Elsevier.

sure.^{77–79} Nauman et al.⁸⁰ combined membrane emulsification with emulsion polymerization to synthesize methyl methacrylate microspheres, achieving precise particle size control by tailoring the membrane pore size.

Membrane emulsification is notable for producing microspheres with uniform, predictable particle sizes, ensuring batch-to-batch consistency. Its mild conditions are ideal for sensitive protein and peptide drugs, while the high emulsion stability reduces the risks of agglomeration and droplet rupture. Additionally, the simplicity of the method supports industrial scalability. However, limitations include potential effects on in vivo drug release profiles and risks of sudden drug release.

2.2. Chemical Synthesis of Microspheres. The chemical preparation of polymer microspheres involves the polymerization of small-molecule monomers and is primarily categorized as emulsion, seed swelling, precipitation, dispersion, and suspension polymerization.

2.2.1. Emulsion Polymerization. Introduced by Harkins in the 1950s, emulsion polymerization is a widely used technique for producing monodisperse polymer microspheres. By combining a monomer, water, a water-soluble emulsifier, and an initiator, this method reliably yields microspheres with

excellent monodispersity and particle sizes ranging from 50 to 800 nm, making it ideal for small-scale applications.⁸¹ As shown in Figure 3a(i), Chen et al.⁸² modified Fe_3O_4 with *O*-(propargyl)-*N*-(triethoxysilyl)carbamic acid methyl ester, introducing polymerizable $\text{C}\equiv\text{C}$ triple bonds, and encapsulated it with a helical polyacetylene (PA) shell via emulsion polymerization to form core–shell $\text{Fe}_3\text{O}_4/\text{PA}$ composite microspheres. While emulsion polymerization is efficient and produces high-molecular-weight products, excessive use of emulsifiers can compromise microsphere performance. To mitigate this, green approaches such as soapless and microemulsion polymerization have been developed for monodisperse microsphere synthesis.

Emulsifiers in emulsion polymerization are difficult to remove and restrict their medical applications. Soapless emulsion polymerization overcomes this by producing monodisperse microspheres with clean surfaces, allowing functional group incorporation without surfactants.⁸³ This method introduces hydrophilic groups onto microsphere surfaces by using initiators and polar monomers, enabling them to act as surfactants. This eliminates emulsifier-related risks while producing smooth-surfaced microspheres, which

can be easily modified with cationic or anionic groups for tailored functionalities.⁸⁴ As shown in Figure 3a(ii), Abdollahi et al.⁸⁵ used soapless emulsion polymerization with ethylene and poly(methyl methacrylate) to synthesize functional polymer nanoparticles. Similarly, Yang et al.⁸⁶ produced monodisperse polystyrene (PS) microspheres with carboxyl and sulfonic acid groups, exploring their nucleation and growth mechanisms.

Fine emulsion polymerization employs emulsifiers and coemulsifiers under high shear stress to create stable, submicron droplets. Unlike conventional methods, it requires coemulsifiers and utilizes microemulsification to reduce the droplet size. Polymerization within these droplets produces microspheres that closely match the initial droplet size.⁸⁷ Cordeiro et al.⁸⁸ utilized fine emulsion polymerization to produce monodisperse poly(methyl methacrylate) microspheres containing magnetic nanoparticles and Cuban oil. Similarly, Mangia et al.⁸⁹ synthesized poly(methyl methacrylate)/acrylic acid copolymer microspheres for enzyme encapsulation. Fine emulsion polymerization offers enhanced stability over conventional methods, facilitating the creation of smaller, monodisperse microspheres with intricate morphologies.

2.2.2. Suspension Polymerization. Emulsion polymerization suspends immiscible liquids in a solution, where polymerization or chemical reactions cause droplets to coalesce into large particles. As shown in Figure 3b,⁹⁰ suspension polymerization is commonly used to synthesize liquid or colloidal particles. Abd El-Mageed et al.⁹¹ prepared uniform, magnetically stable PS microspheres using α -allyl alkylphenol polyoxyethylene ether and Hitenol BC as stabilizers. Although straightforward and eco-friendly, suspension polymerization faces challenges in controlling droplet size. Achieving monodisperse microspheres requires precise regulation of the stirring speed and dispersant usage, leading to the development of advanced systems such as microsuspension polymerization.

Microsuspension polymerization employs ionic surfactants and emulsifiers to reduce surface tension between monomer droplets and the aqueous phase, dispersing the monomer into micrometer- or submicrometer-sized droplets under shear forces. Glasing et al.⁹² used cellulose nanocrystals as stabilizers to polymerize styrene, producing uniform, monodisperse microspheres. Compared to traditional suspension polymerization, microsuspension polymerization simplifies the production of monodisperse microspheres but is constrained by extensive surfactant use, limiting its application in high-purity preparations.

2.2.3. Precipitation Polymerization. In the 1990s, Stöver et al. introduced precipitation polymerization, successfully producing monodisperse PS microspheres (Figure 3c).^{90,93} During polymerization, oligomers form primary nuclei, which grow by capturing monomers and soluble oligomers until critical chain lengths trigger spontaneous precipitation, forming microspheres. Stöver et al.⁹⁴ utilized acetonitrile to synthesize poly(divinylbenzene) microspheres with tailored structures via precipitation polymerization. While simple and stabilizer-free, this method suffers from low efficiency and reliance on toxic solvents, such as toluene and acetonitrile, limiting its environmental viability. To address these issues, advanced techniques, such as distillation and reflux precipitation polymerization, have been developed.

Distillation precipitation polymerization refines traditional precipitation polymerization using solvent distillation to

control the reaction, requiring precise solvent selection. At the distillation temperature, monomers form nuclei that precipitate and grow by capturing monomers and oligomers, yielding monodisperse microspheres. Zhang et al.⁹⁵ employed this method to produce fluorinated hydrophobic PS microspheres with controlled particle sizes. By contrast, reflux precipitation polymerization simplifies the setup by eliminating complex apparatus and utilizing magnetic stirring, reducing particle aggregation, and enhancing reaction control. Wang et al.⁹⁶ utilized this approach to prepare monodisperse poly(ethylene glycol methacrylate phosphate) gel microspheres with a spherical structure and abundant phosphate groups.

2.2.4. Dispersion Polymerization. Dispersion polymerization, a subset of precipitation polymerization, employs dispersants or macromolecular monomers to stabilize insoluble polymers in the reaction medium. Initially, a homogeneous mixture of the monomer, dispersant, initiator, and solvent is formed. As polymerization progresses, growing polymer chains precipitate upon reaching a critical length and aggregate into particles. These particles are stabilized using dispersants and mechanical stirring, forming a dynamically stable microsphere dispersion.

Zhang et al.⁹⁷ utilized water-soluble potassium persulfate as an initiator to synthesize electromagnetic hydroxyl PS/Fe₃O₄ composite microspheres via dispersion polymerization. Similarly, Fan et al.⁹⁸ prepared magnetic core-shell microspheres with Fe₃O₄ as the core and poly(maleic anhydride-co-methyl methacrylate) as the shell (Figure 3d). Dispersion polymerization, known for its simplicity, strong adsorption, and modifiable surfaces, has advanced with innovative initiation methods such as microwave⁹⁹ and ultrasound.¹⁰⁰ These techniques, compared to traditional thermal initiation, considerably reduce reaction time, boost efficiency, and enhance process control.^{101,102}

2.2.5. Seed Swelling Polymerization. Seed swelling polymerization is widely employed to prepare large, monodisperse polymer microspheres.¹⁰³ Small seed microspheres, typically produced via emulsion or dispersion polymerization, serve as templates in seed swelling polymerization. An inert solvent and monomer are introduced, causing the seeds to swell, increasing their size by more than 2-fold while maintaining excellent monodispersity. This approach enables precise control over microsphere size and pore distribution.¹⁰⁴ The process is categorized into one-step and two-step swelling methods based on the swelling procedure.

The two-step swelling method involves monomers, initiators, reaction media, and swelling agents. Seed microspheres are first activated with a specific swelling agent, followed by monomer swelling and heat-induced polymerization. Kao et al.¹⁰⁵ used emulsion polymerization to produce 0.55 μm poly(methyl methacrylate) seed microspheres, which were subsequently activated, swollen, and polymerized to form monodisperse cross-linked microspheres (1–4 μm in diameter). While effective for size expansion, this method relies on swelling agents, which may compromise microsphere performance through two principal pathways: residual swelling agents trapped within the polymer matrix can reduce cross-linking uniformity, weakening the mechanical strength of the microsphere,¹⁰⁶ and incomplete removal of swelling agents during post-treatment can alter porosity and disrupt pore connectivity.¹⁰⁷ Additionally, some polar swelling agents may induce long-term chemical instability under physiological conditions via progressive leaching.¹⁰⁸ The complex post-

treatment workflow, particularly multicycle centrifugation and solvent extraction, further elevates the risks of polydispersity and surface pitting defects when scaling production.

The one-step swelling method simplifies the process by omitting swelling agents and directly activating and swelling seed microspheres with monomers. Tian et al.¹⁰⁹ used polystyrene-4-sodium styrenesulfonate microspheres as seeds, styrene as the swelling monomer, and divinylbenzene as a cross-linker to create polymer microspheres with varied structures (Figure 3e). While this method effectively produces large, monodisperse, and surface-functionalized microspheres, it involves a complex reaction process, lengthy preparation, and high costs.

2.3. Structure of Microspheres. The diversity of the preparation methods and processing techniques leads to a wide variety of polymer microsphere structures. Based on their structural differences, polymer microspheres can be classified into solid microspheres,¹¹⁰ hollow microspheres,¹¹¹ porous microspheres,¹¹² core-shell microspheres,¹¹³ Janus microspheres,¹¹⁴ and multilayer microspheres.¹¹⁵ The structure of microspheres directly influences their stimuli-responsive behavior by modulating diffusion pathways, interfacial interactions, and energy transfer efficiency under external stimuli. For example, hollow and porous structures enhance mass transfer for rapid drug release, while core-shell designs enable sequential or localized responses.^{116–118}

Solid polymer microspheres are composed entirely of uniform polymer material without prominent internal cavities or pores. These microspheres can be prepared using methods such as the emulsion-solvent evaporation method,¹¹⁹ emulsion polymerization,¹²⁰ and precipitation polymerization.¹²¹ As shown in Figure 4a, Ma et al.¹²² successfully synthesized solid polyaniline (PANI) microspheres using a polyvinylpyrrolidone template method. By varying the HCl solution concentration and surfactant type, they controlled the structure of the PANI microspheres. The dense morphology of solid microspheres limits swelling capacity but improves mechanical stability under thermal or mechanical stimuli, making them ideal for sustained-release systems where slow diffusion governs responsiveness.¹²³

Hollow polymer microspheres consist of an external polymer shell and one or more internal cavities. These cavities are connected to the external environment through pores or channels in the shell, which can be adjusted in size and number as needed. Hollow microspheres are typically prepared using methods such as coaxial electrohydrodynamic atomization¹²⁴ or template emulsion polymerization.¹²⁵ As shown in Figure 4b, Contaldi et al.¹²⁶ successfully fabricated hollow PS microspheres using gas foaming technology. Compared with solid microspheres, hollow structures offer lower density and larger internal volume. The hollow cavity acts as a reservoir for cargo (e.g., drugs and nanoparticles),¹²⁷ while the permeability of the shell governs stimulus-triggered drug release. For pH-responsive systems, shell swelling in acidic environments increases pore size, enabling rapid payload release.¹²⁸

Porous microspheres feature numerous interconnected pores both on their surface and within, forming a three-dimensional porous network. The size, shape, and distribution of these pores can be tailored by adjusting the preparation methods and conditions. Porous microspheres are typically produced using techniques such as the emulsion-solvent evaporation method¹²⁹ or freeze-drying.¹³⁰ As shown in Figure 4c, Ding et al.¹³¹ successfully prepared porous poly(D,L-lactide)

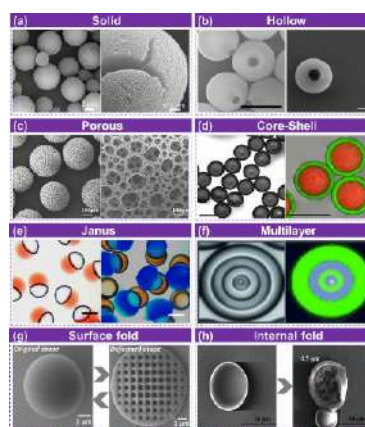


Figure 4. Various structures of polymer microspheres. (a) SEM image of solid PANI microspheres. Reprinted with permission from ref 122. Copyright 2016, Elsevier. (b) SEM image of hollow PS microspheres. Reprinted with permission from ref 126. Copyright 2016, John Wiley and Sons. (c) SEM image of porous PDLA microspheres. Reprinted with permission from ref 131. Available under a CC-BY-NC-ND 4.0. Copyright 2020, Elsevier. (d) X-ray microscopy image of core-shell microspheres. Reprinted with permission from ref 138. Copyright 2013, American Chemical Society. (e) X-ray microscopy image of Janus microspheres. Reprinted with permission from ref 145. Copyright 2018, American Chemical Society. (f) Optical microscopy image of multilayer microspheres. Reprinted with permission from ref 151. Copyright 2014, John Wiley and Sons. (g) SEM image of surface fold microspheres. Reprinted with permission from ref 153. Copyright 2021, American Chemical Society. (h) SEM image of internal fold microspheres. Reprinted with permission from ref 154. Copyright 2023, Taylor & Francis.

(PDLA) microspheres via water-in-oil emulsion-solvent evaporation. Owing to their large specific surface area and high porosity, porous microspheres offer considerably more adsorption and reaction sites compared to other microsphere structures,¹³² accelerating stimuli-triggered phase transitions (e.g., poly(*N*-isopropylacrylamide) (PNIPAM) collapse at lower critical solution temperature (LCST)¹³³) and improving adsorption capacity for environmental applications.¹³⁴

Core-shell polymer microspheres consist of a central core and an outer shell with a distinct interface between the two. The core and shell differ profoundly in their chemical compositions and properties. Core-shell microspheres can be prepared using techniques such as membrane emulsification,¹³⁵ microfluidics,¹³⁶ or soapless emulsion polymerization.¹³⁷ As shown in Figure 4d, Windbergs et al.¹³⁸ demonstrated that coaxial coflow focusing microfluidics enables precise control over core-shell dimensions, achieving monodisperse microspheres with tunable shell thickness. The core-shell structure enables multifunctionality; the core encapsulates substances such as drugs, dyes, or catalysts, providing protection and controlled delivery of these materials,^{139,140} while the shell can respond to external stimuli, regulating the release of substances or enabling specific functions.¹⁴¹

Janus microspheres feature two or more distinct regions with differing chemical compositions or properties, displaying a pronounced asymmetric distribution on the surface or within the microsphere, resembling the dual-faced Roman god Janus.¹⁴² These microspheres can be prepared using techniques such as microfluidics¹⁴³ or electrohydrodynamic

jetting.¹⁴⁴ As shown in Figure 4e, Wang et al.¹⁴⁵ successfully fabricated poly(acrylic acid)-poly(ethoxylated trimethylolpropane triacrylate) (PAA-PETPTA) Janus microspheres using the microfluidic method. The asymmetric structure enables directional responses; for example, one hemisphere may swell under pH changes while the other remains inert, driving self-propelled motion¹⁴⁶ or targeted adhesion.¹⁴⁷

Multilayer microspheres consist of multiple layers of identical or different polymer materials with distinct interfaces between each layer. These different shells can vary in their chemical compositions, physical properties, or stimuli responsiveness. Multilayer microspheres can be prepared using techniques such as solvent evaporation,¹⁴⁸ microfluidics,¹⁴⁹ or self-assembly.¹⁵⁰ As shown in Figure 4f, Haase et al.¹⁵¹ successfully fabricated multilayered microspheres using the microfluidic method. These microspheres respond to multiple stimuli and integrate various functions (e.g., an outer pH-sensitive layer may degrade first in acidic environments, exposing an inner temperature-sensitive layer for secondary activation),¹¹⁶ while the multilayer structure enhances stability and durability, extending the lifespan of microspheres.¹⁵²

With the continuous advancement of smart materials, the controlled transformation of microsphere structures has become a key frontier in research. Central to this is utilizing the intrinsic properties of smart materials to drive tunable variation in the microsphere microstructure, enabling precise structural modulation. As shown in Figure 4g, Li et al.¹⁵³ employed nanoimprint lithography to induce noticeable compression deformation in shape-memory PS microspheres. The shape-memory effect of the microspheres enables reversible switching between a temporary disk-like shape and the original spherical structure. Furthermore, during the recovery of the microspheres from their temporary shape to the original configuration, a thin film of gold nanoparticles was introduced to the surface of the microspheres, combining the shape-memory effect with thermal expansion mismatch, producing microspheres with a surface fold structure.

The surface wrinkle structure of microspheres can be precisely controlled, and their internal cavity can be fine-tuned to exhibit a wrinkled structure. As shown in Figure 4h, Zhang et al.¹⁵⁴ employed an interfacial polymerization method, carefully controlling the oil-phase composition and polymerization conditions, to successfully fabricate polyurethane microspheres with wrinkled structures in their internal cavities. Modulating the wrinkling structure of the internal cavity enables precise control over the drug-loading capacity of microspheres, allowing for fine-tuned regulation of drug encapsulation content.

In conclusion, polymer microspheres can be fabricated into diverse structures through material selection and synthesis methods (Table 1), thereby offering robust support for innovation and advancement across multiple domains.

3. STIMULI-RESPONSIVE PROPERTIES

Smart polymer microspheres (SPMs), also known as smart or environmentally responsive microspheres, encompass a broad range of materials, leading to various classification methods. The most common approach classifies them based on the type of stimuli they respond to, generally divided into physically, chemically, and biologically responsive microspheres. Physical stimuli include factors such as temperature, light, and magnetic fields; chemical stimuli involve pH, ionic strength, and

Table 1. Material, Synthesis, and Structure of Polymer Microspheres

synthesis	material	structure	reference
emulsification-solvent evaporation	polylactide/poly(ethylene oxide)	porous	155
	concanavalin-A/diloxanide furoate	core-shell	156
spray drying	chitosan	porous/solid	157
	poly(D,L-lactic/glycolic acid)	porous/solid	158
microfluidic	—	—	159
	sodium alginate	core-shell	160
electrostatic spraying	calcium alginate/poly(lactic acid-co-glycolic acid)	core-shell	161
	alginate/chitosan	core-shell	162
membrane emulsification	poly(methyl methacrylate)	solid	163
	chitosan	porous	164
emulsion polymerization	poly(methyl methacrylate)	—	165
	poly(styrene-co-butyl acrylate)/polypyrrole	porous	166
suspension polymerization	poly(methyl methacrylate)/graphene	core-shell	167
	dextran	porous	168
precipitation polymerization	styrene	solid	169
	poly(styrene-co-acrylonitrile)	core-shell	170
dispersion polymerization	azobenzene	solid	171
	melamine-formaldehyde	solid	172
seed swelling polymerization	poly(2-methylaniline)-coated/polystyrene	core-shell	173
	poly(acrylamide)/poly(acrylic acid)	core-shell	174

solvents; while biological stimuli include enzymes, antigens, antibodies, and proteins.

3.1. Physical Responsiveness. **3.1.1. Temperature Responsiveness.** Temperature-responsive polymer microspheres adapt to changes in environmental temperature by altering their properties. They are broadly classified into two types: those undergoing volume or phase transitions and shape-memory microspheres, which recover a predefined shape under specific temperature conditions.

Polymers used in the first type of temperature-responsive microspheres typically exhibit a critical solution temperature, where polymer-solvent interactions change with temperature. Within a narrow range, polymer chains transition between soluble and insoluble states, altering intramolecular and intermolecular electrostatic and hydrophilic/hydrophobic interactions. This triggers polymer chain expansion or contraction, causing a volume phase transition. Depending on their thermal transition behavior, these microspheres are categorized into two types: LCST-based systems, which exhibit a lower critical solution temperature, and UCST-based systems, characterized by an upper critical solution temperature.¹⁷⁵

Polymers with LCST remain water-soluble below their LCST values owing to hydrogen bonding. When the temperature exceeds the LCST, these bonds break, and hydrophobic interactions dominate, causing the polymer chains to collapse or aggregate in a phase transition.¹⁷⁶ Common LCST-responsive polymers include PNIPAM, poly(*N*-isopropylmethacrylamide),¹⁷⁷ and poly(*N*-vinylcaprolac-

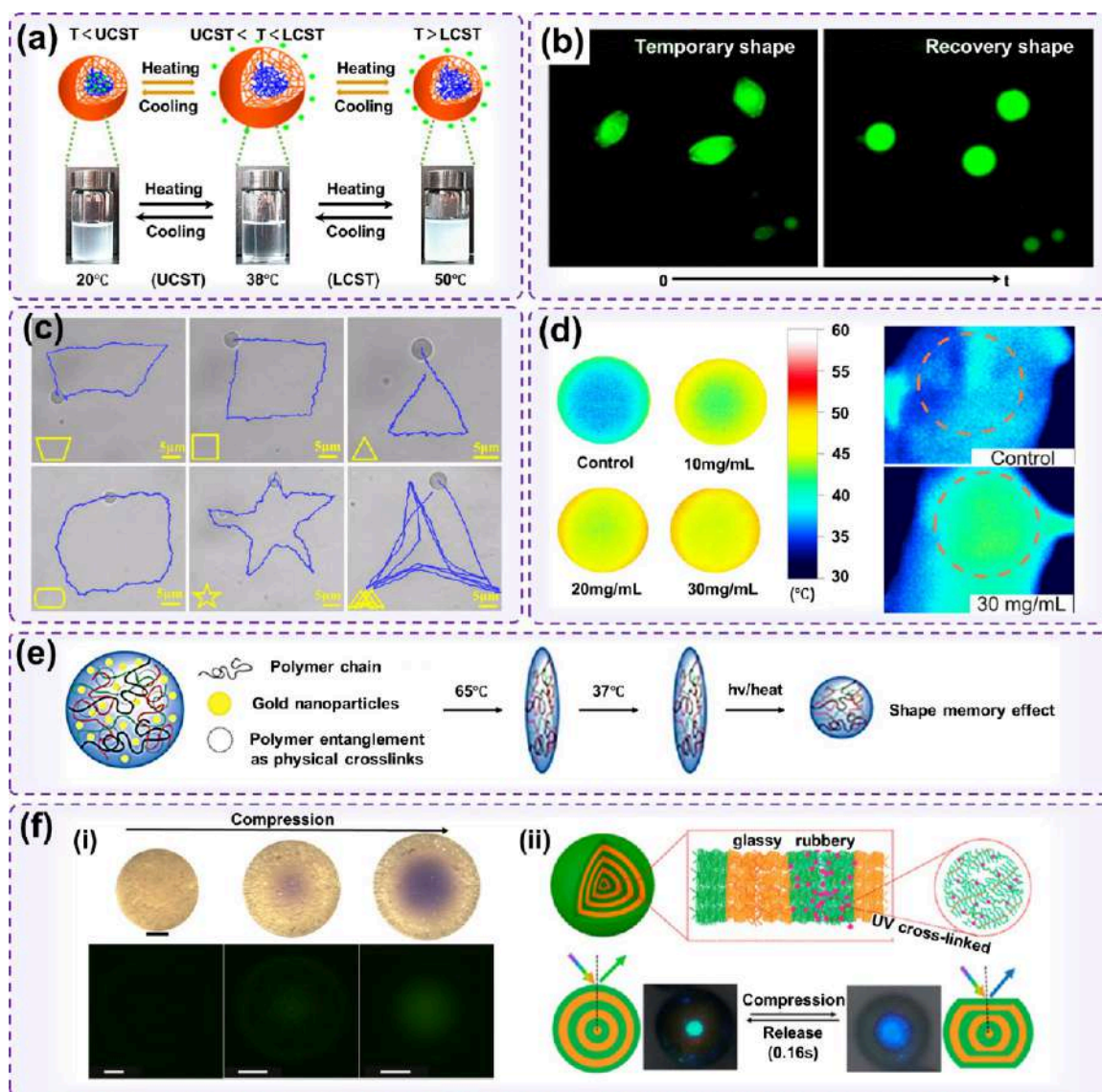


Figure 5. Physically stimuli-responsive polymer microspheres. (a) Microspheres exhibiting different behaviors at varying temperatures. Reprinted with permission from ref 184. Copyright 2014, American Chemical Society. (b) SEM images of shape-memory microspheres at different stretching ratios and after shape recovery. Reprinted with permission from ref 190. Copyright 2020, American Chemical Society. (c) Smart microspheres capable of directional movement under external magnetic fields. (The lines depicted in the figure represent the trajectories of these microspheres when subjected to magnetic fields.) Reprinted with permission from ref 194. Copyright 2024, Elsevier. (d) Smart microspheres generating heat in response to alternating magnetic fields (illustrated using magnetothermal infrared imaging of microspheres *in vitro* and *in vivo*). Reprinted with permission from ref 196. Copyright 2022, Elsevier. (e) Schematic of light-responsive shape-memory microspheres. Reprinted with permission from ref 208. Copyright 2018, American Chemical Society. (f) (i) Mechanochromic smart microspheres with embedded mechanophores. Reprinted with permission from ref 216. Copyright 2009, Springer Nature. (ii) Smart microspheres triggered by mechanical compression for dynamic color changes. Reprinted with permission from ref 217. Copyright 2021, American Chemical Society.

tam).¹⁷⁸ PNIPAM, the most extensively studied temperature-responsive polymer, exhibits an LCST of ~ 32 °C for high-molecular-weight forms.¹⁷⁹ Below the LCST, hydrogen bonding between the amide groups and water molecules stabilizes a hydrated structure. Above the LCST, these bonds break, and hydrophobic interactions dominate, causing bound water to diffuse outward and the polymer to transition from a hydrophilic, soluble state to a hydrophobic, insoluble one.¹⁸⁰ PNIPAM is widely utilized to fabricate temperature-responsive polymer microspheres, enabling thermal control over their size, morphology, and permeability. For example, Cao et al.¹⁸¹ developed PNIPAM/SiO₂ microspheres for phosphate anion

adsorption. Below the LCST, the PNIPAM shell expands, enhancing phosphate adsorption, while above the LCST, the shell collapses, increasing hydrophobicity and reducing adsorption efficiency.

Unlike LCST, UCST marks the threshold below which a polymer phase emerges, while the solution remains homogeneous above this temperature. Polymers with UCST typically exhibit electrostatic or hydrogen bonding interactions, forming insoluble complexes in solution. Heating disrupts these interactions, rendering the polymer soluble.¹⁸² Du et al.¹⁸³ synthesized temperature-responsive microspheres (*c*-PMAD) via dispersion polymerization and investigated their properties.

At elevated temperatures, the cross-linked polymer chains stretched, causing microsphere swelling, whereas low temperatures led to particle size reduction.

Polymer microspheres with both UCST and LCST properties can be engineered through an advanced material design. Yin et al.¹⁸⁴ employed seeded emulsion polymerization to synthesize dual-responsive microspheres, as illustrated in Figure 5a. As the temperature increased from 20 to 38 °C, the microspheres expanded from 150 to 230 nm, resulting in a clear solution. However, further heating to 55 °C caused the microspheres to contract to 188 nm, rendering the solution cloudy again.

The second type of temperature-responsive microsphere incorporates shape-memory polymers (SMPs), which enable shape-memory functionality. SMPs are stimuli-responsive materials that can temporarily deform and recover their original shape when exposed to external stimuli.^{185–187} A critical parameter for SMPs is the glass transition temperature (T_g).¹⁸⁸ For thermally driven SMPs, heating above T_g softens the material, allowing SMPs to deform into a temporary shape under load. Cooling below T_g fixes this shape, and reheating above T_g triggers a spontaneous return to the original configuration.¹⁸⁹ Zhang et al.¹⁹⁰ synthesized core–shell shape-memory polyurethane microspheres via emulsion polymerization and subsequently fabricated them into polymer films. The shape-memory characteristics of these microspheres were assessed through tensile deformation tests on the film, followed by a thermal recovery analysis. As illustrated in Figure 5b, fluorescence microscopy reveals that the microspheres transition from a spherical to a fusiform morphology under tensile strain. Upon reheating above their shape-memory transition temperature, the microspheres nearly completely recovered their original shape, with a recovery rate approaching 100%.

3.1.2. Magnetic Field Responsiveness. Magnetic-responsive polymer microspheres are a novel type of functional microsphere composed of polymers and magnetic functional particles. These microspheres retain the modifiability of polymer microspheres while also exhibiting magnetic responsiveness, owing to the incorporation of magnetic particles. Common magnetic particles used in these microspheres include iron, cobalt, nickel, and their oxides or alloys. Based on their responsive behavior, magnetic-responsive polymer microspheres can be categorized into two types: the first type is directionally controlled in a constant magnetic field,¹⁹¹ while the second type converts magnetic fields into heat when exposed to an alternating magnetic field.¹⁹²

The first type of magnetic-responsive polymer microspheres can be guided to specific locations under the influence of a magnetic field.¹⁹³ Guo et al.¹⁹⁴ encapsulated Fe_3O_4 nanoparticles into PLA microspheres using an emulsion-solvent evaporation method. As shown in Figure 5c, these microspheres can execute complex directional motions under the influence of an external magnetic field.

The second type of magnetic-responsive microsphere not only achieves targeted transport but also generates heat under an alternating magnetic field. When magnetic nanoparticles are exposed to such a field, heat is produced owing to magnetic hysteresis loss, raising the temperature of microspheres.¹⁹⁵ Zhou et al.¹⁹⁶ synthesized $\gamma\text{-Fe}_2\text{O}_3$ @poly(sucrose allyl ether) microspheres that generate heat under the influence of an alternating magnetic field. As shown in Figure 5d, both *in vitro* and *in vivo*, the microspheres generate heat in an alternating

magnetic field, with the maximum temperature achievable increasing with the microsphere concentration in the solution. The magnetothermal efficiency of magnetic-responsive microspheres can be quantified by the specific absorption rate (SAR):¹⁹⁷

$$\text{SAR} = \frac{C}{m} \cdot \frac{dT}{dt} \quad (1)$$

where C is the heat capacity of water, m is the mass of magnetic nanoparticles, and dT/dt is the initial temperature rise rate.

3.1.3. Light Responsiveness. Light responsiveness is another common form of physical stimuli, offering advantages such as rapid response and precisely controllable response regions, making manipulation and control easy.¹⁹⁸ Similar to temperature-responsive polymers, light-responsive polymers can be broadly divided into two categories. The first type consists of polymers with photosensitive groups, enabling a direct response to light exposure. The second type involves incorporating light-sensitive functional particles into SMP, creating composite materials that exhibit light responsiveness—an ability the base polymer would not inherently possess.

Typically, the first type of light-responsive polymer microsphere contains specific photosensitive groups. When exposed to the light of a certain wavelength, the polymer molecules undergo controlled conformational changes, bond cleavage, or decomposition to generate ions, altering polymer properties.¹⁹⁹ Current research on light-responsive polymers primarily focuses on polymers containing azobenzene, triphenylmethane hydroxide, spiropyran, and 2-nitrobenzyl ester groups.^{200,201} A notable characteristic of azo compounds is their photoinduced *cis–trans* isomerization, where functional groups switch between *trans* and *cis* configurations under specific wavelengths of light, ultimately altering the spatial conformation of the polymer. Under ultraviolet light exposure, triphenylmethane hydroxide can decompose into cations and anions, changing the hydrophilicity of the polymer.²⁰² Ultraviolet light of specific wavelengths can also cause the cleavage of 2-nitrobenzyl ester groups and structural changes in spiropyran molecules, resulting in changes in the molecular chains and luminescent properties of the polymer.²⁰³ Yang et al.²⁰⁴ used surface imprinting technology to fabricate hollow photo-responsive molecularly imprinted polymer shell microspheres containing azobenzene photosensitive groups, which exhibited reversible light-responsive behavior in the adsorption and release of griseofulvin. The photoisomerization kinetics of azobenzene groups follows first-order kinetics:²⁰⁵

$$\frac{d[A]}{dt} = -k_{\text{UV}}[A] + k_{\text{vis}}[B] \quad (2)$$

where k_{UV} and k_{vis} are rate constants for UV-induced *trans–cis* and visible-light-induced *cis–trans* transitions and $[A]$ and $[B]$ denote the concentrations of *trans*-azobenzene and *cis*-azobenzene, respectively.

The second type of light-responsive polymer microsphere incorporates functional particles with photothermal effects into SMP microspheres. When exposed to light of a specific wavelength, these functional particles generate Joule heat, raising the temperature of the matrix material. Once the temperature reaches or exceeds the T_g of the polymer, the microspheres exhibit shape-memory behavior.²⁰⁶ Common photothermal functional particles include gold nanoparticles,

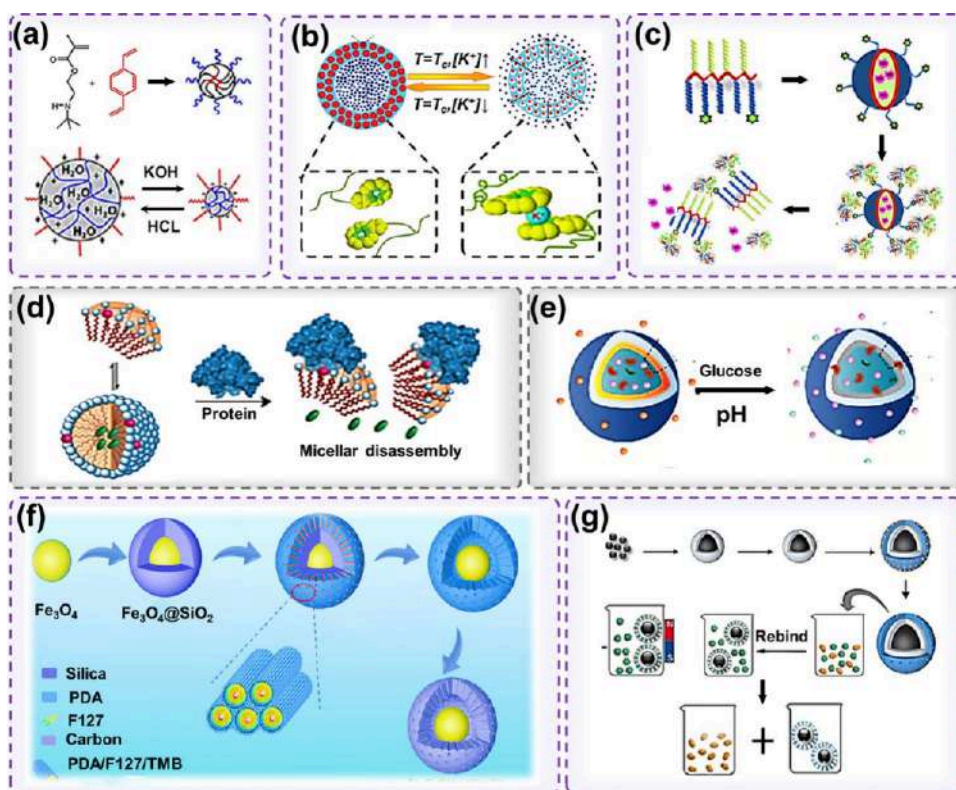


Figure 6. Chemical, biological, and multi-stimuli-responsive polymer microspheres. (a) pH-responsive polymer microspheres with secondary amine groups. Reprinted with permission from ref 229. Copyright 2012, American Chemical Society. (b) Potassium-ion-responsive P(NIPAM-co-AAB15C5) microspheres. Reprinted with permission from ref 232. Copyright 2016, Royal Society of Chemistry. (c) Protein-responsive polypeptide nanospheres. Reprinted with permission from ref 241. Copyright 2015, American Chemical Society. (d) Ligand-protein binding-induced dissociation of dendritic micelle assemblies and guest release. Reprinted with permission from ref 243. Copyright 2010, American Chemical Society. (e) Schematic of glucose-responsive microspheres for controlled insulin release. Reprinted with permission from ref 250. Copyright 2019, Springer Nature. (f) Multiresponsive Fe_3O_4 @Void@mPDA microspheres. Reprinted with permission from ref 252. Copyright 2022, American Chemical Society. (g) Schematic of light and magnetic dual-responsive bovine hemoglobin-molecularly imprinted polymer microspheres and their application. Reprinted with permission from ref 253. Copyright 2019, Elsevier.

multiwalled carbon nanotubes, and carbon quantum dots.²⁰⁷ As shown in Figure 5e, Guo et al.²⁰⁸ developed light-responsive shape-memory microspheres made of PDLLA encapsulating gold nanoparticles. Using thin-film stretching, spherical microspheres were deformed into ellipsoidal shapes. Upon exposure to light of a specific wavelength, the photothermal effect triggered the shape-memory response, causing the microspheres to return to their original spherical shape. Bai et al.²⁰⁹ used the emulsion-solvent evaporation method to incorporate multiwalled carbon nanotubes with photothermal conversion capabilities into cellulose acetate (CA) microspheres. By adjustment of the stretching conditions, the CA microspheres were deformed into various temporary shapes. Upon near-infrared (NIR) light irradiation, the temporarily shaped CA microspheres nearly fully reverted to their original shape, demonstrating an excellent light-responsive shape-memory performance.

3.1.4. Mechanical Responsiveness. Mechanical response polymers are a distinct category of polymeric materials that undergo changes in their macroscopic physical and chemical properties in response to mechanical stimuli, such as compression, shear forces, or ultrasound.²¹⁰ These changes are facilitated by the cleavage and reformation of covalent bonds, as well as alterations in molecular chain conformations.²¹¹ These materials are broadly categorized into two

types: mechanochromic polymers, which generate visible optical signals (color/fluorescence changes) through mechanochemical reactions;²¹² and mechano-drug-release polymers, where mechanical energy triggers controlled payload release via structural disruption.²¹³

Mechanochromic polymer microspheres rely on embedded mechanophores—force-sensitive molecular units that undergo covalent bond scission or conformational changes under stress.²¹⁴ Common mechanical carriers²¹⁵ include spiroactam, spirocyan, dianthracene, and azobenzene. As demonstrated in Figure 5f(i), microspheres fabricated using bilateral mechanophore anchoring across the spiro-junction enabled precise transduction of compressive stress to selective C–O bond cleavage. This energy-controlled activation triggers a reversible electrocyclic ring-opening reaction, converting colorless spirocyan to conjugated merocyanine, which exhibits a characteristic red color and 3.5-fold enhanced fluorescence. Crucially, the mechanochromic response aligned with centrosymmetric stress fields, allowing optical visualization of plastic strain accumulation through progressive green channel attenuation.²¹⁶ Recent advancements introduce glassy-rubbery concentric lamellar nanostructures via confined self-assembly of bottlebrush block copolymers, where alternating PS and photo-cross-linked polydimethylsiloxane (PDMS) domains enable rapid mechanochromism and near-instanta-

neous recovery.²¹⁷ Unlike conventional systems relying on covalent bond scission, these alternating nanostructures achieve color modulation through strain-dependent spacing changes in 1D photonic crystals (Figure 5f(ii)) while leveraging the synergy between PS rigidity and PDMS elasticity for high durability (>250 compression cycles without degradation).

Mechano-drug-release polymer microspheres exploit ultrasonic energy to achieve spatiotemporal payload control.²¹⁸ These systems typically feature a core-shell architecture, where drugs are encapsulated within a polymer matrix containing cavitation-sensitive moieties (e.g., gas-filled pores or thermolabile bonds).²¹⁹ Ultrasound induces localized cavitation bubbles, generating transient shear forces that fracture polymer chains or pores, enhancing drug permeability.²²⁰ Rapoport et al. designed PEG-PLLA/PCL-stabilized perfluoropentane microspheres with ultrasound-stimulated drug release.²²¹ Under tumor-targeted ultrasound, the interfacial shear stress caused the copolymer shell to rupture, releasing paclitaxel from within the microspheres.

3.2. Chemical Responsiveness. **3.2.1. pH Responsiveness.** pH-responsive polymers can be broadly classified into two categories: base-responsive polymers containing carboxylic acid groups and acid-responsive polymers with pyridine, amine, amidine, or guanidine groups. These responsive groups are solely influenced by external pH changes, which affect the degree of polymer ionization. This ionization alters the hydrophilic-hydrophobic balance of the polymer chains, leading to changes in the microsphere volume, permeability, and morphology. Common pH-responsive polymers include poly(acrylic acid),²²² poly(methacrylic acid),²²³ poly(allylamine hydrochloride),²²⁴ and poly(vinylpyridine).²²⁵

Carboxylic-acid-based pH-responsive polymers ionize in alkaline environments, increasing hydrophilicity, while in acidic or neutral environments they revert to an electrically neutral, nonionic state. Yu et al.²²⁶ used a one-step method to synthesize hollow polymer microspheres with a cyclic ether monomer. Owing to the presence of COOH groups, the hollow microspheres exhibited distinct pH-responsive behavior. When the environmental pH was below 5, the cavities in microspheres expanded, increasing their volume, while at pH above 5, both the outer and inner shells of the microspheres contracted sharply, reducing cavity volume. The pH-dependent swelling ratio (SR) is governed by the Henderson-Hasselbalch equation:²²⁷

$$SR = \phi_0 \cdot (1 + 10^{(pK_a - pH)}) \quad (3)$$

where ϕ_0 is the equilibrium volume fraction at neutral pH and pK_a is the strength of the substance's proton dissociation ability in solution.

Polymers with amine or pyridine groups respond to pH through protonation in acidic environments, transitioning from hydrophobic to strongly hydrophilic positively charged states. In alkaline or neutral environments, they deprotonate, causing the polymer chains to revert to a hydrophobic state.²²⁸ As shown in Figure 6a, Armes et al.²²⁹ synthesized pH-responsive poly(ethylene glycol) methacrylate-poly[2-(*tert*-butylamino)-ethyl methacrylate] microspheres via emulsion copolymerization. Owing to the protonation and deprotonation of secondary amine groups, the microspheres expanded when the pH decreased from 10 to 3 and returned to their original size as the pH shifted back to alkaline.

3.2.2. Ion Responsiveness. Polymers used to prepare ion-responsive microspheres typically contain specific ion-responsive and ionizable groups. These polymers often carry opposite charges, allowing them to form host-guest-like complexes through Coulombic interactions. The formation of these complexes induces a phase transition in the polymer chains, altering the molecular structure and hydrophilicity of the polymer, which in turn cause macroscopic changes in the size and dispersion of the polymer microspheres.²³⁰ The ionic strength of the environment also influences the swelling behavior of the microspheres. As ion concentration increases, polymer chains become highly coiled, hydrophobic interactions between chains intensify, and interactions between polymer chains and water molecules weaken, reducing the water content inside the microspheres. Additionally, with increased external ion concentration, the free ion concentration outside the microspheres surpasses that inside, causing the external osmotic pressure to exceed the internal pressure, causing microsphere shrinkage.²³¹

As shown in Figure 6b, Chu et al.²³² developed poly(*N*-isopropylacrylamide-*co*-acryloylamidobenzo-15-crown-5) (P(NIPAM-*co*-AAB15C5)) microspheres that respond to potassium ions. By adjustment of the potassium ion concentration in the environment, the volume of the microspheres can be controlled. As the potassium ion concentration increases, the P(NIPAM-*co*-AAB15C5) microspheres transition from an expanded to a contracted state. Conversely, as the potassium ion concentration decreases, the microspheres expand again, owing to the reduction in host-guest complex formation.

3.3. Biological Responsiveness. Biological stimuli responsiveness refers to the ability of materials to respond to biomacromolecules such as proteins, enzymes, and sugars within living organisms. This responsiveness is crucial, as it represents an ideal form of external stimuli response. In medical diagnostics, changes in the concentration of specific biomacromolecules, such as proteins or sugars, or variations in enzyme activity, are often primary indicators for disease identification.²³³ Furthermore, compared to stimuli such as temperature or pH, biological stimuli such as proteins or enzymes provide higher specificity, resulting in greater diagnostic accuracy.

3.3.1. Enzyme Responsiveness. Enzymes are crucial in biological metabolism and cellular detection owing to their specificity in recognizing target molecules.²³⁴ The types and concentrations of enzymes vary across different tissues, cells, and organelles, with their expression often altered in diseased tissues such as those affected by cancer or inflammation. For example, after a myocardial infarction, the expression of matrix metalloproteinases (MMPs) in myocardial tissue increases.²³⁵ Enzyme-responsive polymer microspheres are widely used in drug delivery systems, where they accumulate at target tissues or reach intracellular organelles, releasing drugs through localized enzymatic cleavage.²³⁶

Among the various enzyme-responsive types, microspheres that respond to MMPs are the most common and practical.²³⁷ MMPs are a class of endonucleases that degrade extracellular matrix proteins and are often overexpressed in pathological environments, such as tumors or rheumatoid arthritis. By leveraging the differences in MMP activity between pathological and normal physiological conditions, MMP-responsive behavior can be achieved. A common strategy is incorporating MMP-cleavable peptide sequences into the polymer to enable MMP responsiveness.²³⁸ Christman et al.²³⁹ designed an

enzyme-responsive micelle capable of targeting myocardial infarction tissue. During a myocardial infarction, the MMP concentration increases at the infarct site. The micelles, transported through the bloodstream, accumulate in the infarct region, where elevated MMP levels degrade the enzyme-responsive micelle structure, facilitating their targeted accumulation in the infarcted tissue. Enzyme-triggered erosion follows Michaelis–Menten kinetics:²⁴⁰

$$v = \frac{V_{\max}[S]}{K_m + [S]} \quad (4)$$

where v is the degradation rate, V_{\max} is the maximum reaction velocity, $[S]$ represents the substrate concentration, and K_m is the substrate affinity.

Cathepsins are also overexpressed in cancerous tissues, with different types of cathepsins exhibiting distinct structures, protein substrates, and catalytic mechanisms, playing various roles in tumor proliferation, angiogenesis, and metastasis. All cathepsins are produced in an inactive form and can be activated under low pH conditions.²³⁷

3.3.2. Protein Responsiveness. Strictly speaking, enzymes are a type of protein. However, in enzyme responsiveness, enzymes cleave specific chemical bonds at target sites within molecules, triggering chemical reactions that release small molecules or cause nanoparticle dissociation. By contrast, protein responsiveness focuses on the specific binding of proteins to certain functional groups, inducing responsive behavior. The underlying mechanisms of protein and enzyme response are fundamentally different.

Carbonic anhydrase is an important protein that catalyzes the reversible hydration of carbon dioxide, helping to regulate the acid–base balance of the body. As shown in Figure 6c, Thayumanavan et al.²⁴¹ used a self-assembly method to create polymer microspheres with a polypeptide backbone, a benzene ring as the hydrophobic segment, and PEG as the primary hydrophilic segment. Part of the hydrophilic chain contains benzenesulfonamide groups that specifically bind to carbonic anhydrase. Upon contact with the enzyme, it binds specifically to the benzenesulfonamide groups on the micelle surface,²⁴² disrupting the hydrophilic–hydrophobic balance of the micelles and triggering the release of hydrophobic cargo from within the micelles.

Thayumanavan et al.²⁴³ synthesized a series of dendrimers with PEG as the hydrophilic segment and aliphatic carbon chains as the hydrophobic segment. As shown in Figure 6d, these dendrimers self-assemble into microspheres owing to the hydrophilic–hydrophobic balance. The dendrimers also contain biotin ligands as terminal groups. When the microspheres encounter avidin (antibiotin protein), the biotin terminal groups bind specifically to avidin, causing the dendrimers to dissociate into monomers. This disrupts the hydrophilic–hydrophobic balance, leading to micelle dissociation and the release of encapsulated cargo.

3.3.3. Glucose Responsiveness. Glucose-responsive polymer microspheres are synthesized from polymers that respond to glucose.²⁴⁴ These materials can be classified into three main categories: polymers containing glucose oxidase (GOX),²⁴⁵ concanavalin-A polymers,²⁴⁶ and polymers with phenylboronic acid structures.²⁴⁷ GOX, an enzyme found in microorganisms, plants, and animals, is a glycoprotein composed of two methylene-linked flavin adenine dinucleotide molecules. In oxygen-rich environments, GOX catalyzes the conversion of

glucose into gluconic acid and hydrogen peroxide.²⁴⁸ As glucose levels rise in the bloodstream, GOX converts glucose to gluconic acid, lowering the surrounding pH. The pH-responsive polymer matrix detects this pH drop, triggering the swelling of the delivery system and facilitating insulin release.²⁴⁹

As shown in Figure 6e, Yu et al.²⁵⁰ developed glucose-responsive microspheres for controlled insulin release using the W/O/W double emulsion method. In high-glucose environments, approximately 61% of insulin encapsulated within the microspheres was continuously released over 15 h.

3.4. Multiple Stimuli Responsiveness. Current research on stimuli-responsive polymer microspheres primarily focuses on single-factor responsive systems. However, given the complexity of external environments and the practical demands of applications, the research focus is gradually shifting from single-factor-responsive to multi-factor-responsive polymer microspheres. For example, in drug delivery systems, microspheres may encounter multiple physical or chemical stimuli in the body. Therefore, these microspheres must be capable of analyzing and responding to several stimuli in complex environments.²⁵¹

A common approach for preparing multiresponsive polymer microspheres involves combining functional groups, polymers, or functional particles that respond to different stimuli. Polydopamine (PDA) has garnered great interest in biomedical applications owing to its strong adhesive properties, biocompatibility, and excellent photothermal conversion capabilities. As shown in Figure 6f, Peng et al.²⁵² successfully fabricated yolk–shell-structured magnetic mesoporous polydopamine microspheres and their carbon-based derivatives through interfacial assembly and selective etching methods. The internal core of these microspheres contains Fe_3O_4 particles, granting them magnetic responsiveness and allowing reversible magnetic separation and redispersion under changes in external magnetic field changes. Additionally, benzene and heterocyclic rings in PDA provide superior NIR light absorption, thus endowing the microspheres with excellent light-responsive properties.

As shown in Figure 6g, Xie et al.²⁵³ developed a novel dual-responsive protein-imprinted polymer through surface imprinting polymerization, which responds to both light and magnetic stimuli. The core of these microspheres consists of Fe_3O_4 magnetic particles, which provide them with excellent magnetic properties for rapid separation. Additionally, the azobenzene chromophores enable photoreversible binding dynamics toward the template protein; under 365 nm UV irradiation, *trans*-to-*cis* isomerization induces contraction of imprinted cavities, triggering a 31.4% release of preadsorbed bovine hemoglobin; conversely, 440 nm visible light reverses the configuration (*cis*-to-*trans*), restoring cavity accessibility for selective rebinding with 67.2% adsorption efficiency.

4. APPLICATIONS

With the rapid advancement of smart materials and micronano technologies, stimuli-responsive polymer microspheres, known for their exceptional multifunctional properties, have found extensive applications across numerous cutting-edge fields. These include, but are not limited to, drug delivery systems,²⁵⁴ tissue engineering,²⁵⁵ microrobots,¹⁹⁴ smart window design,²⁵⁶ intelligent coatings,²⁵⁷ information encryption,²⁵⁸ and wastewater treatment systems.²⁵⁹ Owing to their high sensitivity to external stimuli, these polymer microspheres

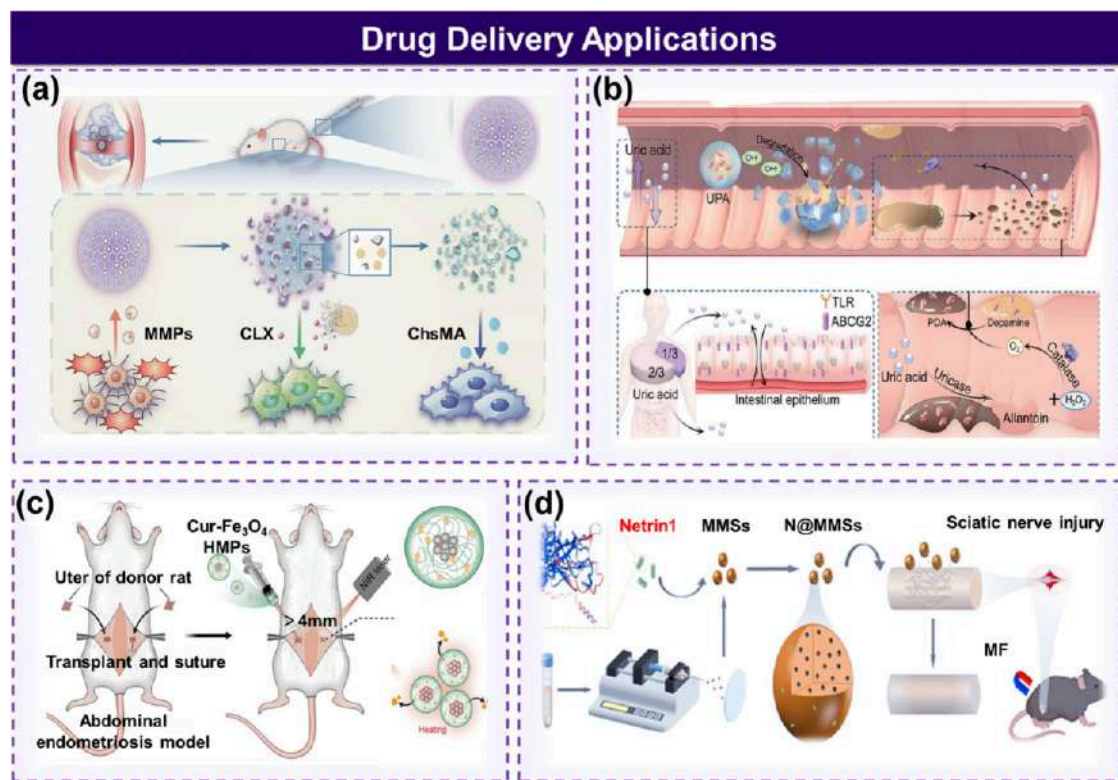


Figure 7. Applications of stimuli-responsive polymer microspheres in drug delivery systems. (a) Enzyme-responsive drug-loaded microspheres for the release of celecoxib and chondroitin sulfate. Reprinted with permission from ref 270. Copyright 2024, Elsevier. (b) pH-responsive polymer microspheres for the release of uricase and dopamine. Reprinted with permission from ref 271. Copyright 2023, John Wiley and Sons. (c) Light-responsive polymer microspheres for the release of curcumin. Reprinted with permission from ref 273. Copyright 2024, John Wiley and Sons. (d) Magnetic-responsive polymer microspheres for the release of Netrin1. Reprinted with permission from ref 275. Copyright 2024, Elsevier.

demonstrate diverse functional behaviors in various environments, further driving innovations and deepening the application of related technologies.

4.1. Drug Delivery. SPMs, which undergo reversible physical or chemical changes in response to environmental stimuli, have shown tremendous potential in drug delivery systems in recent years.^{260,261} Traditional drug delivery methods face challenges such as uncontrolled drug release, uneven distribution within the body, and critical side effects.²⁶² In contrast to conventional methods such as oral administration, injection, transdermal, or inhalation delivery, stimuli-responsive polymer microspheres offer several key advantages: they bypass first-pass metabolism and gastrointestinal degradation, enhancing drug bioavailability;^{263,264} they enable precise drug release at diseased sites in response to specific physiological or external stimuli, minimizing the impact on healthy tissues;^{265,266} and their intelligent responsive properties allow for timed and controlled drug release, reducing dosing frequency and improving patient compliance.^{267,268}

Enzyme-responsive and pH-responsive polymer microspheres primarily exploit the acidic and microenvironmental characteristics of inflammation or tumors for targeted drug release.²⁶⁹ As shown in Figure 7a, Miao et al.²⁷⁰ developed a dual-layer hydrogel microsphere for osteoarthritis (OA) treatment. The outer layer, composed of methacrylated gelatin, rapidly responds to MMPs in the OA microenvironment within 48 h, achieving >90% degradation efficiency under 10 U/mL collagenase III exposure, releasing celecoxib (CLX) to suppress inflammation and alleviate pain. Quantitative

pharmacokinetic analysis revealed a burst release of $68.3\% \pm 4.7\%$ CLX within the first 3 days, followed by sustained diffusion-controlled release over 14 days. The inner layer, composed of methacrylated chondroitin sulfate microspheres, gradually degrades at a rate of $12.8 \pm 1.2 \mu\text{m}/\text{day}$, releasing chondroitin sulfate to promote cartilage repair. This dual-microsphere design, responsive to the disease microenvironment, provides immediate symptom relief through anti-inflammatory action in the early stages of OA (TNF- α suppression by 61.4% vs. phosphate-buffered saline control) and offers long-term therapeutic effects by promoting cartilage regeneration (type II collagen expression increased 2.3-fold at week 8 postimplantation).

As shown in Figure 7b, Tang et al.²⁷¹ developed a pH-responsive, intestine-targeted burst-release hydrogel microsphere for gout treatment. These microspheres exploit a sharp pH threshold of 7.4–7.8, achieving complete disintegration within 25 min in simulated small intestinal fluid (pH 7.8) with a swelling rate exceeding 500% within 1 h. These microspheres remain stable in the acidic gastric environment (pH 1.2–3.0 for up to 6 h) but rapidly disintegrate in the mildly alkaline small intestine, releasing uricase and dopamine. Drug release kinetics shows $76.1 \pm 3.4\%$ uricase release within 1 h in intestinal conditions, facilitated by enzyme-catalyzed H₂O₂ decomposition rates of $28.3 \mu\text{M}/\text{min}$. Through an enzyme cascade reaction, the uricase is anchored to the intestinal mucosa via *in situ* dopamine polymerization (local O₂ concentration increased 5.2-fold under catalase activity), enhancing uric acid transport proteins in intestinal epithelial

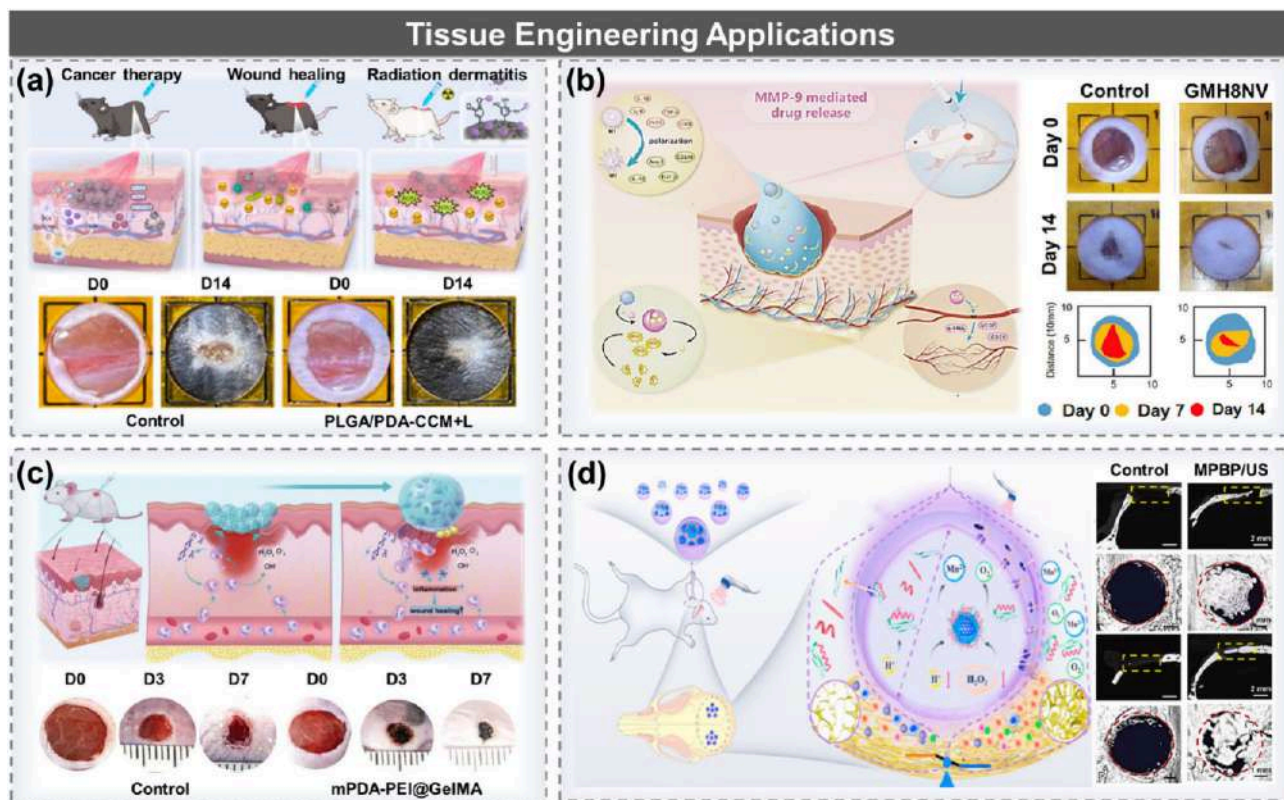


Figure 8. Applications of stimuli-responsive polymer microspheres in tissue engineering. (a) Magnetic-responsive drug-loaded microspheres for wound healing promotion. Reprinted with permission from ref 289. Available under a CC-BY. Copyright 2024, John Wiley and Sons. (b) Enzyme-responsive polymer microspheres for diabetic wound healing. Reprinted with permission from ref 290. Copyright 2024, American Chemical Society. (c) Enzyme-responsive polymer microspheres for enhancing diabetic wound healing. Reprinted with permission from ref 291. Available under a CC-BY 3.0. Copyright 2024, John Wiley and Sons. (d) Ultrasound and microenvironment dual-responsive polymer microspheres for bone defect repair. Reprinted with permission from ref 292. Available under a CC-BY-NC-ND 4.0. Copyright 2024, Elsevier.

cells and promoting fecal uric acid excretion by up to 37% in gout patients. This pH-responsive feature ensures precise drug release at specific intestinal sites, markedly improving therapeutic efficacy (blood uric acid reduction by 71% in hyperuricemia models) and safety by minimizing gastric drug leakage (<12% cumulative release in gastric fluid over 24 h).

Light-responsive microspheres allow precise control over drug release timing and location through external light sources.²⁷² As shown in Figure 7c, Liu et al.²⁷³ developed a light-responsive hydrogel microsphere for endometriosis treatment. These microspheres combine NIR light-triggered curcumin release with Fe₃O₄ nanoparticles (photothermal conversion efficiency = 30.4%), exhibiting remarkable photothermal activity. Drug release studies demonstrate NIR-triggered burst-release kinetics: 68.2% cumulative curcumin release within 18 days under three irradiation cycles, markedly higher than nonirradiated controls (21.3% release). When injected into endometriotic lesions and exposed to NIR light, the microspheres raise the local temperature via the photothermal effect (maintaining 46 °C for 5 min *in vivo*), inducing apoptosis in 98% of lesion cells. Simultaneously, NIR light triggers curcumin release, with anti-inflammatory efficacy reducing TNF- α and IL-6 levels by 82.4% and 75.6%, respectively. This dual mechanism notably suppresses endometriotic lesion growth (49.7% volume reduction) and the fibrotic area.

Magnetic-responsive microspheres enable remote control and precise targeting via external magnetic fields, thereby reducing systemic toxicity.²⁷⁴ Liu et al.²⁷⁵ developed magnetic microspheres loaded with Netrin1 to guide axonal growth, as shown in Figure 7d. In a mouse sciatic nerve injury model, the Netrin1-loaded magnetic microspheres demonstrated prominent nerve regeneration effects. Application of a magnetic field enhanced microsphere localization at the injury site (targeted accumulation increased 4.2-fold vs. nonmagnetic controls) and promoted the expression of neurotrophic factors (NGF protein levels elevated 6.03-fold in spinal cord tissue), effectively restoring nerve function.

Mechanoresponsive polymer microspheres have garnered substantial attention in drug delivery owing to their unique ability to provide noninvasive spatiotemporal control and deep tissue penetration through external physical stimuli. Among these, ultrasound-responsive systems stand out for their exceptional biosafety and precisely tunable energy input. Notably, Guo et al.²⁷⁶ engineered acoustically actuated “microsphere-bombs” via microfluidic synthesis of hyaluronic acid methacrylate hydrogels coloaded with antibacterial polyphenols and osteogenic MoS₂ nanoparticles. Under low-intensity ultrasound (1.5 W/cm²), transient cavitation effects generated localized hydraulic pressure gradients, triggering the structural disintegration of the microspheres within 2 min. This acoustic bursting mechanism enabled on-demand explosive release of therapeutic payloads (>96% within 24 h) through

synergistic fluidic oscillations and bubble collapse-induced network rupture. Ultrasound-directed delivery combines injectable localization and stimulus-programmable dosing, overcoming diffusion-limited drug penetration in dense infectious biofilms.

Beyond traditional stimuli-responsive microspheres, biodegradable variants have emerged as promising candidates for environmentally adaptive drug delivery.^{277–279} Wu et al.²⁸⁰ engineered phosphorylated cellulose microspheres (CMP) via esterification with phosphoric acid for targeted ciprofloxacin (CIP) release. The CMP exhibited pH-dependent degradation kinetics owing to electrostatic interactions between phosphate groups in CMP and ionizable carboxyl/piperazinyl moieties in CIP. Under simulated intestinal conditions (pH 6.8), the porous CMP (95.63% porosity) achieved sustained CIP release (56.7% over 24 h) through non-Fickian diffusion, while rapid pH-triggered CIP release (96.3% within 24 h at gastric pH 1.2) occurred via suppressed electrostatic binding. This design leverages the intrinsic sustainability of cellulose and phosphoric acid modification for dual functionality—pH-responsive drug release and ecological degradation—addressing limitations of synthetic, nondegradable carriers prone to inflammatory responses.

While stimuli-responsive microspheres excel in achieving precise spatiotemporal control of drug release, their engineered interactions with biological interfaces markedly enhance clinical efficacy. A transformative application is in mitigating sensory challenges associated with oral medications, particularly taste aversion.²⁸¹ Conventional bitter drugs frequently encounter low patient adherence owing to unpleasant flavor perception during swallowing.²⁸² To address this, stimuli-responsive microspheres have been specifically engineered to encapsulate bitter active compounds and prevent their premature release until reaching the gastrointestinal tract.²⁸³ For instance, Seo et al.²⁸⁴ developed pullulan-g-poly(L-lactide) nanogels with sharp temperature-triggered drug release behavior. These nanogels retained >90% encapsulated doxorubicin (DOX) at oral cavity temperatures (25–37 °C) but rapidly released 78% of the payload within 5 h at gastric conditions (42 °C) owing to hydrophobic chain collapse and nanogel contraction. This mechanism could prevent drug leaching during oral transit while enabling gastric release. By combining thermally stable encapsulation with pH/thermal dual-responsive materials, such systems may spatially separate drug exposure from taste receptors.

4.2. Tissue Regeneration. Traditional tissue engineering approaches typically rely on static scaffold materials that fail to adapt dynamically to changes in the tissue environment, limiting their ability to replicate complex biological conditions.²⁸⁵ SPMs, with their ability to respond sensitively to environmental changes, offer a dynamically adjustable microenvironment that substantially enhances cell-implant interactions.²⁸⁶ Specifically, these microspheres can precisely regulate behaviors such as swelling, degradation, or drug release, providing timely cellular support and signal transmission, thereby effectively promoting tissue regeneration.^{287,288}

As shown in Figure 8a, Zhang et al.²⁸⁹ developed copper-based metal–organic framework-modified microspheres for the comprehensive treatment of melanoma. Under 808 nm NIR irradiation (1.5 W/cm²), the PLGA/PDA-CCM microspheres exhibited rapid photothermal conversion, raising the temperature from 25 to 56.7 °C within 300 s, enabling targeted

therapy through photothermal responsiveness. The release kinetics of Cu²⁺ demonstrated a biphasic profile, with 43.5% cumulative release within 6 h, followed by sustained release over 21 days. This photothermal-ionic coupling mechanism induced immunogenic cell death with >80% calreticulin exposure and HMGB1 release (24.17 ± 6.75 pg/mL), triggering a potent antitumor immune response. Notably, oxygen depletion in hypoxic tumors reduced the photothermal conversion efficiency by 18%, highlighting the need for optimized irradiation parameters in low-oxygen microenvironments. This platform prevents tumor recurrence through 71.09% distal tumor suppression and promotes wound healing by enhancing the vascular density while mitigating radiation dermatitis.

Diabetes causes numerous complications, including but not limited to cardiovascular disease, nerve damage, kidney dysfunction, and impaired wound healing, the latter being one of the most challenging. To address this issue, Li et al. designed a gelatin microsphere responsive to matrix metalloproteinase-9 (MMP9),²⁹⁰ as shown in Figure 8b. MMP9 is typically overexpressed in diabetic wounds, and this microsphere can precisely release H8 nanovesicles, which possess both anti-inflammatory and antioxidant properties in such environments. This MMP9-responsive microsphere system effectively promotes angiogenesis, alleviates oxidative stress damage, suppresses inflammation, and accelerates diabetic wound healing by promoting collagen deposition. Additionally, diabetic wounds often contain high concentrations of neutrophil extracellular traps (NETs), the formation of which exacerbates the inflammatory response and impedes wound healing. As shown in Figure 8c, Xiao et al.²⁹¹ developed an MMP9-responsive gelatin microsphere that clears NETs. In the MMP9-rich diabetic wound environment, the microsphere precisely releases functional agents, profoundly reducing NET formation and inflammation, promoting angiogenesis and collagen deposition and ultimately accelerating wound healing.

Stimuli-responsive polymer microspheres have also been applied to bone defect repair. As shown in Figure 8d, Song et al.²⁹² developed a multifunctional microsphere system that is dual-responsive to ultrasound (1 MHz, 1 W/cm² for 3 min) and the bone injury microenvironment (pH threshold ≤ 5.5, H₂O₂ concentration ≥ 100 μM), promoting bone defect repair. Under acidic conditions (pH = 5.5) with 100 μM H₂O₂, the system achieved 83.6% cumulative release of Mn²⁺ and 76.1% BMP-2 release within 30 days, while ultrasound-triggered bursts increased their release rates by 1.5× compared to passive diffusion. MnO₂ neutralized the acidic microenvironment and scavenged 98.7% of reactive oxygen species (ROS) within 2 h, generating Mn²⁺ and O₂. This dual action enhanced osteoblast proliferation by 2.1× and accelerated mineralization. Furthermore, M1-to-M2 macrophage polarization efficiency reached 71.3%, reducing TNF-α expression by 65% and elevating IL-10 by 2.8 times. Mechanistically, MnO₂-mediated ROS clearance suppressed NF-κB activation, creating an immunoregulatory niche that synergized with the osteogenic effects of BMP-2, achieving 89.7% bone volume/tissue volume recovery at 8 weeks postimplantation.

Emerging as mechanoactive therapeutic platforms, ultrasound-responsive microspheres have demonstrated unprecedented capabilities in orchestrating the bone regeneration microenvironment. Chen et al.²⁹³ engineered oxygen-spatio-temporizing hydrogel microspheres (US@O₂@GHB) via microfluidic fabrication of GelMA/HepMA matrices embed-

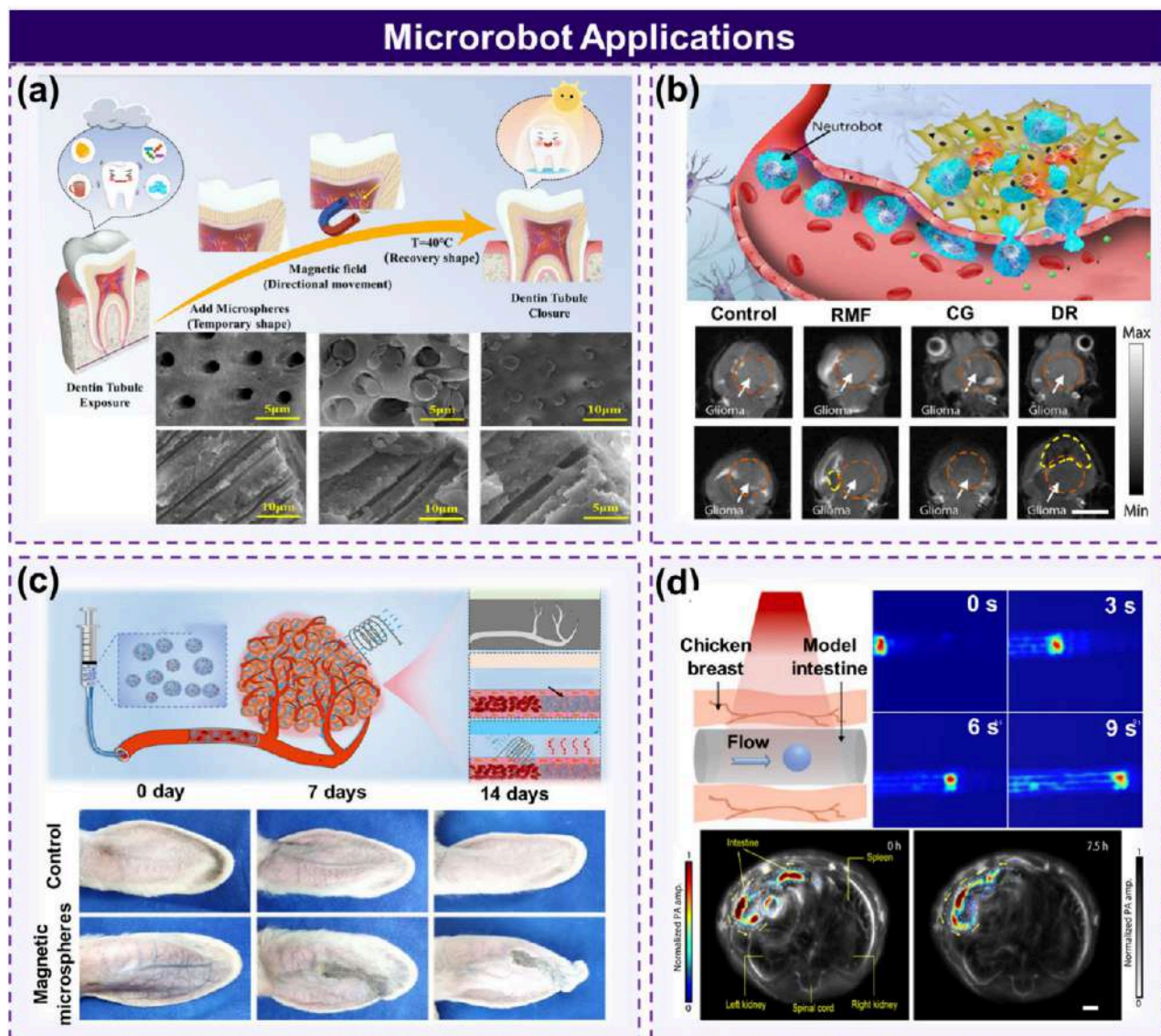


Figure 9. Applications of stimuli-responsive polymer microspheres in microrobots. (a) Multifunctional microrobot for occluding dental tubules. Reprinted with permission from ref 194. Copyright 2024, Elsevier. (b) Microrobot for targeted treatment of malignant glioma. Reprinted with permission from ref 303. Copyright 2024, Elsevier. (c) Microrobot for the treatment of hepatocellular carcinoma. Reprinted with permission from ref 304. Copyright 2022, Elsevier. (d) Microrobot enabling *in vivo* imaging. Reprinted with permission from ref 302. Copyright 2019, The American Association for the Advancement of Science.

ded with perfluorohexane-loaded PLGA nanobubbles. These microspheres leverage ultrasound-induced cavitation (650 kHz, $1\text{--}4\text{ W/cm}^2$) to generate transient hydraulic pressure gradients, triggering on-demand oxygen bursts within 9 h postinjury—a critical window for VEGF-mediated angiogenesis. Through spatiotemporal oxygen modulation, the released oxygen elevated HIF-1 α /VEGF axis activity by 1.95–2.29 times compared to static oxygen carriers, while BMP-2 sustained release via heparin-binding enhanced osteogenic differentiation. In rat femoral defect models, this biomechanically actuated system achieved 96% vascular network reconstitution and 2.1 times higher bone mineral density than conventional hydrogels at 8 weeks, demonstrating precise coupling of mechanical stimuli with biochemical signaling.

Polyvinyl fluoride (PVF), a polymer material with distinctive electrical properties, has recently given rise to novel intelligent PVF materials characterized by their photoinduced surface

charge regeneration²⁹⁴ and triboelectric self-polarization.²⁹⁵ These materials have been successfully applied in nerve and blood vessel remodeling and repair,^{296,297} as well as in the development of intelligent control systems that operate without external drivers.²⁹⁸ Research has demonstrated that through programmed design, PVF materials can achieve particle sorting, cell assembly, and cellular stimulation.²⁹⁹ Consequently, micronano structures fabricated from PVF materials can facilitate the transport of bioactive substances such as growth factors and extracellular matrix, along with the capture, transfer, and manipulation of specific cells. This capability offers a valuable tool for tissue engineering research and treatment and holds promise for further advancements in this field.

4.3. Microrobots. Microrobots and nanorobots are robotic systems that operate at the micrometer or nanometer scale, exhibiting autonomy or control over performing specific tasks within microscopic environments. Stimuli-responsive polymer

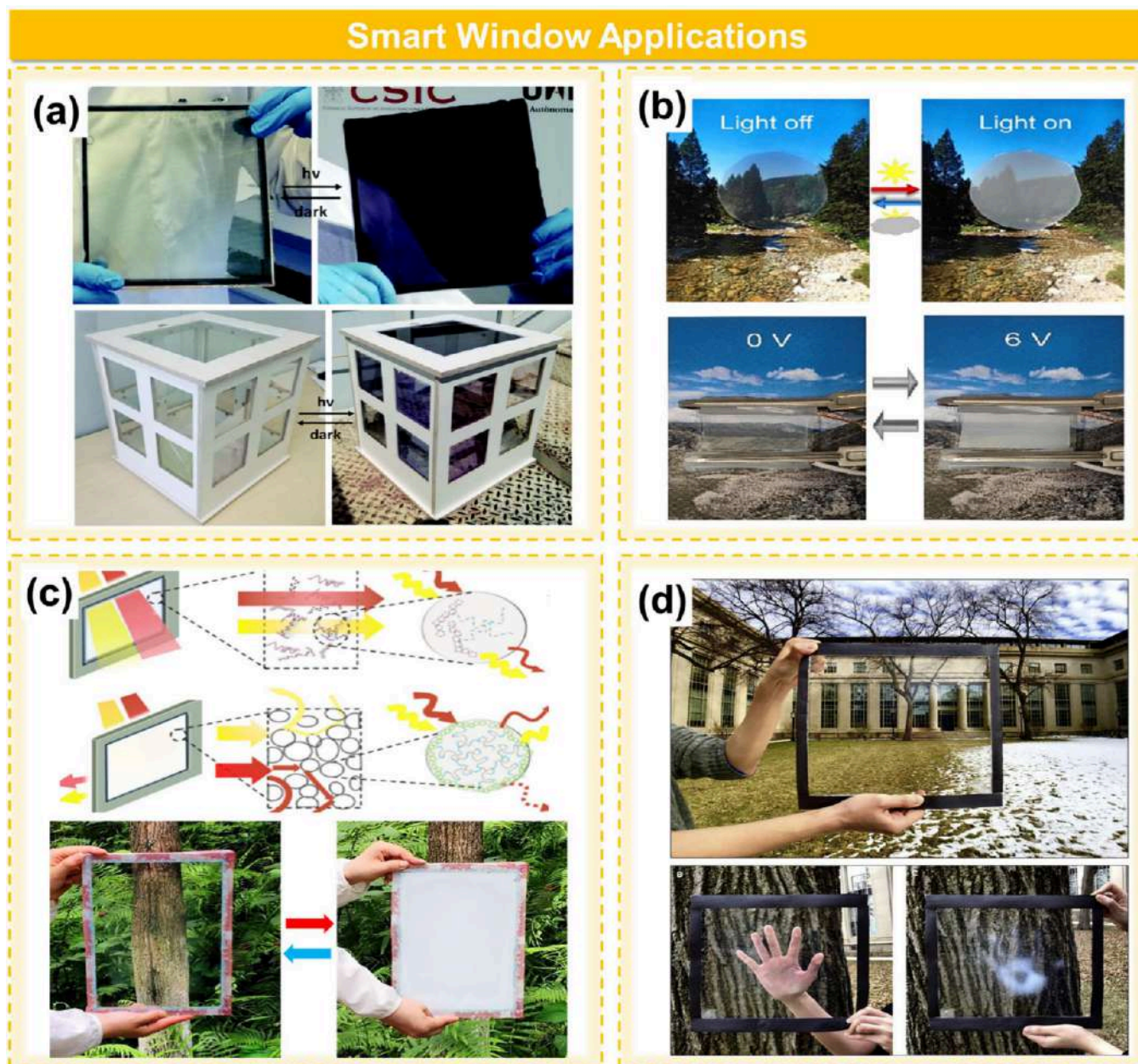


Figure 10. Applications of stimuli-responsive polymer microspheres in smart windows. (a) Thermoresponsive polymer microspheres for photochromic windows. Reprinted with permission from ref 307. Copyright 2020, Royal Society of Chemistry. (b) Thermoresponsive polymer microspheres for transparency-adjustable smart windows. Reprinted with permission from ref 308. Copyright 2023, Elsevier. (c) Thermoresponsive polymer microspheres for light transmittance-adjustable smart windows. Reprinted with permission from ref 309. Copyright 2021, Elsevier. (d) Thermoresponsive polymer microspheres for NIR light transmittance-adjustable smart windows. Reprinted with permission from ref 310. Copyright 2019, Elsevier.

microspheres, which respond to environmental stimuli and convert them into functional outputs, are crucial in the development of advanced devices such as microrobots and nanorobots. By leveraging the unique properties of stimuli-responsive polymers or functional particles, functional modules for microrobots and nanorobots can be designed to respond to external environmental changes, enabling tasks such as occluding specialized tissue structures,³⁰⁰ targeted destruction of tumors,³² embolization,³⁰¹ and *in vivo* imaging.³⁰²

Guo et al.¹⁹⁴ developed a micronanorobot for the occlusion of dentinal tubules, integrating magnetic-guided motion and shape-memory functionality. As shown in Figure 9a, the micronanorobot, initially in its temporary shape, can be

magnetically guided into dentinal tubules, where it recovers its original shape through shape-memory capabilities, effectively sealing the tubules. This micronanorobot achieved an entry rate of 93.33% into the dentinal tubules and an occlusion rate of 85.41%, offering an innovative solution for the treatment of tooth sensitivity.

Zhang et al.³⁰³ developed magnetically/chemically dual-responsive micronanorobots for targeted treatment of malignant gliomas. As shown in Figure 9b, these biohybrid "neurobots" achieve precise motion control under a rotating magnetic field (15 mT amplitude and 2 Hz frequency), reaching a maximum propulsion speed of 16.4 $\mu\text{m/s}$. Their directional navigation relies on chemotactic gradients of

inflammatory factors (threshold concentration ≥ 10 nM fMLP; chemotactic velocity = $0.21 \mu\text{m/s}$ under a $100 \text{ pM}/\mu\text{m}$ gradient). When exposed to pathological hydrogen peroxide levels ($\geq 100 \mu\text{M H}_2\text{O}_2$), the embedded MnO_2 nanoparticles scavenge 98.7% ROS within 2 h while generating therapeutic Mn^{2+} and O_2 . Crucially, the neutroBots cross the blood–brain barrier using a combination of magnetic propulsion and chemotaxis, enhancing glioma accumulation by 43% in the dual-responsive mode compared to controls. *E. coli* membrane camouflage enables $\geq 97.7\%$ neutrophil phagocytosis efficiency and reduces paclitaxel leakage. In postoperative glioma models, the dual-responsive treatment prolonged the median survival to 43 days, demonstrating the synergy of external actuation and biological responsiveness in complex physiological environments.

Wei et al.³⁰⁴ developed a micronanorobot for hepatocellular carcinoma treatment. As shown in Figure 9c, these micronanorobots achieve precise hyperthermic control through optimized AC magnetic fields (200 Oe, and 100 kHz), maintaining tumor-targeted temperature of $50.7 \pm 0.8 \text{ }^\circ\text{C}$ via low-Curie-point SPIONs ($T_c = 55.6 \text{ }^\circ\text{C}$). Furthermore, they can load and release DOX in a controlled manner under an alternating magnetic field. Experimental results showed that these micronanorobots effectively occlude target blood vessels and are detectable via computed tomography/nuclear magnetic resonance imaging. This multifunctional micronanorobot, integrating embolization, chemotherapy, magnetic hyperthermia, and imaging monitoring, provides a novel technological pathway for precision therapy.

Wu et al.³⁰² developed a photoacoustic tomography-guided microrobotic system for intestinal-targeted navigation. As shown in Figure 9d, these Mg/Au Janus micromotors encapsulated in gelatin/alginate microcapsules maintained gastric stability for >2 h in pH 2 HCl and achieved pH-responsive release in intestinal fluid upon NIR exposure (808 nm, $2 \text{ W}/\text{cm}^2$ for 0.1 s). The micromotors demonstrated bubble-propelled motion at $43 \pm 5 \mu\text{m/s}$ in the intestinal fluid. Real-time tracking via PACT precisely localized migration toward tumor regions at $1.2 \text{ cm}/6 \text{ h}$, while triggered drug release (DOX encapsulation efficiency = 75.9%; sustained release over 72 h) and local pH elevation to ~ 12.0 via $\text{Mg}(\text{OH})_2$ hydrolysis enhanced mucus penetration and tumor accumulation. This integrated platform achieved 80% drug retention in target intestinal segments vs. 20% passive diffusion, bridging precise imaging and active propulsion for GI therapeutics.

4.4. Smart Windows. Stimuli-responsive polymer microspheres hold great promise in the field of smart windows. By responding to external stimuli such as light, heat, and electricity, these microspheres can dynamically regulate the transparency, thermal conductivity, and color changes of a window, enabling energy-saving effects through environmental adaptability.³⁰⁵ Their application in smart windows not only enhances building intelligence but also substantially improves energy efficiency, paving the way for green buildings.³⁰⁶

Torres-Pierna et al.³⁰⁷ successfully fabricated a highly transparent, fast-responsive photochromic film by encapsulating temperature-responsive polymer microspheres within a polymer matrix. As shown in Figure 10a, when applied to a glass surface, the film enables the glass to rapidly transition from colorless to colored upon light stimulation and quickly reverts to its original state once the light source is removed. This method overcomes the limitations of traditional photo-

chromic materials in solid-state applications, allowing precise control of optical properties in solid materials. Additionally, by adjusting the combination of dyes and oil phases, both the wavelength of the photochromic response and fading time can be finely tuned.

Otaegui et al.³⁰⁸ developed smart windows capable of transparency modulation at different temperatures by dispersing thermoresponsive microspheres within a polymer matrix. As shown in Figure 10b, at room temperature the refractive index of the microspheres matches that of the polymer matrix, maintaining high transparency. When the temperature exceeds the melting point of the microspheres, the refractive index mismatch causes light scattering, making the window opaque. Additionally, the incorporation of photothermal agents or heating elements allows for the adjustment of light transmittance under applied voltage. This method features low material costs, ease of fabrication, high optical stability, and mechanical flexibility, making it suitable for large-scale production.

Tan et al.³⁰⁹ developed a temperature-responsive “cloud” material for smart windows, enabling light transmittance modulation through the controlled self-assembly of microspheres. As shown in Figure 10c, these microspheres are fully dissolved in water below their LCST, exhibiting up to 95.7% visible light transmittance. When the temperature exceeds the LCST, the microspheres self-assemble into large particles, effectively scattering NIR light and reducing transmittance to 0.8%, thereby providing remarkable optical modulation.

Li et al.³¹⁰ synthesized thermochromic hydrogel microspheres that undergo volumetric phase transitions in response to temperature changes, leading to noticeable alterations in their scattering properties and, consequently, modulating the light transmittance of windows. As shown in Figure 10d, by uniformly dispersing these microspheres in a film and placing them between two layers of glass, the NIR light transmittance of the window can be effectively controlled, achieving efficient solar shielding near room temperature.

4.5. Smart Coating. Stimuli-responsive polymer microspheres in smart coatings offer remarkable functionality, controllability, and environmental responsiveness.³¹¹ By tuning the chemical composition, structure, and surface functionalization of polymer microspheres, these microsphere-infused coatings can adapt to external stimuli, enabling functions such as microdamage detection, damage extent assessment,³¹² self-healing,³¹³ corrosion resistance,³¹⁴ and antifouling properties.³¹⁵ The intelligent characteristics of stimuli-responsive microspheres enhance the durability and performance of coatings, paving the way for the next generation of efficient, eco-friendly smart materials.³¹⁶

Robb et al.²⁵⁷ developed a smart coating containing microspheres that exhibit aggregation-induced emission (AIE) luminescence. As shown in Figure 11a, mechanical damage to the coating causes the microspheres to rupture, releasing a luminophore solution. Upon solvent evaporation, the luminophores aggregate and emit a fluorescent signal, enabling real-time self-reporting of microdamage. This coating system is highly sensitive and broadly applicable, allowing for rapid and reliable damage detection across various coating materials and damage modes. Notably, this single-use mechanism relies on the irreversible depletion of encapsulants, prioritizing immediate damage visualization over repeated responsiveness.

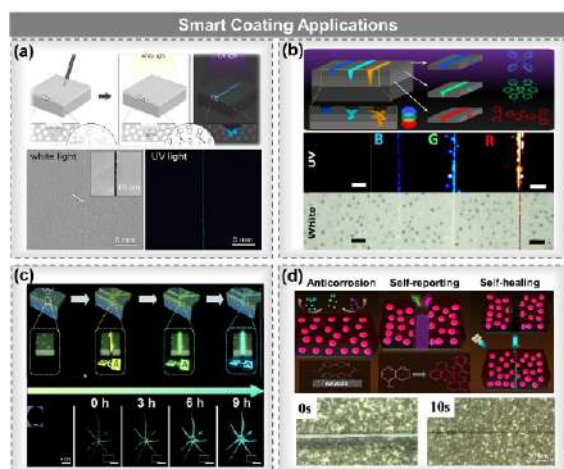


Figure 11. Applications of stimuli-responsive polymer microspheres in smart coatings. (a) Light-responsive polymer microspheres for monitoring microdamage in smart coatings. Reprinted with permission from ref 257. Available under a CC-BY-NC 4.0. Copyright 2016, American Chemical Society. (b) Light-responsive polymer microspheres for assessing damage severity in smart coatings. Reprinted with permission from ref 317. Copyright 2018, American Chemical Society. (c) Stimuli-responsive polymer microspheres for self-healing and visualized damage repair in smart coatings. Reprinted with permission from ref 318. Copyright 2022, Royal Society of Chemistry. (d) Stimuli-responsive polymer microspheres for corrosion protection, self-healing, and corrosion sensing in smart coatings. Reprinted with permission from ref 314. Copyright 2024, American Chemical Society.

Building on this, Lu et al.³¹⁷ encapsulated AIE luminophores of different emission colors into microspheres and embedded these microspheres within the coating layers, creating a smart coating capable of detecting both damage and damage severity. As shown in Figure 11b, when the coating is mechanically damaged, the microspheres rupture according to the crack depth, releasing luminophores that emit different fluorescent colors, thereby enabling the visual detection of the damage depth. Similar to the system developed by Robb et al.,²⁵⁷ the release-triggered fluorescence signaling operates irreversibly, forming a semipermanent record of the damage.

Chen et al.³¹⁸ utilized AIE-functionalized microspheres to detect coating damage and enable real-time visualization of the self-healing process at the damaged site. As shown in Figure 11c, when the coating is damaged, the diisocyanate solution encapsulated in microcapsules is released, reacting with moisture in air to form a solid polymer that fills the damaged area. This process activates the AIE mechanism, enabling the repair process to be visually monitored by changes in the fluorescent signal. The dual functionality of damage reporting and self-healing combines an irreversible chemical reaction (moisture curing) with a one-time optical feedback loop.

Zhang et al.³¹⁴ developed a multifunctional smart coating with corrosion protection, self-healing, and corrosion sensing capabilities by embedding stimuli-responsive polymer microspheres within the coating. As shown in Figure 11d, when the coating is mechanically damaged, 8-hydroxyquinoline is released from the microspheres and chelates with Al^{3+} , emitting a distinct fluorescence signal to detect corrosion. The photothermal properties of the microspheres allow the coating to heat rapidly under NIR light, inducing polymer chain mobility and enabling crack self-healing. This smart

coating, formed by mixing the microspheres with UV-cured resin and applying it to an aluminum alloy substrate, exhibited excellent corrosion resistance, rapid self-healing efficiency, and reliable corrosion monitoring, providing an innovative solution to extend the service life of metal materials. Contrastingly, the photothermal self-healing component exhibits partial reversibility, as cyclic NIR exposure can reactivate polymer chain dynamics without microsphere exhaustion, highlighting tunable reversibility in material design.

The strategic selection between single-use and reversible responsiveness is critical for real-world applications. Mechanistically, irreversible systems (e.g., Figures 11a–11c)^{257,317,318} achieve high-intensity localized activation via total payload release, making them ideal for one-time damage reporting³¹² but preventing repeated functionality. Conversely, thermodynamically reversible mechanisms (e.g., temperature-dependent swelling of PNIPAM microspheres³¹⁹ or electrochemical redox-responsive films)³²⁰ enable cyclic adaptation, as demonstrated in photothermal repair by Zhang (Figure 11d).³¹⁴ Future designs should hybridize both paradigms: combining irreversible “first-aid” sensing with reversible regulators for long-term environmental interaction. For example, phase-change microspheres with spatially segregated compartments could offer simultaneous crack-sealing (reversible thermal flow) and corrosion inhibitor release (single-use). Such multimodal systems would align stimulus reversibility with application timelines to maximize the operational lifespans.

4.6. Encrypted Messages. The application of stimuli-responsive polymer microspheres in information encryption reveals the vast potential of cross-disciplinary innovations between cutting-edge technology and material science.³²¹ By precisely tuning the molecular structure and surface properties of these microspheres, they can undergo highly controlled and reversible physical or chemical changes in response to specific external stimuli, enabling concealed data storage and selective data retrieval.^{322,323} This unique capability not only introduces dynamic adjustability and stealth to information encryption but also surpasses the limitations of traditional encryption techniques, elevating information security to a new level.³²⁴ With continued technological advancements, stimuli-responsive polymer microspheres are poised to drive disruptive innovations in information encryption, offering highly reliable and intelligent solutions for data protection.³²⁵

Otaegui et al.³²⁶ successfully developed thermally responsive multicolor fluorescent pixels by combining fluorescent dyes with organic phase-change materials, utilizing temperature regulation to achieve reversible fluorescence emission. These mixtures were encapsulated into microspheres containing different dye and phase-change material combinations through a microencapsulation technology. Embedding the microspheres into a polymer matrix resulted in pixel arrays that exhibited a dynamic multicolor luminescent behavior. As shown in Figure 12a, these pixel arrays demonstrate excellent potential in high-security 3D information encryption and 4D data storage, greatly enhancing information storage density and security.

Cai et al.³²⁷ developed an information encryption technology using stimuli-responsive polymer microspheres embedded with hydrophobic carbon dots and integrated with responsive hydrogel photonic crystal particles. By adjustment of the surrounding solvent, these microspheres achieved reversible fluorescence and structural color changes. As shown in Figure

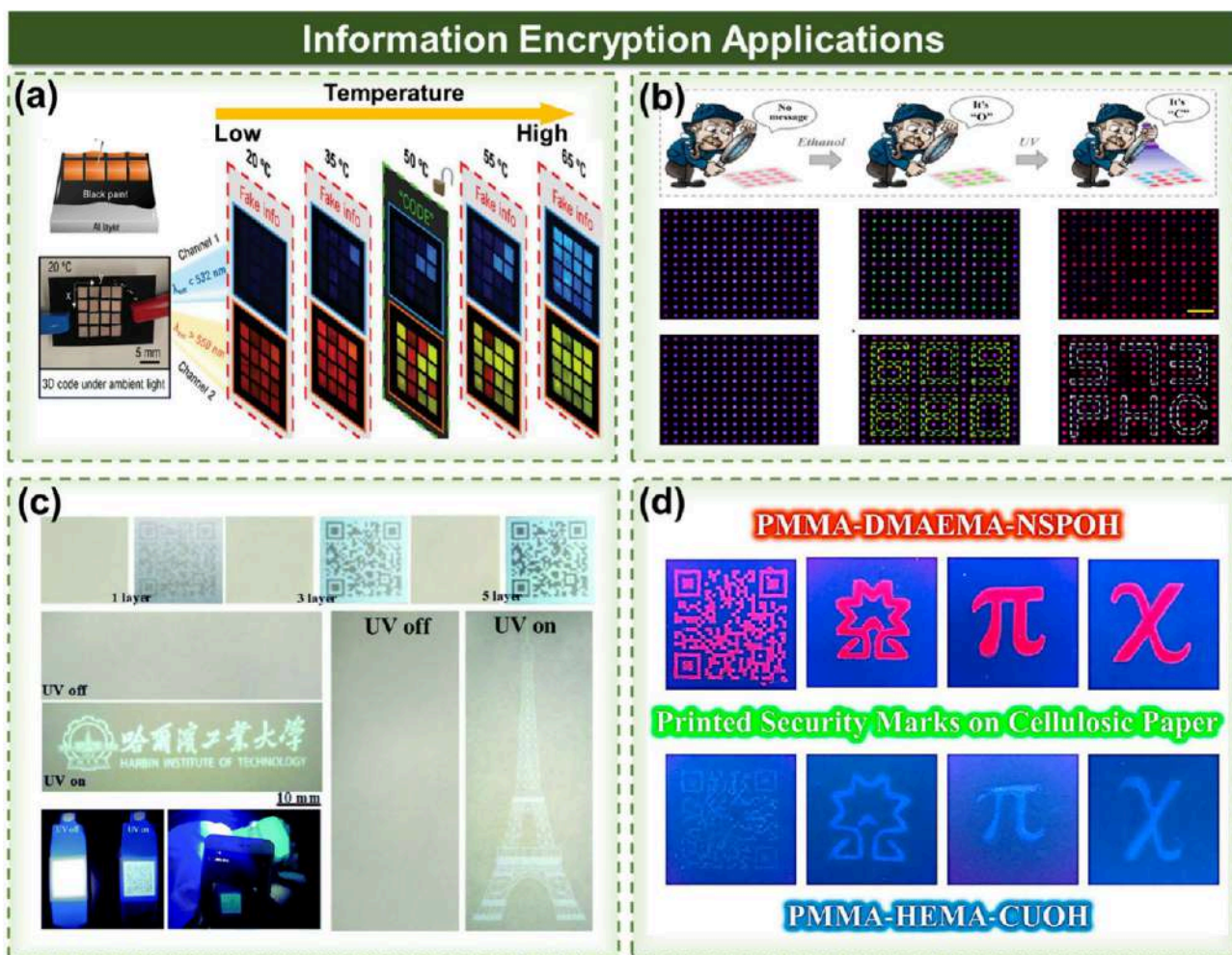


Figure 12. Applications of stimulus-responsive polymer microspheres in information encryption. (a) Temperature-responsive polymer microspheres enabling pixel arrays with dynamic multicolor luminescent behavior. Reprinted with permission from ref 326. Available under a CC-BY 3.0. Copyright 2024, John Wiley and Sons. (b) Stimuli-responsive polymer microspheres generating dynamic patterns for complex information encryption and decryption. Reprinted with permission from ref 327. Copyright 2023, Elsevier. (c) Light-responsive polymer microspheres enabling microscale pattern encryption. Reprinted with permission from ref 328. Copyright 2021, RSC Pub. (d) Light-responsive polymer microspheres facilitating encrypted information printing. Reprinted with permission from ref 329. Copyright 2020, Elsevier.

12b, this dual-mode color-switching feature enabled the construction of dynamic patterns for complex information encryption and decryption, enhancing encryption efficiency while providing a wide viewing angle and a convenient method for decryption.

Wang et al.³²⁸ successfully fabricated conjugated polymer fluorescent nanospheres with adjustable fluorescence intensity for high-resolution inkjet printing in microscale pattern encryption. By precise control of the nanoparticle size, loaded materials, and fluorescence properties, these nanospheres were transformed into invisible ink. When combined with inkjet printing technology, they enabled highly accurate pattern encryption. As shown in Figure 12c, these patterns remain undetectable under natural light but become visible under UV light, demonstrating strong potential for encryption and anticounterfeiting applications.

Abdollahi et al.³²⁹ developed microspheres capable of emitting multiple colors under UV light, applying them to encrypted information printing on cellulose-based paper. As shown in Figure 12d, these fluorescent markers are completely invisible under natural light but become visible under UV light,

remarkably enhancing the security and anticounterfeiting properties of the information. This technology offers promising applications in high-security domains such as passports, banknotes, and identification cards while providing an efficient, eco-friendly solution for anticounterfeiting and identity authentication.

4.7. Water Treatment. The rapid pace of industrialization and urbanization has intensified environmental pollution, creating an urgent need for efficient and intelligent environmental technologies and materials. Stimuli-responsive polymer microspheres, with their sensitivity to environmental changes, controllable size, and modifiable surfaces, are innovative solutions to various environmental challenges.³³⁰ In water pollution, soluble contaminants—such as heavy metal ions commonly used in various industries, including lead ions (Pb^{2+}),³³¹ antimony ions (Sb^{3+}),³³² chromium ions (Cr^{6+}),³³³ and copper ions (Cu^{2+})²⁵⁹—as well as certain organic dyes³³⁴ and antibiotics,³³⁵ pose serious environmental hazards owing to their toxicity. Current techniques employed for the detoxification and removal of heavy metal ions and dyes include extraction, adsorption, electrocatalytic oxidation, and

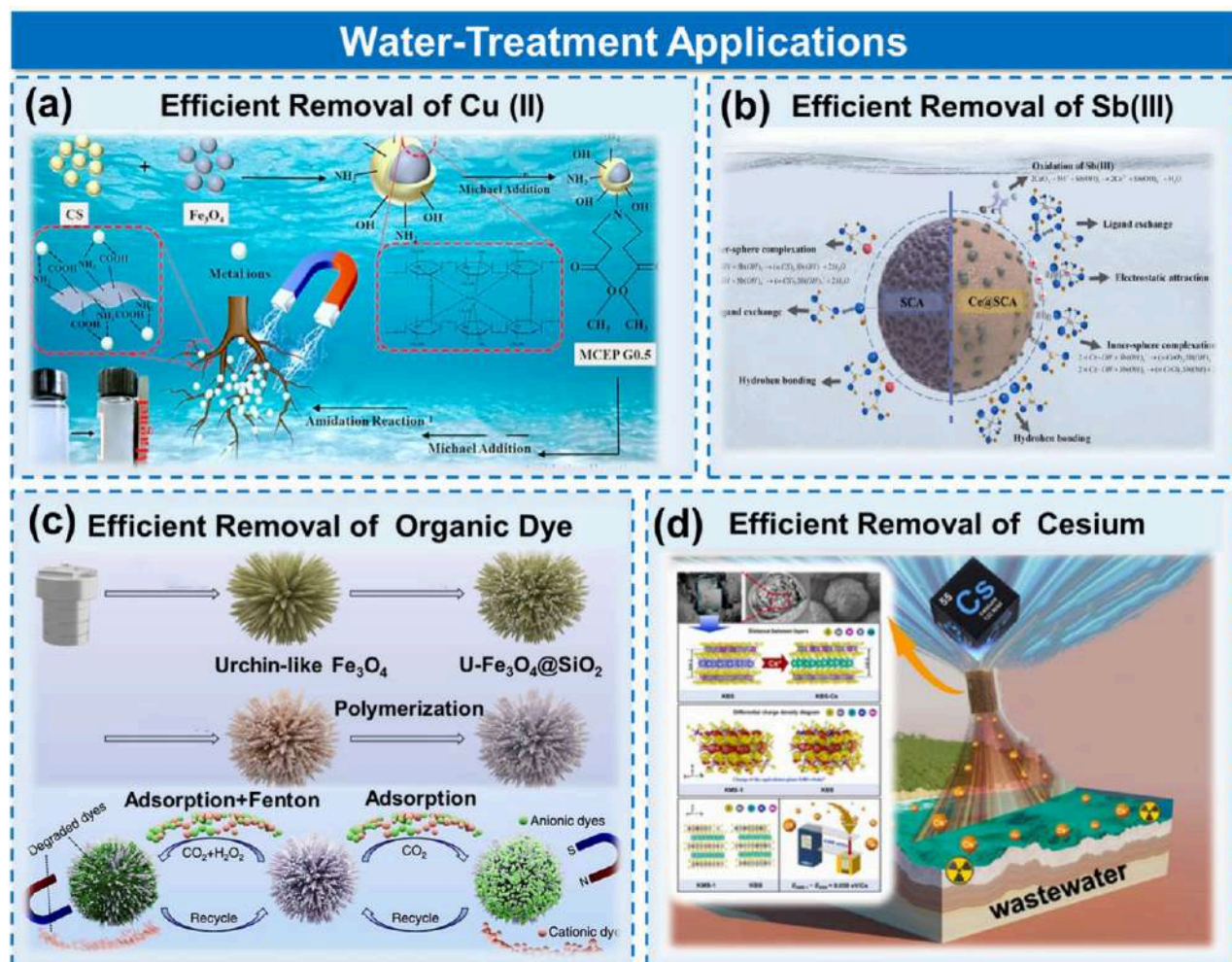


Figure 13. Environmental applications of stimulus-responsive polymer microspheres. (a) Magnetic-responsive polymer microspheres for the adsorption of Cu^{2+} from industrial wastewater. Reprinted with permission from ref 341. Copyright 2024, Springer Nature. (b) pH-responsive polymer microspheres for the adsorption of Sb^{3+} from industrial wastewater. Reprinted with permission from ref 342. Copyright 2024, Elsevier. (c) CO_2 -responsive magnetic polymer microspheres for the removal of organic dyes from wastewater. Reprinted with permission from ref 343. Copyright 2024, Elsevier. (d) Stimuli-responsive polymer microspheres for the adsorption of Cs^+ from industrial wastewater. Reprinted with permission from ref 344. Copyright 2024, Elsevier.

membrane separation.³³⁶ Among these, adsorption is particularly effective owing to its mild operating conditions, cost-efficiency, and lack of secondary pollution.³³⁷ Stimuli-responsive polymer microspheres, featuring high surface areas and easy recovery after use, have emerged as promising adsorbents.³³⁸ Furthermore, they can provide structural support or protective networks for other materials, enhancing the stability, mechanical properties, and adsorption efficiency of adsorbents.³³⁹ Consequently, environmentally friendly, efficient, and cost-effective stimuli-responsive polymer microspheres have already been successfully applied in industrial wastewater treatment.³⁴⁰

As illustrated in Figure 13a, Wang et al.³⁴¹ developed magnetic chitosan microspheres (MCEPs) for the removal of Cu^{2+} from industrial wastewater. Their study demonstrated that MCEPs exhibit a high selective adsorption capacity for Cu^{2+} , reaching a maximum of 702.9 mg/g, with adsorption completing within 60 min. Additionally, the adsorbent is highly regenerative, retaining over 80% adsorption efficiency after five cycles. The incorporation of magnetic particles endows the MCEPs with magnetically responsive properties, allowing for easy recovery under an external magnetic field after Cu^{2+}

adsorption. This innovation addresses the challenge of difficult adsorbent recovery in heavy metal removal and detection, offering a novel solution for efficient waste treatment.

Wastewater contamination by antimony ions poses serious health risks, including cancer and congenital malformations. As illustrated in Figure 13b, Zeng et al.³⁴² developed a hydrophilic porous sulfur-doped carbon aerogel microsphere (Ce@SCA) using microemulsion technology and hydrothermal synthesis for Sb^{3+} removal from wastewater. Ce@SCA exhibits pH-responsive adsorption behavior, with the adsorption capacity for Sb^{3+} gradually decreasing as the pH of the solution increases from 2 to 10. This pH-dependent response enhances the adaptability of the material to various wastewater treatment conditions, particularly improving adsorption efficiency in acidic environments.

As illustrated in Figure 13c, Yang et al.³⁴³ developed a novel urchin-like CO_2 -responsive magnetic microsphere (U- Fe_3O_4 @P) for organic dye removal. U- Fe_3O_4 @P exhibits a CO_2 -triggered responsiveness, enabling ultrafast, selective, and reversible adsorption of anionic dyes. Simultaneously, U- Fe_3O_4 @P demonstrates Fenton-like degradation for non-adsorbed cationic dyes. In practical applications, when exposed

to complex synthetic dye wastewater containing various inorganic salts, dissolved organic substances, and surfactants, U-Fe₃O₄@P rapidly and selectively adsorbs and separates anionic dyes while efficiently removing both anionic and cationic dyes. Additionally, its strong antibacterial activity effectively extends their lifespan, making them suitable for wastewater disinfection.

Efficient cesium removal from wastewater is crucial for the sustainable development of nuclear energy and public health yet challenging owing to high concentrations of competing sodium and potassium ions. As depicted in Figure 13d, Ma et al.³⁴⁴ addressed this issue by developing Zein@SA/KBS microspheres with exceptional Cs⁺ adsorption capacity. These microspheres demonstrate stable adsorption performance across varying pH conditions, outperforming most composite adsorbents in Cs⁺ removal while maintaining structural integrity. In fixed-bed experiments, Zein@SA/KBS microspheres exhibited outstanding adsorption efficiency for Cs⁺, reaching a maximum efficiency of 96.71%.

Furthermore, cellulose-based magnetic microspheres have emerged as sustainable alternatives for heavy metal and dye removal in wastewater treatment.^{345,346} Leveraging the natural abundance and biodegradability of cellulose, these composites integrate magnetic functionality with eco-compatibility.³⁴⁷ Inspired by this concept, Luo et al.³⁴⁸ engineered magnetic chitosan/cellulose microspheres (MCCM) by embedding γ -Fe₂O₃ nanoparticles within a biopolymer matrix. This system efficiently removed Cu²⁺, Cd²⁺, and Pb²⁺ (adsorption capacities = 88.2, 61.1, and 45.9 mg/g, respectively) while maintaining over 85% regeneration efficiency after 10 cycles using eco-friendly sodium citrate desorption. The superparamagnetic MCCM enabled rapid separation (<30 s) while preserving 94.4% porosity for enhanced ion diffusion. By integrating magnetic operability with the inherent biodegradability of cellulose, this approach minimizes secondary pollution risks.

5. SUMMARY AND OUTLOOK

SPMs represent a breakthrough in materials science, offering unparalleled adaptability and functionality across diverse fields, including biomedicine, environmental remediation, and smart technologies. Their ability for reversible transformations in response to external stimuli—such as temperature, pH, light, and magnetic fields—positions them as vital tools for addressing complex, real-world challenges. This review underscore their versatility, with diverse structural designs, including solid, porous, core-shell, and Janus microspheres, enabling precise control over their properties and behavior. These innovations have expanded their application potential, from targeted drug delivery to environmental sensing and advanced information encryption.

From a technological readiness perspective, stimuli-responsive microspheres currently span multiple technology readiness levels (TRLs) depending on their application domains. In biomedicine (e.g., drug delivery and tissue engineering), most systems operate at TRL 3–4 (lab-scale validation), with proof-of-concept demonstrations in cell cultures and small animal models. Advancing toward clinical translation (TRL 6–7) requires addressing long-term biocompatibility, scalable manufacturing, and regulatory compliance. Environmental applications (e.g., heavy metal adsorption and smart coatings) have progressed to TRL 5–6, with pilot-scale demonstrations showing adsorption efficiency of >700 mg/g for Cu²⁺ and

cyclic stability of >85% after 10 cycles. However, industrial adoption remains hindered by cost-effectiveness benchmarks. Meanwhile, emerging applications in microrobotics (e.g., dentinal tubule occlusion) and information encryption (e.g., thermoresponsive fluorescent pixels) are still in the early stages (TRL 2–3), requiring robust material integration strategies and reliability optimization under real-world conditions.

Despite notable progress, critical challenges persist. Scaling production while maintaining functionality and uniformity poses a major hurdle, particularly for industrial applications. Moreover, the development of multi-stimuli-responsive systems capable of interacting with complex environments will be essential for advancing precision medicine and adaptive environmental technologies. Biocompatibility and biodegradability are crucial for biomedical applications. While strides have been made in creating safe and effective materials, ensuring their degradation into nontoxic byproducts remains a priority. Advancements in natural polymer systems and synthetic routes will be key to meeting the rigorous demands of *in vivo* use. Sustainability is another pressing issue, as stimulus-responsive microspheres gain wide industrial adoption. The design of eco-friendly, recyclable materials and green synthesis processes will be paramount for ensuring their long-term environmental viability.

Future research should prioritize three directions to elevate TRL across applications: (1) cross-disciplinary collaborations to bridge the “valley of death” between TRL 4 and 6 for biomedical systems, emphasizing Good Manufacturing Practice (GMP)-compliant production (e.g., microfluidic encapsulation standardization) and toxicological profiling; (2) development of unified TRL assessment frameworks for stimuli-responsive materials, integrating metrics for scalability metrics (e.g., batch-to-batch consistency >95%), long-term stability (e.g., >1 year shelf life), and lifecycle environmental impacts (e.g., CO₂ footprint reduction); and (3) adoption of circular economy models for high-TRL applications, such as magnetically retrievable microspheres in wastewater treatment, aligning with industrial Environmental, Social, Governance criteria through closed-loop recycling (>90% recovery efficiency).

Looking forward, the integration of polymer science with cutting-edge technologies—such as nanotechnology, artificial intelligence, and bioengineering—will drive these materials to unprecedented levels of precision and efficiency. These synergies are expected to enable next-generation adaptive systems with a transformative impact across disciplines. In conclusion, SPMs hold immense promise, but realizing their full potential requires continued innovation in material design, scalable production, and sustainable practices. These materials are poised to redefine intelligent systems, shaping the future of advanced technologies and responsive applications.

AUTHOR INFORMATION

Corresponding Authors

Fenghua Zhang – Centre for Composite Materials and Structures, Harbin Institute of Technology (HIT), Harbin 150080, People's Republic of China; orcid.org/0000-0001-6136-9707; Email: fhzhang_hit@163.com

Jinsong Leng – Centre for Composite Materials and Structures, Harbin Institute of Technology (HIT), Harbin 150080, People's Republic of China; orcid.org/0000-0001-5098-9871; Email: lengjs@hit.edu.cn

Authors

Tao Guo – Centre for Composite Materials and Structures, Harbin Institute of Technology (HIT), Harbin 150080, People's Republic of China

Lan Luo – Centre for Composite Materials and Structures, Harbin Institute of Technology (HIT), Harbin 150080, People's Republic of China

Linlin Wang – Centre for Composite Materials and Structures, Harbin Institute of Technology (HIT), Harbin 150080, People's Republic of China

Yanju Liu – Department of Astronautic Science and Mechanics, Harbin Institute of Technology (HIT), Harbin 150001, People's Republic of China; orcid.org/0000-0001-8269-1594

Complete contact information is available at: <https://pubs.acs.org/10.1021/acsnano.5c00998>

Author Contributions

[†]T.G. and L.L. contributed equally to this work. F.Z., Y.L., and J.L. conceived the idea. T.G., L.L., F.Z., Y.L., and J.L. wrote the manuscript. L.W. made revisions to the manuscript of the article. All authors discussed the results and commented on the manuscript.

Funding

This work was supported by the National Natural Science Foundation of China (Grant 92271112) and the Heilongjiang Provincial Natural Science Foundation of China (Grant 2022ZX02C25).

Notes

The authors declare no competing financial interest.

VOCABULARY

Smart materials: materials that are manipulated to respond in a controllable and reversible way, modifying some of their properties as a result of external stimuli such as certain mechanical stress or a certain temperature, among others.

Polymer microspheres: microscopic, spherical particles composed of synthetic or natural polymers, typically ranging in size from tens of nanometers to several hundred micrometers in diameter.

Microstructures: small-scale physical and morphological features of a material, typically observed at the nanometer to micrometer scale.

Physical stimulus: a substance engineered to dynamically alter its physical, chemical, or mechanical properties in response to external physical stimuli, such as mechanical force, temperature, light, electric/magnetic fields, or acoustic waves.

Chemical stimulus: a substance designed to undergo controlled changes in its structure, properties, or functionality in response to specific chemical stimuli, such as pH, ionic strength, redox conditions, or the presence of particular molecules (e.g., enzymes, glucose, toxins).

Biological stimulus: a substance engineered to detect and respond to biological signals or entities, such as enzymes, antibodies, nucleic acids, cells, pathogens, or specific biomolecular interactions (e.g., antigen–antibody binding).

REFERENCES

- (1) Green, N. W.; Dennison, J. R. Deep Dielectric Charging of Spacecraft Polymers by Energetic Protons. *IEEE Trans. Plasma Sci.* **2008**, *36* (5), 2482–2490.
- (2) Natarajan, E.; Freitas, L. I.; Santhosh, M. S.; Markandan, K.; Majeed Al-Talib, A. A.; Hassan, C. S. Experimental and Numerical Analysis on Suitability of S-Glass-Carbon Fiber Reinforced Polymer Composites for Submarine Hull. *Def. Technol.* **2023**, *19*, 1–11.
- (3) Liu, F.; Wang, X. Synthetic Polymers for Organ 3D Printing. *Polymers* **2020**, *12* (8), 1765.
- (4) Zheng, X.-Y.; Li, T.; Cai, H.-W.; Wang, X.-H.; Sun, X.-L.; Wan, W.-M. Polymerization-Induced Emission of Borinic Acid towards Stimuli-Responsive Luminescent Polymers. *Polymer* **2024**, *300*, 126996.
- (5) Musarurwa, H.; Tawanda Tavengwa, N. Stimuli-Responsive Polymer-Based Aqueous Two-Phase Extraction of Analytes in Complex Matrices. *J. Mol. Liq.* **2022**, *360*, 119508.
- (6) Chikh Alard, I.; Soubhye, J.; Berger, G.; Gelbcke, M.; Spassov, S.; Amighi, K.; Goole, J.; Meyer, F. Triple-Stimuli Responsive Polymers with Fine Tuneable Magnetic Responses. *Polym. Chem.* **2017**, *8* (16), 2450–2456.
- (7) Peng, L.; Liu, S.; Feng, A.; Yuan, J. Polymeric Nanocarriers Based on Cyclodextrins for Drug Delivery: Host-Guest Interaction as Stimuli Responsive Linker. *Mol. Pharmaceutics* **2017**, *14* (8), 2475–2486.
- (8) Kim, J.; Park, J.; Jung, K.; Kim, E. J.; Tan, Z.; Xu, M.; Lee, Y. J.; Ku, K. H.; Kim, B. J. Light-Responsive Shape- and Color-Changing Block Copolymer Particles with Fast Switching Speed. *ACS Nano* **2024**, *18* (11), 8180–8189.
- (9) Islam, M. R.; Lu, Z.; Li, X.; Sarker, A. K.; Hu, L.; Choi, P.; Li, X.; Hakobyan, N.; Serpe, M. J. Responsive Polymers for Analytical Applications: A Review. *Anal. Chim. Acta* **2013**, *789*, 17–32.
- (10) Cao, Z.-Q.; Wang, G.-J. Multi-Stimuli-Responsive Polymer Materials: Particles, Films, and Bulk Gels. *Chem. Rec.* **2016**, *16* (3), 1398–1435.
- (11) Meng, H.; Li, G. Reversible Switching Transitions of Stimuli-Responsive Shape Changing Polymers. *J. Mater. Chem. A* **2013**, *1* (27), 7838–7845.
- (12) Tian, X.; Zhang, K.; Zhang, Y.; Wang, N.; Wang, H.; Xu, H.; Guang, S. Preparation and Mechanism Study of Hydrogen Bond Induced Enhanced Compositing Gelatin Microsphere Probe. *Int. J. Biol. Macromol.* **2024**, *266*, 130752.
- (13) Yang, A.-L.; Sun, S.-B.; Qu, L.-Y.; Li, X.-Y.; Liu, J.-L.; Zhou, F.; Xu, Y.-J. Polysaccharide Hydrogel Containing Silver Nanoparticle@Catechol Microspheres with Photothermal, Antibacterial and Anti-Inflammatory Activities for Infected-Wounds Repair. *Int. J. Biol. Macromol.* **2024**, *265*, 130898.
- (14) Tariq, A.; Arif, Z. U.; Khalid, M. Y.; Hossain, M.; Rasool, P. I.; Umer, R.; Ramakrishna, S. Recent Advances in the Additive Manufacturing of Stimuli-Responsive Soft Polymers. *Adv. Eng. Mater.* **2023**, *25* (21), 2301074.
- (15) He, R.; Sun, J.; Bai, X.; Lin, Q.; Yuan, Y.; Zhang, Y.; Dai, K.; Xu, Z. A Novel Alginate-Embedded Magnetic Biochar-Anoxygenic Photosynthetic Bacteria Composite Microspheres for Multipollutant Removal: Mechanisms of Photo-Bioelectrochemical Enhancement and Excellent Reusability Performance. *Environ. Res.* **2024**, *247*, 118158.
- (16) Yuan, Z.; Ding, J.; Zhang, Y.; Huang, B.; Song, Z.; Meng, X.; Ma, X.; Gong, X.; Huang, Z.; Ma, S.; Xiang, S.; Xu, W. Components, Mechanisms and Applications of Stimuli-Responsive Polymer Gels. *Eur. Polym. J.* **2022**, *177*, 111473.
- (17) Su, J.; Cao, Z.; Mao, Y.; Shen, W.; Wang, X.; Zhang, S.; Chen, Y.; Ge, X. Preparation of Eugenol/1-Methylcyclopropene Composite Microsphere by S/O/W Method and Study on the Postharvest Quality of Loquat. *J. Stored Prod. Res.* **2024**, *105*, 102252.
- (18) Sun, J.; Wei, Z.; Xue, C. Porous Gelatin Microspheres for High Loading and Improved Stability of Anthocyanins: Serving as Antioxidant Factors and Food Freshness Indicators. *Food Hydrocoll.* **2024**, *148*, 109494.
- (19) Kim, J. H.; Jeong, H.-S.; Hwang, J.; Kweon, D.-H.; Choi, C.-H.; Park, J. P. Affinity Peptide-Tethered Suspension Hydrogel Sensor for Selective and Sensitive Detection of Influenza Virus. *ACS Appl. Mater. Interfaces* **2023**, *15* (44), 52051–52064.

- (20) Wang, X.; Li, X.; Ou, G.; Shi, X.; Liu, Z. Morphological Transformation of Calcium Phenylphosphonate Microspheres Induced by Micellization of γ -Polyglutamic Acid. *J. Colloid Interface Sci.* **2019**, *556*, 33–46.
- (21) Zhou, L.; Xu, Z.; Hua, C.; Cao, H.; Qin, B.; Zhao, H.; Xie, Y. Facile Synthesis of Nitrogen and Sulfur Co-Doped Hollow Microsphere Polymers from Benzothiazole Containing Wastewater for Water Treatment. *Chemosphere* **2022**, *287*, 131982.
- (22) Guo, M.; Cao, X.; Meijer, E. W.; Dankers, P. Y. W. Core-Shell Capsules Based on Supramolecular Hydrogels Show Shell-Related Erosion and Release Due to Confinement. *Macromol. Biosci.* **2013**, *13* (1), 77–83.
- (23) Zhang, C.; Tang, J.; Liu, D.; Li, X.; Cheng, L.; Tang, X. Design and Evaluation of an Innovative Floating and Bioadhesive Multiparticulate Drug Delivery System Based on Hollow Structure. *Int. J. Pharm.* **2016**, *503* (1), 41–55.
- (24) Deng, W.; Guo, H.-C.; Li, G.-A.; Kan, C.-Y. Fabrication of Polymeric-Laponite Composite Hollow Microspheres via LBL Assembly. *Chin. Chem. Lett.* **2017**, *28* (2), 367–371.
- (25) Yu, B.; Xue, T.; Pang, L.; Zhang, X.; Shen, Y.; Cong, H. The Effect of Different Porogens on Porous PMMA Microspheres by Seed Swelling Polymerization and Its Application in High-Performance Liquid Chromatography. *Materials* **2018**, *11* (5), 705.
- (26) Li, P.; Li, K.; Niu, X.; Fan, Y. Electrospinning Magnetic-Fluorescent Bifunctional Janus PLGA Microspheres with Dual Rare Earth Ions Fluorescent-Labeling Drugs. *RSC Adv.* **2016**, *6* (101), 99034–99043.
- (27) Xia, T.; Wang, Y.; Awasthi, P.; Dong, W.; Li, M.; Qiao, X.; Chen, D.; Ling, S.; Fan, X. Strategies Towards Submicron Size and High-Performance Magnetic PGMA@Fe₃O₄@SiO₂-COOH Microspheres with Biological Application. *J. Inorg. Organomet. Polym. Mater.* **2024**, *34* (6), 2432–2444.
- (28) Zhang, Q.; Ma, X.; Du, X.; Song, P.; Xia, L. Silver-Nanoparticle-Coated Fe₃O₄/Chitosan Core-Shell Microspheres for Rapid and Ultrasensitive Detection of Thiram Using Surface Magnetic Solid-Phase Extraction-Surface-Enhanced Raman Scattering (SMSPE-SERS). *Sci. Total Environ.* **2024**, *914*, 170027.
- (29) Du, P.; Yang, H.; Zeng, J.; Liu, P. Folic Acid-Conjugated Temperature and pH Dual-Responsive Yolk/Shell Microspheres as a Drug Delivery System. *J. Mater. Chem. B* **2013**, *1* (39), 5298–5306.
- (30) Lin, Y. L.; Zhao, M. X.; Yu, Y. L.; Liu, S. L.; Li, M.; Jiang, A. L.; Deng, M. The Treatment of Oily Wastewater by Thermo-Responsive Calcium Alginate Capsules Immobilized *Pseudomonas aeruginosa*. *Water Environ. Res.* **2024**, *96* (4), No. e11022.
- (31) Shen, Y.; Xu, Y.; Yu, Z.; Chen, G.; Chen, B.; Liao, L. Multifunctional Injectable Microspheres Containing “Naturally-Derived” Photothermal Transducer for Synergistic Physical and Chemical Treating of Acute Osteomyelitis through Sequential Immunomodulation. *ACS Nano* **2024**, *18* (7), 5483–5497.
- (32) Chen, P.; Xiao, Q.; Guo, Z.; Liang, W.; Liu, O.; Lin, L.; Huang, Y.; Zhu, K.; Ye, G. Synthesis and Characterization of 3-in-1 Multifunctional Lipiodol-Doped Fe₃O₄@Poly(Diallyl Isophthalate) Microspheres for Arterial Embolization, Chemotherapy, and Imaging. *Biomed. Mater.* **2024**, *19* (3), 035011.
- (33) Chiang, W.-L.; Lin, T.-T.; Sureshbabu, R.; Chia, W.-T.; Hsiao, H.-C.; Liu, H.-Y.; Yang, C.-M.; Sung, H.-W. A Rapid Drug Release System with a NIR Light-Activated Molecular Switch for Dual-Modality Photothermal/Antibiotic Treatments of Subcutaneous Abscesses. *J. Controlled Release* **2015**, *199*, 53–62.
- (34) Villar-Alvarez, E.; Parron-Onate, S.; Wienskowska, O.; Carrascull-Marín, A.; Bellacanzone, C.; Lorenzo, J.; Ruiz-Molina, D.; Roscini, C. Multimodal HOCl-Responsive MEH-PPV Nanoparticles for Anti-Inflammatory Imaging and Therapy. *Sens. Actuators B Chem.* **2024**, *417*, 136150.
- (35) Yang, J.; Long, Q.; Zhu, Y.; Lin, C.; Xu, X.; Pan, B.; Shi, W.; Guo, Y.; Deng, J.; Yao, Q.; Wang, Z. Multifunctional Self-Assembled Adsorption Microspheres Based on Waste Bamboo Shoot Shells for Multi-Pollutant Water Purification. *Environ. Res.* **2024**, *249*, 118452.
- (36) Abdollahi, A.; Hanaei, N.; Rahmanidoust, M.; Dashti, A. Photoluminescent Janus Oxazolidine Nanoparticles for Development of Organic Light-Emitting Diodes, Anticounterfeiting, Information Encryption, and Optical Detection of Scratch. *J. Colloid Interface Sci.* **2023**, *630*, 242–256.
- (37) Sawant, A.; Kamath, S.; kg, H.; Kulyadi, G. P. Solid-in-Oil-in-Water Emulsion: An Innovative Paradigm to Improve Drug Stability and Biological Activity. *AAPS PharmSciTech* **2021**, *22* (1), 52.
- (38) Deliormanli, A. M.; Yenice, A. C. Preparation of Hollow PCL Microspheres by o/w Single Emulsion-Solvent Evaporation Method in the Presence of Graphene Nanopowders. *Express Polym. Lett.* **2021**, *15* (7), 641–653.
- (39) Wu, J.; Ding, J.; Xiao, B.; Chen, D.; Huang, D.; Ma, P.; Xiong, Z. A Facile Strategy for Controlling Porous PLGA Microspheres via o/w Emulsion Method. *J. Polym. Res.* **2022**, *29* (12), 508.
- (40) Li, X.; et al. Preparation of Ropivacaine Loaded PLGA Microspheres as Controlled-Release System with Narrow Size Distribution and High Loading Efficiency. *AAPS PharmSciTech* **2019**, *20* (8), 330.
- (41) Xu, J.; Bai, Y.; Li, X.; Wei, Z.; Sun, L.; Yu, H.; Xu, H. Porous Core/Dense Shell PLA Microspheres Embedded with High Drug Loading of Bupivacaine Crystals for Injectable Prolonged Release. *AAPS PharmSciTech* **2021**, *22* (1), 27.
- (42) Luo, P. P.; Li, J. D.; Zuo, Y.; Wu, X.; Li, Y. B. A Novel Antimicrobial Nano-Composite Porous Material for Bone Repair. *Mater. Sci. Forum* **2011**, *695*, 517–520.
- (43) Mei, Q.; Luo, P.; Zuo, Y.; Li, J.; Zou, Q.; Li, Y.; Jiang, D.; Wang, Y. Formulation and *In Vitro* Characterization of Rifampicin-Loaded Porous Poly(ϵ -Caprolactone) Microspheres for Sustained Skeletal Delivery. *Drug Des. Devel. Ther.* **2018**, *12*, 1533–1544.
- (44) Ji, J.; Deng, C.; Liu, X.; Qin, J. Fabrication of Porous Polyimide Hollow Microspheres through O/W/O Multiple Emulsion. *Colloids Surf. Physicochem. Eng. Asp.* **2020**, *591*, 124537.
- (45) Lin, J.; Wang, L.; Lin, J.; Liu, Q. Dual Delivery of TGF- β 3 and Ghrelin in Microsphere/Hydrogel Systems for Cartilage Regeneration. *Molecules* **2021**, *26* (19), 5732.
- (46) Park, H.; Ha, D.-H.; Ha, E.-S.; Kim, J.-S.; Kim, M.-S.; Hwang, S.-J. Effect of Stabilizers on Encapsulation Efficiency and Release Behavior of Exenatide-Loaded PLGA Microsphere Prepared by the W/O/W Solvent Evaporation Method. *Pharmaceutics* **2019**, *11* (12), 627.
- (47) Castellanos, I. J.; Cruz, G.; Crespo, R.; Griebenow, K. Encapsulation-Induced Aggregation and Loss in Activity of γ -Chymotrypsin and Their Prevention. *J. Controlled Release* **2002**, *81* (3), 307–319.
- (48) Sheikh Hasan, A.; Sapin, A.; Damgé, C.; Leroy, P.; Socha, M.; Maincent, P. Reduction of the *In Vivo* Burst Release of Insulin-Loaded Microparticles. *J. Drug Delivery Sci. Technol.* **2015**, *30*, 486–493.
- (49) Marquette, S.; Peerboom, C.; Yates, A.; Denis, L.; Goole, J.; Amighi, K. Encapsulation of Immunoglobulin G by Solid-in-Oil-in-Water: Effect of Process Parameters on Microsphere Properties. *Eur. J. Pharm. Biopharm.* **2014**, *86* (3), 393–403.
- (50) Chen, L.; Mei, L.; Feng, D.; Huang, D.; Tong, X.; Pan, X.; Zhu, C.; Wu, C. Anhydrous Reverse Micelle Lecithin Nanoparticles/PLGA Composite Microspheres for Long-Term Protein Delivery with Reduced Initial Burst. *Colloids Surf. B Biointerfaces* **2018**, *163*, 146–154.
- (51) Shi, N.-Q.; Zhou, J.; Walker, J.; Li, L.; Hong, J. K.Y.; Olsen, K. F.; Tang, J.; Ackermann, R.; Wang, Y.; Qin, B.; Schwendeman, A.; Schwendeman, S. P. Microencapsulation of Luteinizing Hormone-Releasing Hormone Agonist in Poly(Lactic-co-Glycolic Acid) Microspheres by Spray-Drying. *J. Controlled Release* **2020**, *321*, 756–772.
- (52) Rassu, G.; Gavini, E.; Spada, G.; Giunchedi, P.; Marceddu, S. Ketoprofen Spray-Dried Microspheres Based on Eudragit® RS and RL: Study of the Manufacturing Parameters. *Drug Dev. Ind. Pharm.* **2008**, *34* (11), 1178–1187.
- (53) Zhang, Z.; Li, L.; Sun, D.; Wang, M.; Shi, J.; Yang, D.; Wang, L.; Zou, S. Preparation and Properties of Chitosan-Based Microspheres by Spray Drying. *Food Sci. Nutr.* **2020**, *8* (4), 1933–1941.

- (54) França, D.; Medina, Â. F.; Messa, L. L.; Souza, C. F.; Faez, R. Chitosan Spray-Dried Microcapsule and Microsphere as Fertilizer Host for Swellable-Controlled Release Materials. *Carbohydr. Polym.* **2018**, *196*, 47–55.
- (55) Wei, H.; Li, W.; Chen, H.; Wen, X.; He, J.; Li, J. Simultaneous Diels-Alder Click Reaction and Starch Hydrogel Microsphere Production via Spray Drying. *Carbohydr. Polym.* **2020**, *241*, 116351.
- (56) Johansen, P.; Merkle, H. P.; Gander, B. Technological Considerations Related to the Up-Scaling of Protein Microencapsulation by Spray-Drying. *Eur. J. Pharm. Biopharm.* **2000**, *50* (3), 413–417.
- (57) Whitesides, G. M. The Origins and the Future of Microfluidics. *Nature* **2006**, *442* (7101), 368–373.
- (58) Zhang, M.; Guo, W.; Ren, M.; Ren, X. Fabrication of Porous Cellulose Microspheres with Controllable Structures by Microfluidic and Flash Freezing Method. *Mater. Lett.* **2020**, *262*, 127193.
- (59) Su, Y.; Liu, J.; Tan, S.; Liu, W.; Wang, R.; Chen, C. PLGA Sustained-Release Microspheres Loaded with an Insoluble Small-Molecule Drug: Microfluidic-Based Preparation, Optimization, Characterization, and Evaluation *In Vitro* and *In Vivo*. *Drug Delivery* **2022**, *29* (1), 1437–1446.
- (60) Utada, A. S.; Lorenceau, E.; Link, D. R.; Kaplan, P. D.; Stone, H. A.; Weitz, D. A. Monodisperse Double Emulsions Generated from a Microcapillary Device. *Science* **2005**, *308* (5721), 537–541.
- (61) Abate, A. R.; Weitz, D. A. High-Order Multiple Emulsions Formed in Poly(Dimethylsiloxane) Microfluidics. *Small* **2009**, *5* (18), 2030–2032.
- (62) Adams, L. L. A.; Kodger, T. E.; Kim, S.-H.; Shum, H. C.; Franke, T.; Weitz, D. A. Single Step Emulsification for the Generation of Multi-Component Double Emulsions. *Soft Matter* **2012**, *8* (41), 10719–10724.
- (63) Zhao, Y.; Gu, H.; Xie, Z.; Shum, H. C.; Wang, B.; Gu, Z. Bioinspired Multifunctional Janus Particles for Droplet Manipulation. *J. Am. Chem. Soc.* **2013**, *135* (1), 54–57.
- (64) Kim, C. M.; Park, S. J.; Kim, G. M. Applications of PLGA Microcarriers Prepared Using Geometrically Passive Breakup on Microfluidic Chip. *Int. J. Precis. Eng. Manuf.* **2015**, *16* (12), 2545–2551.
- (65) Zhu, L.; Li, Y.; Zhang, Q.; Wang, H.; Zhu, M. Fabrication of Monodisperse, Large-Sized, Functional Biopolymeric Microspheres Using a Low-Cost and Facile Microfluidic Device. *Biomed. Microdevices* **2010**, *12* (1), 169–177.
- (66) Wang, X.; Zuo, X.; Wang, J.; Zhang, W.; Xu, H.; Wang, D.; Zhang, Y.; Zhao, T. Experimental Investigation on Electrostatic Breakup Characteristics of Non-Newtonian Zeolite Molecular Sieve Suspension Fluid. *Chem. Eng. Sci.* **2022**, *253*, 117506.
- (67) Lu, Z.; Zhou, Y.; Liu, B. Preparation of Chitosan Microcarriers by High Voltage Electrostatic Field and Freeze Drying. *J. Biosci. Bioeng.* **2019**, *128* (4), 504–509.
- (68) Ma, L.; Liu, C. Preparation of Chitosan Microspheres by Ionotropic Gelation under a High Voltage Electrostatic Field for Protein Delivery. *Colloids Surf. B Biointerfaces* **2010**, *75* (2), 448–453.
- (69) Kuo, S. M.; Niu, G. C.; Chang, S. J.; Kuo, C. H.; Bair, M. S. A One-Step Method for Fabricating Chitosan Microspheres. *J. Appl. Polym. Sci.* **2004**, *94* (5), 2150–2157.
- (70) Li, C.; Li, L.; Ma, R.; Wang, Z.; Shi, X.; Yang, X.; Wang, Y.; Zhang, P. Preparation of Polycarbonate/Gelatine Microspheres Using a High-Voltage Electrostatic Technique for Enhancing the Adhesion and Proliferation of Mesenchymal Stem Cells. *J. Mater. Sci.* **2019**, *54* (9), 7180–7197.
- (71) Han, S.; Dwivedi, P.; Mangrio, F. A.; Dwivedi, M.; Khatik, R.; Cohn, D. E.; Si, T.; Xu, R. X. Sustained Release Paclitaxel-Loaded Core-Shell-Structured Solid Lipid Microparticles for Intraperitoneal Chemotherapy of Ovarian Cancer. *Artif. Cells Nanomed. Biotechnol.* **2019**, *47* (1), 957–967.
- (72) Liang, X.; Xie, L.; Zhang, Q.; Wang, G.; Zhang, S.; Jiang, M.; Zhang, R.; Yang, T.; Hu, X.; Yang, Z.; Tian, W. Gelatin Methacryloyl-Alginate Core-Shell Microcapsules as Efficient Delivery Platforms for Prevascularized Microtissues in Endodontic Regeneration. *Acta Biomater.* **2022**, *144*, 242–257.
- (73) Charcosset, C.; Limayem, I.; Fessi, H. The Membrane Emulsification Process—A Review. *J. Chem. Technol. Biotechnol.* **2004**, *79* (3), 209–218.
- (74) Vladislavjević, G. T.; Kobayashi, I.; Nakajima, M. Production of Uniform Droplets Using Membrane, Microchannel and Microfluidic Emulsification Devices. *Microfluid. Nanofluidics* **2012**, *13* (1), 151–178.
- (75) Zhou, Q.-Z.; Ma, G.-H.; Su, Z.-G. Effect of Membrane Parameters on the Size and Uniformity in Preparing Agarose Beads by Premix Membrane Emulsification. *J. Membr. Sci.* **2009**, *326* (2), 694–700.
- (76) Mi, Y.; Zhou, W.; Li, Q.; Gong, F.; Zhang, R.; Ma, G.; Su, Z. Preparation of Water-in-Oil Emulsions Using a Hydrophobic Polymer Membrane with 3D Bicontinuous Skeleton Structure. *J. Membr. Sci.* **2015**, *490*, 113–119.
- (77) Vladislavjevic, G. Influence of Process Parameters on Droplet Size Distribution in SPG Membrane Emulsification and Stability of Prepared Emulsion Droplets. *J. Membr. Sci.* **2003**, *225* (1–2), 15–23.
- (78) Oh, D. H.; Balakrishnan, P.; Oh, Y.-K.; Kim, D.-D.; Yong, C. S.; Choi, H.-G. Effect of Process Parameters on Nanoemulsion Droplet Size and Distribution in SPG Membrane Emulsification. *Int. J. Pharm.* **2011**, *404* (1–2), 191–197.
- (79) Yuyama, H.; Watanabe, T.; Ma, G.-H.; Nagai, M.; Omi, S. Preparation and Analysis of Uniform Emulsion Droplets Using SPG Membrane Emulsification Technique. *Colloids Surf. Physicochem. Eng. Asp.* **2000**, *168* (2), 159–174.
- (80) Nauman, N.; Zaquen, N.; Junkers, T.; Boyer, C.; Zetterlund, P. B. Particle Size Control in Miniemulsion Polymerization via Membrane Emulsification. *Macromolecules* **2019**, *52* (12), 4492–4499.
- (81) Sundberg, D. Structured, Composite Nanoparticles from Emulsion Polymerization - Morphological Possibilities. *Biomacromolecules* **2020**, *21* (11), 4388–4395.
- (82) Chen, H.; Zhou, J.; Deng, J. Helical Polymer/Fe₃O₄ NPs Constructing Optically Active, Magnetic Core/Shell Microspheres: Preparation by Emulsion Polymerization and Recycling Application in Enantioselective Crystallization. *Polym. Chem.* **2016**, *7* (1), 125–134.
- (83) Zhu, Y.; Wu, G. Preparation of Monodisperse Polystyrene Nanoparticles with Tunable Sizes Based on Soap-Free Emulsion Polymerization Technology. *Colloid Polym. Sci.* **2021**, *299* (1), 73–79.
- (84) Ishihara, M.; Kaeda, T.; Sasaki, T. Silica/Polymer Core-Shell Particles Prepared via Soap-Free Emulsion Polymerization. *e-Polym.* **2020**, *20* (1), 254–261.
- (85) Abdollahi, A.; Roghani-Mamaqani, H.; Salami-Kalajahi, M. Morphology Evolution of Functionalized Styrene and Methyl Methacrylate Copolymer Latex Nanoparticles by One-Step Emulsifier-Free Emulsion Polymerization. *Eur. Polym. J.* **2020**, *133*, 109790.
- (86) Yang, B.; Xu, L.; Liu, Y.; Liu, B.; Zhang, M. Preparation of Monodisperse Polystyrene Microspheres with Different Functional Groups Using Soap-Free Emulsion Polymerization. *Colloid Polym. Sci.* **2021**, *299* (7), 1095–1102.
- (87) Gharieh, A.; Khoei, S.; Mahdavian, A. R. Emulsion and Miniemulsion Techniques in Preparation of Polymer Nanoparticles with Versatile Characteristics. *Adv. Colloid Interface Sci.* **2019**, *269*, 152–186.
- (88) Cordeiro, A. P.; Feuser, P. E.; Araújo, P. H. H.; Sayer, C. Encapsulation of Magnetic Nanoparticles and Copaiba Oil in Poly(Methyl Methacrylate) Nanoparticles via Miniemulsion Polymerization for Biomedical Application. *Macromol. Symp.* **2020**, *394* (1), 2000112.
- (89) Mangia, L. H. R.; Ferraz, H. C.; Souza, R. S. D.; Pereira, M. C. S.; Pinto, J. C. *In Situ* Encapsulation of Rivastigmine in TAT-Functionalized P(MMA-Co-AA) Nanoparticles through Miniemulsion Polymerization. *Colloids Surf. Physicochem. Eng. Asp.* **2021**, *624*, 126776.

- (90) Orowitz, T. E.; Ana Sombo, P. P. A. A.; Rahayu, D.; Hasanah, A. N. Microsphere Polymers in Molecular Imprinting: Current and Future Perspectives. *Molecules* **2020**, *25* (14), 3256.
- (91) Abd El-Mageed, A. I. A.; Dyab, A. K. F.; Mohamed, L. A.; Taha, F.; Essawy, H. A. Suspension Polymerization for Fabrication of Magnetic Polystyrene Microspheres Stabilized with Hitenol BC-20. *Polym. Bull.* **2022**, *79* (5), 3379–3393.
- (92) Glasing, J.; Jessop, P. G.; Champagne, P.; Hamad, W. Y.; Cunningham, M. F. Microsuspension Polymerization of Styrene Using Cellulose Nanocrystals as Pickering Emulsifiers: On the Evolution of Latex Particles. *Langmuir* **2020**, *36* (3), 796–809.
- (93) Li, K.; Stöver, H. D. H. Synthesis of Monodisperse Poly(Divinylbenzene) Microspheres. *J. Polym. Sci. Part A Polym. Chem.* **1993**, *31* (13), 3257–3263.
- (94) Li, W.-H.; Stöver, H. D. H. Monodisperse Cross-Linked Core-Shell Polymer Microspheres by Precipitation Polymerization. *Macromolecules* **2000**, *33* (12), 4354–4360.
- (95) Zhang, D.; Liu, J.; Liu, T.; Yang, X. Synthesis of Superhydrophobic Fluorinated Polystyrene Microspheres via Distillation Precipitation Polymerization. *Colloid Polym. Sci.* **2015**, *293* (6), 1799–1807.
- (96) Wang, F.; Zhang, Y.; Yang, P.; Jin, S.; Yu, M.; Guo, J.; Wang, C. Fabrication of Polymeric Microgels Using Reflux-Precipitation Polymerization and Its Application for Phosphoprotein Enrichment. *J. Mater. Chem. B* **2014**, *2* (17), 2575–2581.
- (97) Zhang, J.; Ding, X.; Peng, Y.; Mang, W. Magnetic Polymer Microsphere with Photoconductivity: Preparation and Characterization of Iron(III) Phthalocyanine Covalently Bonded on to Polystyrene Microsphere Surface. *Polym. Int.* **2002**, *51* (7), 617–621.
- (98) Fan, L.-H.; Luo, Y.-L.; Chen, Y.-S.; Zhang, C.-H.; Wei, Q.-B. Preparation and Characterization of Fe₃O₄ Magnetic Composite Microspheres Covered by a P(MAH-Co-MAA) Copolymer. *J. Nanopart. Res.* **2009**, *11* (2), 449–458.
- (99) Zhu, M.-Q.; Chen, G.-C.; Li, Y.-M.; Fan, J.-B.; Zhu, M.-F.; Tang, Z. One-Step Template-Free Synthesis of Monoporous Polymer Microspheres with Uniform Sizes via Microwave-Mediated Dispersion Polymerization. *Nanoscale* **2011**, *3* (11), 4608–4612.
- (100) Geng, G. Q.; Liu, X. J.; Bian, G. X. Study on Preparation of Silica Aerogels/Polystyrene Microspheres with Core-Shell Structure. *Mater. Sci. Forum* **2010**, *658*, 93–96.
- (101) Xu, Z. S.; Deng, Z. W.; Hu, X. X.; Li, L.; Yi, C. F. Monodisperse Polystyrene Microspheres Prepared by Dispersion Polymerization with Microwave Irradiation. *J. Polym. Sci. Part A Polym. Chem.* **2005**, *43* (11), 2368–2376.
- (102) Deng, Z. W.; Xu, Z. S.; Yi, C. F. Preparation of Monodisperse Polystyrene-g-Poly(Ethylene Oxide) Microspheres by Microwave Dispersion Polymerization. *Acta Polym. Sin.* **2006**, *006* (1), 185–188.
- (103) Yu, B.; Xue, T.; Pang, L.; Zhang, X.; Shen, Y.; Cong, H. The Effect of Different Porogens on Porous PMMA Microspheres by Seed Swelling Polymerization and Its Application in High-Performance Liquid Chromatography. *Materials* **2018**, *11* (5), 705.
- (104) Cong, H.; Yu, B.; Gao, L.; Yang, B.; Gao, F.; Zhang, H.; Liu, Y. Preparation of Morphology-Controllable PGMA-DVB Microspheres by Introducing Span 80 into Seed Emulsion Polymerization. *RSC Adv.* **2018**, *8* (5), 2593–2598.
- (105) Kao, Y.-C.; Whang, W.-T.; Chen, Y.-C.; Chen, K.-C. Effect of Crosslinking Agents on the Dispersive Behaviour of Polymer Particles in Seed Swelling Polymerisation. *J. Ind. Eng. Chem.* **2017**, *51*, 216–222.
- (106) Yang, M.; Guo, Y.; Wu, Q.; Luan, Y.; Wang, G. Synthesis and Properties of Amphiphilic Nonspherical SPS/PS Composite Particles by Multi-Step Seeded Swelling Polymerization. *Polymer* **2014**, *55* (8), 1948–1954.
- (107) Yuan, W.; Cai, Y.; Chen, Y.; Hong, X.; Liu, Z. Porous Microsphere and Its Applications. *Int. J. Nanomedicine* **2013**, *8*, 1111–1120.
- (108) Ghosh Dastidar, D.; Saha, S.; Chowdhury, M. Porous Microspheres: Synthesis, Characterisation and Applications in Pharmaceutical & Medical Fields. *Int. J. Pharm.* **2018**, *548* (1), 34–48.
- (109) Tian, Q.; Yu, D.; Zhu, K.; Hu, G.; Zhang, L.; Liu, Y. Multi-Hollow Polymer Microspheres with Enclosed Surfaces and Compartmentalized Voids Prepared by Seeded Swelling Polymerization Method. *J. Colloid Interface Sci.* **2016**, *473*, 44–51.
- (110) Zhang, L.; Zhang, B.; Yu, R.; Wu, S.; Han, S.; Tang, R.; Zhao, R.; Kong, X. Simulation of *In Vitro* Embolization Effect of Drug-Loaded Microspheres. *Mater. Today Commun.* **2024**, *40*, 109649.
- (111) Liu, X.; Jin, X.; Ma, P. X. Nanofibrous Hollow Microspheres Self-Assembled from Star-Shaped Polymers as Injectable Cell Carriers for Knee Repair. *Nat. Mater.* **2011**, *10* (5), 398–406.
- (112) Song, L.; Sun, L.; Jiang, N.; Gan, Z. Structural Control and Hemostatic Properties of Porous Microspheres Fabricated by Hydroxyapatite-Graft-Poly(D,L-Lactide) Nanocomposites. *Compos. Sci. Technol.* **2016**, *134*, 234–241.
- (113) Ren, P.-W.; Ju, X.-J.; Xie, R.; Chu, L.-Y. Monodisperse Alginate Microcapsules with Oil Core Generated from a Microfluidic Device. *J. Colloid Interface Sci.* **2010**, *343* (1), 392–395.
- (114) Li, X.; Gao, D.; Liu, M.; Zheng, L.; Li, P.; Lyu, B. Synthesis of Amphiphilic Janus SiO₂/Styrene Butyl Acrylate Polymer Microspheres and Their Application in Oil Recovery. *Colloids Surf. A Physicochem. Eng. Asp.* **2023**, *675*, 132076.
- (115) Ryu, W. H.; Vyakarnam, M.; Greco, R. S.; Prinz, F. B.; Fasching, R. J. Fabrication of Multi-Layered Biodegradable Drug Delivery Device Based on Micro-Structuring of PLGA Polymers. *Biomed. Microdevices* **2007**, *9* (6), 845–853.
- (116) Mu, B.; Liu, P.; Li, X.; Du, P.; Dong, Y.; Wang, Y. Fabrication of Flocculation-Resistant pH/Ionic Strength/Temperature Multi-responsive Hollow Microspheres and Their Controlled Release. *Mol. Pharmaceutics* **2012**, *9* (1), 91–101.
- (117) Xiong, B.; Chen, Y.; Liu, Y.; Hu, X.; Han, H.; Li, Q. Artesunate-Loaded Porous PLGA Microsphere as a Pulmonary Delivery System for the Treatment of Non-Small Cell Lung Cancer. *Colloids Surf. B Biointerfaces* **2021**, *206*, 111937.
- (118) Liu, Y.-M.; Ju, X.-J.; Xin, Y.; Zheng, W.-C.; Wang, W.; Wei, J.; Xie, R.; Liu, Z.; Chu, L.-Y. A Novel Smart Microsphere with Magnetic Core and Ion-Recognizable Shell for Pb²⁺ Adsorption and Separation. *ACS Appl. Mater. Interfaces* **2014**, *6* (12), 9530–9542.
- (119) Wang, S.; Shi, X.; Gan, Z.; Wang, F. Preparation of PLGA Microspheres with Different Porous Morphologies. *Chin. J. Polym. Sci.* **2015**, *33* (1), 128–136.
- (120) Ji, S.; Srivastava, D.; Parker, N. J.; Lee, I. Transitional Behavior of Polymeric Hollow Microsphere Formation in Turbulent Shear Flow by Emulsion Diffusion Method. *Polymer* **2012**, *53* (1), 205–212.
- (121) Xie, X.; Wang, Y.; Xiong, Z.; Li, H.; Yao, C. Highly Efficient Removal of Uranium(VI) from Aqueous Solution Using Poly-(Cyclotriphosphazene-Co-Polyethyleneimine) Microspheres. *J. Radioanal. Nucl. Chem.* **2020**, *326* (3), 1867–1877.
- (122) Ma, Y.; Hou, C.; Zhang, H.; Zhang, H.; Zhang, Q. Synthesis of PANI Solid Microspheres with Convex-Fold Surface via Using Polyvinylpyrrolidone Micellar Template. *Synth. Met.* **2016**, *222*, 388–392.
- (123) Schnieders, J.; Gbureck, U.; Thull, R.; Kissel, T. Controlled Release of Gentamicin from Calcium Phosphate-Poly(Lactic Acid-Co-Glycolic Acid) Composite Bone Cement. *Biomaterials* **2006**, *27* (23), 4239–4249.
- (124) Chang, M. W.; Stride, E.; Edirisinghe, M. A New Method for the Preparation of Monoporous Hollow Microspheres. *Langmuir* **2010**, *26* (7), 5115–5121.
- (125) Parvate, S.; Dixit, P.; Chattopadhyay, S. Hierarchical Polymeric Hollow Microspheres with Size Tunable Single Holes and Their Application as Catalytic Microreactor. *Colloid Polym. Sci.* **2022**, *300* (9), 1101–1109.
- (126) Contaldi, V.; Imperato, L.; Orsi, S.; Di Maio, E.; Netti, P. A.; Iannace, S. Morphology Modulation of Gas-Foamed, Micrometric, Hollow Polystyrene Particles. *J. Appl. Polym. Sci.* **2016**, *133* (48), n/a.
- (127) Brand, T.; Ratinac, K.; Castro, J. V.; Gilbert, R. G. Hollow Latex Particles as Submicrometer Reactors for Polymerization in

- Confined Geometries. *J. Polym. Sci. Part A Polym. Chem.* **2004**, *42* (22), 5706–5713.
- (128) Du, P.; Zeng, J.; Mu, B.; Liu, P. Biocompatible Magnetic and Molecular Dual-Targeting Polyelectrolyte Hybrid Hollow Microspheres for Controlled Drug Release. *Mol. Pharmaceutics* **2013**, *10* (5), 1705–1715.
- (129) Shi, X.-D.; Sun, P.-J.; Gan, Z.-H. Preparation of Porous Polylactide Microspheres and Their Application in Tissue Engineering. *Chin. J. Polym. Sci.* **2018**, *36* (6), 712–719.
- (130) Song, W.; Tong, T.; Xu, J.; Wu, N.; Ren, L.; Li, M.; Tong, J. Preparation and Application of Green Chitosan/Poly(Vinyl Alcohol) Porous Microspheres for the Removal of Hexavalent Chromium. *Mater. Sci. Eng., B* **2022**, *284*, 115922.
- (131) Ding, Q.; Zha, R.; He, X.; Sun, A.; Shi, K.; Qu, Y.; Qian, Z. A Novel Injectable Fibroblasts-Porous PDLA Microspheres/Collagen Gel Composite for Soft-Tissue Augmentation. *Prog. Nat. Sci. Mater. Int.* **2020**, *30* (5), 651–660.
- (132) Yuan, Y.; Shi, X.; Gan, Z.; Wang, F. Modification of Porous PLGA Microspheres by Poly-L-Lysine for Use as Tissue Engineering Scaffolds. *Colloids Surf. B Biointerfaces* **2018**, *161*, 162–168.
- (133) Zhang, F.; Wu, W.; Zhang, X.; Meng, X.; Tong, G.; Deng, Y. Temperature-Sensitive Poly-NIPAm Modified Cellulose Nanofibril Cryogel Microspheres for Controlled Drug Release. *Cellulose* **2016**, *23* (1), 415–425.
- (134) Ren, L.; Xu, J.; Zhang, Y.; Zhou, J.; Chen, D.; Chang, Z. Preparation and Characterization of Porous Chitosan Microspheres and Adsorption Performance for Hexavalent Chromium. *Int. J. Biol. Macromol.* **2019**, *135*, 898–906.
- (135) Cheng, J.; Zhao, N.; Zhang, Y.; Huang, Y.; Huang, Q.; Xiao, C. Facile Preparation of PMMA@PLA Core-Shell Microspheres by PTFE Membrane Emulsification. *J. Membr. Sci.* **2022**, *644*, 120178.
- (136) Wu, J.; Kong, T.; Yeung, K. W. K.; Shum, H. C.; Cheung, K. M. C.; Wang, L.; To, M. K. T. Fabrication and Characterization of Monodisperse PLGA-Alginate Core-Shell Microspheres with Monodisperse Size and Homogeneous Shells for Controlled Drug Release. *Acta Biomater.* **2013**, *9* (7), 7410–7419.
- (137) Wen, F.; Zhang, W.; Zheng, P.; Zhang, X.; Yang, X.; Wang, Y.; Jiang, X.; Wei, G.; Shi, L. One-Stage Synthesis of Narrowly Dispersed Polymeric Core-Shell Microspheres. *J. Polym. Sci. Part A Polym. Chem.* **2008**, *46* (4), 1192–1202.
- (138) Windbergs, M.; Zhao, Y.; Heyman, J.; Weitz, D. A. Biodegradable Core-Shell Carriers for Simultaneous Encapsulation of Synergistic Actives. *J. Am. Chem. Soc.* **2013**, *135* (21), 7933–7937.
- (139) Zhang, Z.; He, X.; Yan, T.; He, Y.; Zeng, C.; Guo, S.; Li, Q.; Xia, H. Preparation of Gelatin-Starch Shell-Yolk Microspheres by Water-in-Water Emulsion Method: Effects of Starch Crystal Type and Cross-Linking. *Food Hydrocoll.* **2024**, *154*, 110134.
- (140) Nie, H.; Dong, Z.; Arifin, D. Y.; Hu, Y.; Wang, C. H. Core/Shell Microspheres via Coaxial Electrohydrodynamic Atomization for Sequential and Parallel Release of Drugs. *J. Biomed. Mater. Res., Part A* **2010**, *95A* (3), 709–716.
- (141) Xiao, C.-D.; Shen, X.-C.; Tao, L. Modified Emulsion Solvent Evaporation Method for Fabricating Core-Shell Microspheres. *Int. J. Pharm.* **2013**, *452* (1), 227–232.
- (142) Cui, Y.; Wang, Y.; Wu, J.; He, X.; Xuan, S.; Gong, X. Magneto-Thermochromic Coupling Janus Sphere for Dual Response Display. *RSC Adv.* **2019**, *9* (31), 17959–17966.
- (143) Lone, S.; Kim, S. H.; Nam, S. W.; Park, S.; Joo, J.; Cheong, I. W. Microfluidic Synthesis of Janus Particles by UV-Directed Phase Separation. *Chem. Commun.* **2011**, *47* (9), 2634–2636.
- (144) Li, K.; Li, P.; Jia, Z.; Qi, B.; Xu, J.; Kang, D.; Liu, M.; Fan, Y. Enhanced Fluorescent Intensity of Magnetic-Fluorescent Bifunctional PLGA Microspheres Based on Janus Electrospinning for Bioapplication. *Sci. Rep.* **2018**, *8* (1), 17117.
- (145) Wang, L.; Yu, L.; Zeng, C.; Wang, C.; Zhang, L. Fabrication of PAA-PETPTA Janus Microspheres with Respiratory Function for Controlled Release of Guests with Different Sizes. *Langmuir* **2018**, *34* (24), 7106–7116.
- (146) Xie, W.; Zhou, C.; Zhang, X.; Du, S.; Wang, W.; Wang, H.; Zhang, Z. Large-Scale Synthesis of Uniform and Shape-Tunable ZnO/Polysiloxane Janus Micromotors Powered by Visible Light and Pure Water. *ChemNanoMat* **2020**, *6* (12), 1749–1753.
- (147) Thomas, R. G.; Unnithan, A. R.; Moon, M. J.; Surendran, S. P.; Batgerel, T.; Park, C. H.; Kim, C. S.; Jeong, Y. Y. Electromagnetic Manipulation Enabled Calcium Alginate Janus Microsphere for Targeted Delivery of Mesenchymal Stem Cells. *Int. J. Biol. Macromol.* **2018**, *110*, 465–471.
- (148) Lee, W. L.; Widjaja, E.; Loo, S. C. J. One-Step Fabrication of Triple-Layered Polymeric Microparticles with Layer Localization of Drugs as a Novel Drug-Delivery System. *Small* **2010**, *6* (9), 1003–1011.
- (149) Xia, H.; Li, A.; Man, J.; Li, J.; Li, J. Fabrication of Multi-Layered Microspheres Based on Phase Separation for Drug Delivery. *Micromachines* **2021**, *12* (6), 723.
- (150) Szczepanowicz, K.; Hoel, H. J.; Szyk-Warszynska, L.; Bielańska, E.; Bouzga, A. M.; Gaudernack, G.; Simon, C.; Warszynski, P. Formation of Biocompatible Nanocapsules with Emulsion Core and PEGylated Shell by Polyelectrolyte Multilayer Adsorption. *Langmuir* **2010**, *26* (16), 12592–12597.
- (151) Haase, M. F.; Brujic, J. Tailoring of High-Order Multiple Emulsions by the Liquid-Liquid Phase Separation of Ternary Mixtures. *Angew. Chem., Int. Ed.* **2014**, *53* (44), 11793–11797.
- (152) Dwivedi, P.; Han, S.; Mangrino, F.; Fan, R.; Dwivedi, M.; Zhu, Z.; Huang, F.; Wu, Q.; Khatik, R.; Cohn, D. E.; Si, T.; Hu, S.; Sparreboom, A.; Xu, R. X. Engineered Multifunctional Biodegradable Hybrid Microparticles for Paclitaxel Delivery in Cancer Therapy. *Mater. Sci. Eng., C* **2019**, *102*, 113–123.
- (153) Li, W.; Liu, Y.; Leng, J. Harnessing Wrinkling Patterns Using Shape Memory Polymer Microparticles. *ACS Appl. Mater. Interfaces* **2021**, *13* (19), 23074–23080.
- (154) Zhang, F.; Wang, L.; Geng, Q.; Liu, Y.; Leng, J.; Smoukov, S. K. Adjustable Volume and Loading Release of Shape Memory Polymer Microcapsules. *Int. J. Smart Nano Mater.* **2023**, *14* (1), 77–89.
- (155) Chen, D.; Chen, H.; Bei, J.; Wang, S. Morphology and Biodegradation of Microspheres of Polyester-Polyether Block Copolymer Based on Polycaprolactone/Poly(lactide)/Poly(Ethylene Oxide). *Polym. Int.* **2000**, *49* (3), 269–276.
- (156) Anande, N. M.; Jain, S. K.; Jain, N. K. Con-A Conjugated Mucoadhesive Microspheres for the Colonic Delivery of Diloxanide Furoate. *Int. J. Pharm.* **2008**, *359* (1–2), 182–189.
- (157) Mi, F.-L.; Wong, T.-B.; Shyu, S.-S.; Chang, S.-F. Chitosan Microspheres: Modification of Polymeric Chem-Physical Properties of Spray-Dried Microspheres to Control the Release of Antibiotic Drug. *J. Appl. Polym. Sci.* **1999**, *71* (5), 747–759.
- (158) Fu, Y.-J.; Shyu, S.-S.; Su, F.-H.; Yu, P.-C. Development of Biodegradable Co-Poly(d,l-Lactic/Glycolic Acid) Microspheres for the Controlled Release of 5-FU by the Spray Drying Method. *Colloids Surf. B Biointerfaces* **2002**, *25* (4), 269–279.
- (159) Zhao, Q.; Cui, H.; Wang, Y.; Du, X. Microfluidic Platforms toward Rational Material Fabrication for Biomedical Applications. *Small* **2020**, *16* (9), 1903798.
- (160) Qiao, S.; Chen, W.; Zheng, X.; Ma, L. Preparation of pH-Sensitive Alginate-Based Hydrogel by Microfluidic Technology for Intestinal Targeting Drug Delivery. *Int. J. Biol. Macromol.* **2024**, *254*, 127649.
- (161) Zhang, X.; Zhu, R.; Wang, X.; Wang, H.; Xu, Z.; Wang, Y.; Quan, D.; Shen, L. Core-Shell Microspheres Prepared Using Coaxial Electrostatic Spray for Local Chemotherapy of Solid Tumors. *Pharmaceutics* **2023**, *16* (1), 45.
- (162) Fukui, Y.; Maruyama, T.; Iwamatsu, Y.; Fujii, A.; Tanaka, T.; Ohmukai, Y.; Matsuyama, H. Preparation of Monodispersed Polyelectrolyte Microcapsules with High Encapsulation Efficiency by an Electro Spray Technique. *Colloids Surf. Physicochem. Eng. Asp.* **2010**, *370* (1–3), 28–34.

- (163) Bux, J.; Manga, M. S.; Hunter, T. N.; Biggs, S. Manufacture of Poly(Methyl Methacrylate) Microspheres Using Membrane Emulsification. *Philos. Trans. R. Soc. A* **2016**, *374* (2072), 20150134.
- (164) Wu, J.; Wei, W.; Wang, L.-Y.; Su, Z.-G.; Ma, G.-H. Preparation of Uniform-Sized pH-Sensitive Quaternized Chitosan Microsphere by Combining Membrane Emulsification Technique and Thermal-Gelation Method. *Colloids Surf. B Biointerfaces* **2008**, *63* (2), 164–175.
- (165) Gao, Y.; Zhang, J.; Liang, J.; Yuan, D.; Zhao, W. Research Progress of Poly(Methyl Methacrylate) Microspheres: Preparation, Functionalization and Application. *Eur. Polym. J.* **2022**, *175*, 111379.
- (166) Zhang, J.; Wang, X.; Qi, G.; Li, B.; Song, Z.; Jiang, H.; Zhang, X.; Qiao, J. A Novel N-Doped Porous Carbon Microsphere Composed of Hollow Carbon Nanospheres. *Carbon* **2016**, *96*, 864–870.
- (167) Dao, T. D.; Erdenedelger, G.; Jeong, H. M. Water-Dispersible Graphene Designed as a Pickering Stabilizer for the Suspension Polymerization of Poly(Methyl Methacrylate)/Graphene Core-Shell Microsphere Exhibiting Ultra-Low Percolation Threshold of Electrical Conductivity. *Polymer* **2014**, *55* (18), 4709–4719.
- (168) Dai, C.; Wang, Y.; Hou, X. Preparation and Protein Adsorption of Porous Dextran Microspheres. *Carbohydr. Polym.* **2012**, *87* (3), 2338–2343.
- (169) Zhang, Z.; Gu, X.-L.; Zhu, X.-L.; Kong, X.-Z. Preparation and Formation Mechanism of Uniform Polymer Microspheres in Precipitation Polymerization of Pentaerythritol Triacrylate and Styrene. *Acta Phys.-Chim. Sin.* **2012**, *28* (4), 892–896.
- (170) Yang, H.; Kang, H.; Wang, B.; Liu, R. Facile Synthesis of Monodisperse Poly(Styrene-co-Acrylonitrile) Microspheres Using Redox Initiator in Ethanol/Water: Special Formation Mechanism. *Colloids Surf. Physicochem. Eng. Asp.* **2020**, *587*, 124315.
- (171) He, Z.; Shen, S.; Zhang, G.; Miao, T.; Cheng, X.; Wang, Z.; Song, Q.; Zhang, W. Photo-Induced Fusion of Monodisperse Polymer Microspheres: A Novel Strategy for Constructing Topological Microsphere Clusters with Improved Stability. *Aggregate* **2023**, *4* (5), No. e351.
- (172) Liu, X. J.; Li, H. Q.; Lin, X. Y.; Liu, H. Y.; Gao, G. H. Synthesis of Siloxane-Modified Melamine-Formaldehyde Microsphere and Its Heavy Metal Ions Adsorption by Coordination Effects. *Colloids Surf. Physicochem. Eng. Asp.* **2015**, *482*, 491–499.
- (173) Kwon, S. H.; Liu, Y. D.; Choi, H. J. Monodisperse Poly(2-Methylaniline) Coated Polystyrene Core-Shell Microspheres Fabricated by Controlled Releasing Process and Their Electrorheological Stimuli-Response under Electric Fields. *J. Colloid Interface Sci.* **2015**, *440*, 9–15.
- (174) Xiao, X.-C.; Chu, L.-Y.; Chen, W.-M.; Wang, S.; Li, Y. Positively Thermo-Sensitive Monodisperse Core-Shell Microspheres. *Adv. Funct. Mater.* **2003**, *13* (11), 847–852.
- (175) Bordat, A.; Boissenot, T.; Nicolas, J.; Tsapis, N. Thermoresponsive Polymer Nanocarriers for Biomedical Applications. *Adv. Drug Delivery Rev.* **2019**, *138*, 167–192.
- (176) Bulut, E.; Turhan, Y. Synthesis and Characterization of Temperature-Sensitive Microspheres Based on Acrylamide Grafted Hydroxypropyl Cellulose and Chitosan for the Controlled Release of Amoxicillin Trihydrate. *Int. J. Biol. Macromol.* **2021**, *191*, 1191–1203.
- (177) Cors, M.; Wiehemeier, L.; Oberdisse, J.; Hellweg, T. Deuteration-Induced Volume Phase Transition Temperature Shift of PNIPAM Microgels. *Polymers* **2019**, *11* (4), 620.
- (178) Etchenausia, L.; Villar-Alvarez, E.; Forcada, J.; Save, M.; Taboada, P. Evaluation of Cationic Core-Shell Thermoresponsive Poly(N-Vinylcaprolactam)-Based Microgels as Potential Drug Delivery Nanocarriers. *Mater. Sci. Eng., C* **2019**, *104*, 109871.
- (179) Nishizawa, Y.; Matsui, S.; Urayama, K.; Kureha, T.; Shibayama, M.; Uchihashi, T.; Suzuki, D. Non-Thermoresponsive Decanano-Sized Domains in Thermoresponsive Hydrogel Microspheres Revealed by Temperature-Controlled High-Speed Atomic Force Microscopy. *Angew. Chem., Int. Ed.* **2019**, *58* (26), 8809–8813.
- (180) Li, Z.; Liu, L.; Zheng, H.; Meng, F.; Wang, F. Thermoresponsive PNIPAm on Anti-Corrosion Antibacterial Coating for Controlled Ag Ions Release. *Compos. Commun.* **2022**, *35*, 101327.
- (181) Cao, Z.; Chen, Y.; Li, D.; Cheng, J.; Liu, C. Fabrication of Phosphate-Imprinted PNIPAM/SiO₂ Hybrid Particles and Their Phosphate Binding Property. *Polymers* **2019**, *11* (2), 253.
- (182) Du, H.-H.; Xiao, X.-C. Fabrication of Rapidly-Responsive Switches Based on the Coupling Effect of Polyacrylamide and Poly(Acrylic Acid) without IPN Structures. *RSC Adv.* **2015**, *5* (107), 88021–88026.
- (183) Du, W.; Wu, P.; Zhao, Z.; Zhang, X. Facile Preparation and Characterization of Temperature-Responsive Hydrophilic Crosslinked Polymer Microspheres by Aqueous Dispersion Polymerization. *Eur. Polym. J.* **2020**, *128*, 109610.
- (184) Yin, J.; Hu, J.; Zhang, G.; Liu, S. Schizophrenic Core-Shell Microgels: Thermoregulated Core and Shell Swelling/Collapse by Combining UCST and LCST Phase Transitions. *Langmuir* **2014**, *30* (9), 2551–2558.
- (185) Yan, S.; Zhang, F.; Luo, L.; Wang, L.; Liu, Y.; Leng, J. Shape Memory Polymer Composites: 4D Printing, Smart Structures, and Applications. *Research* **2023**, *6*, 0234.
- (186) Luo, L.; Zhang, F.; Leng, J. Shape Memory Epoxy Resin and Its Composites: From Materials to Applications. *Research* **2022**, *2022*, 9767830.
- (187) Montero de Espinosa, L.; Meesorn, W.; Moatsou, D.; Weder, C. Bioinspired Polymer Systems with Stimuli-Responsive Mechanical Properties. *Chem. Rev.* **2017**, *117* (20), 12851–12892.
- (188) Zhang, F.; Wen, N.; Wang, L.; Bai, Y.; Leng, J. Design of 4D Printed Shape-Changing Tracheal Stent and Remote Controlling Actuation. *Int. J. Smart Nano Mater.* **2021**, *12* (4), 375–389.
- (189) Xia, Y.; He, Y.; Zhang, F.; Liu, Y.; Leng, J. A Review of Shape Memory Polymers and Composites: Mechanisms, Materials, and Applications. *Adv. Mater.* **2021**, *33* (6), 2000713.
- (190) Zhang, F.; Zhao, T.; Ruiz-Molina, D.; Liu, Y.; Roscini, C.; Leng, J.; Smoukov, S. K. Shape Memory Polyurethane Microcapsules with Active Deformation. *ACS Appl. Mater. Interfaces* **2020**, *12* (41), 47059–47064.
- (191) Han, J.; Wang, L.; Wang, L.; Li, C.; Mao, Y.; Wang, Y. Fabrication of a Core-Shell-Shell Magnetic Polymeric Microsphere with Excellent Performance for Separation and Purification of Bromelain. *Food Chem.* **2019**, *283*, 1–10.
- (192) Yin, P.; Wei, C.; Jin, X.; Yu, X.; Wu, C.; Zhang, W. Magnetic Polyvinyl Alcohol Microspheres with Self-Regulating Temperature Hyperthermia and CT/MR Imaging for Arterial Embolization. *Polym. Bull.* **2023**, *80* (3), 2697–2711.
- (193) Wang, Z.; Wang, W.; Meng, Z.; Xue, M. Mono-Sized Anion-Exchange Magnetic Microspheres for Protein Adsorption. *Int. J. Mol. Sci.* **2022**, *23* (9), 4963.
- (194) Guo, T.; Chen, J.; Luo, L.; Geng, Q.; Wang, L.; Zhang, F.; Hu, N.; Liu, Y.; Leng, J. Magnetic Guidance Shape Memory PLA/TBC/Fe₃O₄ Microspheres for Dentin Tubule Sealing. *Compos. Part A Appl. Sci. Manuf.* **2024**, *180*, 108083.
- (195) Liang, Y.-J.; Wang, H.; Yu, H.; Feng, G.; Liu, F.; Ma, M.; Zhang, Y.; Gu, N. Magnetic Navigation Helps PLGA Drug Loaded Magnetic Microspheres Achieve Precise Chemoembolization and Hyperthermia. *Colloids Surf. Physicochem. Eng. Asp.* **2020**, *588*, 124364.
- (196) Zhou, Y.; Chen, P.; Chen, M.; Li, J.; Li, X.; Lin, L.; Lun, Y.; Li, Q.; Xiao, Q.; Huang, Y.; Wang, X.; Zou, H.; Ye, G. γ -Fe₂O₃@Poly(Sucrose Allyl Ether) Magnetic Microspheres for Tumor Enhanced Magnetic Resonance Imaging and High-Efficiency Cooperative Magnetothermal Therapy. *Mater. Des.* **2022**, *222*, 111062.
- (197) He, Y.; Chen, X.; Zhang, Y.; Wang, Y.; Cui, M.; Li, G.; Liu, X.; Fan, H. Magneto-responsive Nanozyme: Magnetic Stimulation on the Nanozyme Activity of Iron Oxide Nanoparticles. *Sci. China Life Sci.* **2022**, *65* (1), 184–192.

- (198) Brighenti, R.; Cosma, M. P. Mechanics of Multi-Stimuli Temperature-Responsive Hydrogels. *J. Mech. Phys. Solids* **2022**, *169*, 105045.
- (199) Jin, H.; Zheng, Y.; Liu, Y.; Cheng, H.; Zhou, Y.; Yan, D. Reversible and Large-Scale Cytomimetic Vesicle Aggregation: Light-Responsive Host-Guest Interactions. *Angew. Chem., Int. Ed.* **2011**, *123* (44), 10536–10540.
- (200) Gong, C.-B.; Wei, Y.-B.; Liu, L.-T.; Zheng, A.-X.; Yang, Y.-H.; Chow, C.; Tang, Q. Photoresponsive Hollow Molecularly Imprinted Polymer for Trace Triamterene in Biological Samples. *Mater. Sci. Eng., C* **2017**, *76*, 568–578.
- (201) Such, G. K.; Evans, R. A.; Davis, T. P. Control of Photochromism through Local Environment Effects Using Living Radical Polymerization (ATRP). *Macromolecules* **2004**, *37* (26), 9664–9666.
- (202) Jiang, Y.; Wan, P.; Xu, H.; Wang, Z.; Zhang, X.; Smet, M. Facile Reversible UV-Controlled and Fast Transition from Emulsion to Gel by Using a Photoresponsive Polymer with a Malachite Green Group. *Langmuir* **2009**, *25* (17), 10134–10138.
- (203) Yan, F.; Chen, L.; Tang, Q.; Wang, R. Synthesis and Characterization of a Photocleavable Cross-Linker and Its Application on Tunable Surface Modification and Protein Photodelivery. *Bioconjugate Chem.* **2004**, *15* (5), 1030–1036.
- (204) Yang, Y.-H.; Liu, L.-T.; Chen, M.-J.; Liu, S.; Gong, C.-B.; Wei, Y.-B.; Chow, C.-F.; Tang, Q. A Photoresponsive Surface Molecularly Imprinted Polymer Shell for Determination of Trace Griseofulvin in Milk. *Mater. Sci. Eng., C* **2018**, *92*, 365–373.
- (205) Tamada, K.; Akiyama, H.; Wei, T. X. Photoisomerization Reaction of Unsymmetrical Azobenzene Disulfide Self-Assembled Monolayers Studied by Surface Plasmon Spectroscopy: Influences of Side Chain Length and Contacting Medium. *Langmuir* **2002**, *18* (13), 5239–5246.
- (206) Wu, S.; Li, W.; Sun, Y.; Pang, X.; Zhang, X.; Zhuang, J.; Zhang, H.; Hu, C.; Lei, B.; Liu, Y. Facile Fabrication of a CD/PVA Composite Polymer to Access Light-Responsive Shape-Memory Effects. *J. Mater. Chem. C* **2020**, *8* (26), 8935–8941.
- (207) Zhou, T.; Huang, Z.; Wan, F.; Sun, Y. Carbon Quantum Dots-Stabilized Pickering Emulsion to Prepare NIR Light-Responsive PLGA Drug Delivery System. *Mater. Today Commun.* **2020**, *23*, 100951.
- (208) Guo, Q.; Bishop, C. J.; Meyer, R. A.; Wilson, D. R.; Olsav, L.; Schlesinger, D. E.; Mather, P. T.; Spicer, J. B.; Elisseff, J. H.; Green, J. J. Entanglement-Based Thermoplastic Shape Memory Polymeric Particles with Photothermal Actuation for Biomedical Applications. *ACS Appl. Mater. Interfaces* **2018**, *10* (16), 13333–13341.
- (209) Bai, Y.; Zhang, J.; Ju, J.; Liu, J.; Chen, X. Shape Memory Microparticles with Permanent Shape Reconfiguration Ability and Near Infrared Light Responsiveness. *React. Funct. Polym.* **2020**, *157*, 104770.
- (210) Brighenti, R.; Li, Y.; Vernerey, F. J. Smart Polymers for Advanced Applications: A Mechanical Perspective Review. *Front. Mater.* **2020**, *7*, 196.
- (211) Roy, D.; Cambre, J. N.; Sumerlin, B. S. Future Perspectives and Recent Advances in Stimuli-Responsive Materials. *Prog. Polym. Sci.* **2010**, *35* (1–2), 278–301.
- (212) Sagara, Y.; Traeger, H.; Li, J.; Okado, Y.; Schrettl, S.; Tamaoki, N.; Weder, C. Mechanically Responsive Luminescent Polymers Based on Supramolecular Cyclophane Mechanophores. *J. Am. Chem. Soc.* **2021**, *143* (14), 5519–5525.
- (213) Cosma, M. P.; Brighenti, R. From Responsiveness in Biological Matter to Functional Materials: Analogies and Inspiration towards the Systematic Design and Synthesis of New Smart Materials and Systems. *Appl. Mater. Today* **2023**, *32*, 101842.
- (214) Li, Y.; Xue, B.; Yang, J.; Jiang, J.; Liu, J.; Zhou, Y.; Zhang, J.; Wu, M.; Yuan, Y.; Zhu, Z.; Wang, Z. J.; Chen, Y.; Harabuchi, Y.; Nakajima, T.; Wang, W.; Maeda, S.; Gong, J. P.; Cao, Y. Azobenzene as a Photoswitchable Mechanophore. *Nat. Chem.* **2024**, *16* (3), 446–455.
- (215) Deneke, N.; Rencheck, M. L.; Davis, C. S. An Engineer's Introduction to Mechanophores. *Soft Matter* **2020**, *16* (27), 6230–6252.
- (216) Davis, D. A.; Hamilton, A.; Yang, J.; Cremer, L. D.; Van Gough, D.; Potisek, S. L.; Ong, M. T.; Braun, P. V.; Martínez, T. J.; White, S. R.; Moore, J. S.; Sottos, N. R. Force-Induced Activation of Covalent Bonds in Mechanoresponsive Polymeric Materials. *Nature* **2009**, *459* (7243), 68–72.
- (217) Dong, Y.; Ma, Z.; Song, D. P.; Ma, G.; Li, Y. Rapid Responsive Mechanochromic Photonic Pigments with Alternating Glassy-Rubbery Concentric Lamellar Nanostructures. *ACS Nano* **2021**, *15* (5), 8770–8779.
- (218) Zhang, M.; Hu, W.; Cai, C.; Wu, Y.; Li, J.; Dong, S. Advanced Application of Stimuli-Responsive Drug Delivery System for Inflammatory Arthritis Treatment. *Mater. Today Bio* **2022**, *14*, 100223.
- (219) Lu, C.-T.; Ying-Zheng Zhao; Shu-Ping Ge; Jin, Y.-G.; Du, L.-N. Potential and Problems in Ultrasound-Responsive Drug Delivery Systems. *Int. J. Nanomedicine* **2013**, *8*, 1621–1631.
- (220) Mura, S.; Nicolas, J.; Couvreur, P. Stimuli-Responsive Nanocarriers for Drug Delivery. *Nat. Mater.* **2013**, *12* (11), 991–1003.
- (221) Rapoport, N. Y.; Kennedy, A. M.; Shea, J. E.; Scaife, C. L.; Nam, K.-H. Controlled and Targeted Tumor Chemotherapy by Ultrasound-Activated Nanoemulsions/Microbubbles. *J. Controlled Release* **2009**, *138* (3), 268–276.
- (222) Li, L.; Liu, C.; Zhang, L.; Wang, T.; Yu, H.; Wang, C.; Su, Z. Multifunctional Magnetic-Fluorescent Eccentric-(Concentric-Fe₃O₄@SiO₂)@Polyacrylic Acid Core-Shell Nanocomposites for Cell Imaging and pH-Responsive Drug Delivery. *Nanoscale* **2013**, *5* (6), 2249–2253.
- (223) Kozlovskaya, V.; Higgins, W.; Chen, J.; Kharlampieva, E. Shape Switching of Hollow Layer-by-Layer Hydrogel Microcontainers. *Chem. Commun.* **2011**, *47* (29), 8352–8354.
- (224) Li, X.; Huang, Y.; Xiao, J.; Yan, C. pH Responsive PAIAm-g-PIPA Microspheres: Preparation and Drug Release. *J. Appl. Polym. Sci.* **1995**, *55* (13), 1779–1785.
- (225) Yang, G.; Wu, F.; Wei, Z.; Yang, K.; Zhang, C.; Ma, Y.; Pan, J. Capturing Lithium Using Functional Macroporous Microspheres with Multiple Chambers from One-Step Double Emulsion via a Tailoring Supramolecular Route and Postsynthetic Interface Modification. *Chem. Eng. J.* **2020**, *389*, 124372.
- (226) Yu, C.; Peng, J.; Li, J.; Zhai, M. pH-Responsive Hollow Polymeric Microspheres from Irradiated Cyclic Ether Aqueous Solution. *Appl. Sci.* **2021**, *11* (18), 8652.
- (227) Beyer, D.; Košovan, P.; Holm, C. Simulations Explain the Swelling Behavior of Hydrogels with Alternating Neutral and Weakly Acidic Blocks. *Macromolecules* **2022**, *55* (23), 10751–10760.
- (228) Dupin, D.; Fujii, S.; Armes, S. P.; Reeve, P.; Baxter, S. M. Efficient Synthesis of Sterically Stabilized pH-Responsive Microgels of Controllable Particle Diameter by Emulsion Polymerization. *Langmuir* **2006**, *22* (7), 3381–3387.
- (229) Morse, A. J.; Dupin, D.; Thompson, K. L.; Armes, S. P.; Ouzineb, K.; Mills, P.; Swart, R. Novel Pickering Emulsifiers Based on pH-Responsive Poly(Tert-Butylaminoethyl Methacrylate) Latexes. *Langmuir* **2012**, *28* (32), 11733–11744.
- (230) Slaughter, B. V.; Blanchard, A. T.; Maass, K. F.; Peppas, N. A. Dynamic Swelling Behavior of Interpenetrating Polymer Networks in Response to Temperature and pH. *J. Appl. Polym. Sci.* **2015**, *132* (24), 42076.
- (231) Wan, Y.; Liu, X.; Liu, P.; Zhao, L.; Zou, W. Optimization Adsorption of Norfloxacin onto Polydopamine Microspheres from Aqueous Solution: Kinetic, Equilibrium and Adsorption Mechanism Studies. *Sci. Total Environ.* **2018**, *639*, 428–437.
- (232) Jiang, M. Y.; Ju, X. J.; Deng, K.; Fan, X. X.; He, X. H.; Wu, F.; He, F.; Liu, Z.; Wang, W.; Xie, R.; Chu, L.-Y. The Microfluidic Synthesis of Composite Hollow Microfibers for K⁺-Responsive Controlled Release Based on a Host-Guest System. *J. Mater. Chem. B* **2016**, *4* (22), 3925–3935.

- (233) Kamaly, N.; Xiao, Z.; Valencia, P. M.; Radovic-Moreno, A. F.; Farokhzad, O. C. Targeted Polymeric Therapeutic Nanoparticles: Design, Development and Clinical Translation. *Chem. Soc. Rev.* **2012**, *41* (7), 2971–3010.
- (234) Chang, L.; Liu, C.; He, Y.; Xiao, H.; Cai, X. Small-Volume Solution Current-Time Behavior Study for Application in Reverse Iontophoresis-Based Non-Invasive Blood Glucose Monitoring. *Sci. China Chem.* **2011**, *54* (1), 223–230.
- (235) Purcell, B. P.; Lobb, D.; Charati, M. B.; Dorsey, S. M.; Wade, R. J.; Zellars, K. N.; Doviak, H.; Pettaway, S.; Logdon, C. B.; Shuman, J. A.; Freels, P. D.; Gorman, J. H., III; Gorman, R. C.; Spinale, F. G.; Burdick, J. A. Injectable and Bioresponsive Hydrogels for On-Demand Matrix Metalloproteinase Inhibition. *Nat. Mater.* **2014**, *13* (6), 653–661.
- (236) Kuang, T.; Liu, Y.; Gong, T.; Peng, X.; Hu, X.; Yu, Z. Enzyme-Responsive Nanoparticles for Anticancer Drug Delivery. *Curr. Nanosci.* **2015**, *12* (1), 38–46.
- (237) Barve, A.; Jin, W.; Cheng, K. Prostate Cancer Relevant Antigens and Enzymes for Targeted Drug Delivery. *J. Controlled Release* **2014**, *187*, 118–132.
- (238) Ozden, F.; Saygin, C.; Uzunaslan, D.; Onal, B.; Durak, H.; Aki, H. Expression of MMP-1, MMP-9 and TIMP-2 in Prostate Carcinoma and Their Influence on Prognosis and Survival. *J. Cancer Res. Clin. Oncol.* **2013**, *139* (8), 1373–1382.
- (239) Nguyen, M. M.; Carlini, A. S.; Chien, M.; Sonnenberg, S.; Luo, C.; Braden, R. L.; Osborn, K. G.; Li, Y.; Gianneschi, N. C.; Christman, K. L. Enzyme-Responsive Nanoparticles for Targeted Accumulation and Prolonged Retention in Heart Tissue after Myocardial Infarction. *Adv. Mater.* **2015**, *27* (37), 5547–5552.
- (240) Liu, L.; Liu, G.; Mu, X.; Zhao, S.; Tian, J. Simple Enzyme-Free Detection of Uric Acid by an in Situ Fluorescence and Colorimetric Method Based on Co-PBA with High Oxidase Activity. *Analyst* **2024**, *149* (5), 1455–1463.
- (241) Molla, M. R.; Prasad, P.; Thayumanavan, S. Protein-Induced Supramolecular Disassembly of Amphiphilic Polypeptide Nanoassemblies. *J. Am. Chem. Soc.* **2015**, *137* (23), 7286–7289.
- (242) Krishnamurthy, V. M.; Kaufman, G. K.; Urbach, A. R.; Gitlin, I.; Gudiksen, K. L.; Weibel, D. B.; Whitesides, G. M. Carbonic Anhydrase as a Model for Biophysical and Physical-Organic Studies of Proteins and Protein-Ligand Binding. *Chem. Rev.* **2008**, *108* (3), 946–1051.
- (243) Azagarsamy, M. A.; Yesilyurt, V.; Thayumanavan, S. Disassembly of Dendritic Micellar Containers Due to Protein Binding. *J. Am. Chem. Soc.* **2010**, *132* (13), 4550–4551.
- (244) Lin, K.; Yi, J.; Mao, X.; Wu, H.; Zhang, L.-M.; Yang, L. Glucose-Sensitive Hydrogels from Covalently Modified Carboxylated Pullulan and Concanavalin A for Smart Controlled Release of Insulin. *React. Funct. Polym.* **2019**, *139*, 112–119.
- (245) Kreuter, J. Nanoparticles and Microparticles for Drug and Vaccine Delivery. *J. Anat.* **1996**, *189* (Pt 3), 503–505.
- (246) Chang, R.; Li, M.; Ge, S.; Yang, J.; Sun, Q.; Xiong, L. Glucose-Responsive Biopolymer Nanoparticles Prepared by Co-Assembly of Concanavalin A and Amylopectin for Insulin Delivery. *Ind. Crops Prod.* **2018**, *112*, 98–104.
- (247) Nishiyabu, R.; Kubo, Y.; James, T. D.; Fossey, J. S. Boronic Acid Building Blocks: Tools for Self Assembly. *Chem. Commun.* **2011**, *47* (4), 1124–1150.
- (248) Zhao, L.; Xiao, C.; Wang, L.; Gai, G.; Ding, J. Glucose-Sensitive Polymer Nanoparticles for Self-Regulated Drug Delivery. *Chem. Commun.* **2016**, *52* (49), 7633–7652.
- (249) Wang, J.; Ye, Y.; Yu, J.; Kahkoska, A. R.; Zhang, X.; Wang, C.; Sun, W.; Corder, R. D.; Chen, Z.; Khan, S. A.; Buse, J. B.; Gu, Z. Core-Shell Microneedle Gel for Self-Regulated Insulin Delivery. *ACS Nano* **2018**, *12* (3), 2466–2473.
- (250) Yu, J.; Wang, Q.; Liu, H.; Shan, X.; Pang, Z.; Song, P.; Niu, F.; Hu, L. Glucose-Responsive Microspheres as a Smart Drug Delivery System for Controlled Release of Insulin. *Eur. J. Drug Metab. Pharmacokinet.* **2020**, *45* (1), 113–121.
- (251) Yang, F.; Wang, J.; Song, S.; Rao, P.; Wang, R.; Liu, S.; Xu, L.; Zhang, F. Novel Controlled Release Microspheric Soil Conditioner Based on the Temperature and pH Dual-Stimuli Response. *J. Agric. Food Chem.* **2020**, *68* (30), 7819–7829.
- (252) Peng, H.; Wang, D.; Ma, D.; Zhou, Y.; Zhang, J.; Kang, Y.; Yue, Q. Multifunctional Yolk-Shell Structured Magnetic Mesoporous Polydopamine/Carbon Microspheres for Photothermal Therapy and Heterogenous Catalysis. *ACS Appl. Mater. Interfaces* **2022**, *14* (20), 23888–23895.
- (253) Xie, X.; Hu, Q.; Ke, R.; Zhen, X.; Bu, Y.; Wang, S. Facile Preparation of Photonic and Magnetic Dual Responsive Protein Imprinted Nanomaterial for Specific Recognition of Bovine Hemoglobin. *Chem. Eng. J.* **2019**, *371*, 130–137.
- (254) Zeng, H.; Song, J.; Li, Y.; Guo, C.; Zhang, Y.; Yin, T.; He, H.; Gou, J.; Tang, X. Effect of Hydroxyethyl Starch on Drug Stability and Release of Semaglutide in PLGA Microspheres. *Int. J. Pharm.* **2024**, *654*, 123991.
- (255) Yang, A.-L.; Sun, S.-B.; Qu, L.-Y.; Li, X.-Y.; Liu, J.-L.; Zhou, F.; Xu, Y.-J. Polysaccharide Hydrogel Containing Silver Nanoparticle@catechol Microspheres with Photothermal, Antibacterial and Anti-Inflammatory Activities for Infected-Wounds Repair. *Int. J. Biol. Macromol.* **2024**, *265*, 130898.
- (256) Ge, D.; Lee, E.; Yang, L.; Cho, Y.; Li, M.; Gianola, D. S.; Yang, S. A Robust Smart Window: Reversibly Switching from High Transparency to Angle-Independent Structural Color Display. *Adv. Mater.* **2015**, *27* (15), 2489–2495.
- (257) Robb, M. J.; Li, W.; Gergely, R. C. R.; Matthews, C. C.; White, S. R.; Sottos, N. R.; Moore, J. S. A Robust Damage-Reporting Strategy for Polymeric Materials Enabled by Aggregation-Induced Emission. *ACS Cent. Sci.* **2016**, *2* (9), 598–603.
- (258) Zhang, X.; Wang, B.; Zheng, Z.; Yang, G.; Zhang, C.; Liao, L. A Robust Photoswitchable Dual-Color Fluorescent Poly(Vinyl Alcohol) Composite Hydrogel Constructed by Photo-Responsive FRET Effect. *Dyes Pigm.* **2023**, *208*, 110800.
- (259) Xiong, J.; He, Y.; Cui, X.; Liu, L. Preparation of Amino-Bagasse/Metakaolin Based Geopolymer Hybrid Microsphere as a Low-Cost and Effective Adsorbent for Cu(II). *J. Environ. Chem. Eng.* **2023**, *11* (5), 110954.
- (260) Jiang, F.; Zheng, Q.; Zhao, Q.; Qi, Z.; Wu, D.; Li, W.; Wu, X.; Han, C. Magnetic Propelled Hydrogel Microrobots for Actively Enhancing the Efficiency of Lycorine Hydrochloride to Suppress Colorectal Cancer. *Front. Bioeng. Biotechnol.* **2024**, *12*, 1361617.
- (261) Zhang, B.; Wang, C.; Guo, M.; Zhu, F.; Yu, Z.; Zhang, W.; Li, W.; Zhang, Y.; Tian, W. Circadian Rhythm-Dependent Therapy by Composite Targeted Polyphenol Nanoparticles for Myocardial Ischemia-Reperfusion Injury. *ACS Nano* **2024**, *18* (41), 28154–28169.
- (262) Liu, L.; Zheng, M.; Liang, R. Improvement of Liraglutide Release from PLGA Microspheres by a Porous Microsphere-Gel Composite System. *Pharm. Dev. Technol.* **2024**, *29* (4), 291–299.
- (263) Huang, D.; Wang, Y.; Xu, C.; Zou, M.; Ming, Y.; Luo, F.; Xu, Z.; Miao, Y.; Wang, N.; Lin, Z.; Weng, Z. Colon-Targeted Hydroxyethyl Starch-Curcumin Microspheres with High Loading Capacity Ameliorate Ulcerative Colitis via Alleviating Oxidative Stress, Regulating Inflammation, and Modulating Gut Microbiota. *Int. J. Biol. Macromol.* **2024**, *266*, 131107.
- (264) Cai, L.; Chen, G.; Wang, Y.; Zhao, C.; Shang, L.; Zhao, Y. Boston Ivy-Inspired Disc-Like Adhesive Microparticles for Drug Delivery. *Research* **2021**, *2021*, 9895674.
- (265) Xiao, S.; Sun, X.; Wang, C.; Wu, J.; Zhang, K.; Guo, M.; Liu, B. Nanomicrosphere Sustained-Release Urokinase Systems with Antioxidant Properties for Deep Vein Thrombosis Therapy. *RSC Adv.* **2024**, *14* (10), 7195–7205.
- (266) Li, X.; Li, X.; Yang, J.; Du, Y.; Chen, L.; Zhao, G.; Ye, T.; Zhu, Y.; Xu, X.; Deng, L.; Cui, W. In Situ Sustained Macrophage-Targeted Nanomicelle-Hydrogel Microspheres for Inhibiting Osteoarthritis. *Research* **2023**, *6*, 0131.

- (267) Li, Y.; Chen, Y.; Xue, Y.; Jin, J.; Xu, Y.; Zeng, W.; Liu, J.; Xie, J. Injectable Hydrogel Delivery System with High Drug Loading for Prolonging Local Anesthesia. *Adv. Sci.* **2024**, *11* (24), 2309482.
- (268) Choi, W.; Kohane, D. S. Hybrid Nanoparticle-Hydrogel Systems for Drug Delivery Depots and Other Biomedical Applications. *ACS Nano* **2024**, *18*, 22780.
- (269) Xiang, H.; Zhang, C.; Xiong, Y.; Wang, Y.; Pu, C.; He, J.; Chen, L.; Jiang, K.; Zhao, W.; Yang, H.; Wang, F.; Li, Y. MMP13-Responsive Hydrogel Microspheres for Osteoarthritis Treatment by Precise Delivery of Celecoxib. *Mater. Des.* **2024**, *241*, 112966.
- (270) Miao, K.; Zhou, Y.; He, X.; Xu, Y.; Zhang, X.; Zhao, H.; Zhou, X.; Gu, Q.; Yang, H.; Liu, X.; Huang, L.; Shi, Q. Microenvironment-Responsive Bilayer Hydrogel Microspheres with Gelatin-Shell for Osteoarthritis Treatment. *Int. J. Biol. Macromol.* **2024**, *261*, 129862.
- (271) Tang, Y.; Du, Y.; Ye, J.; Deng, L.; Cui, W. Intestine-Targeted Explosive Hydrogel Microsphere Promotes Uric Acid Excretion for Gout Therapy. *Adv. Mater.* **2024**, *36* (3), 2310492.
- (272) Su, H.; Zhang, H.; Zhang, D.; Wang, H.; Wang, H. Black Phosphorus-Loaded Inverse Opal Microspheres for Intelligent Drug Delivery. *J. Drug Delivery Sci. Technol.* **2024**, *92*, 105374.
- (273) Liu, X.; Yan, S.; Wu, H.; Chen, M.; Dai, H.; Wang, Z.; Chai, M.; Hu, Q.; Li, D.; Chen, L.; Diao, R.; Chen, S.; Wang, L.; Shi, X. Interventional Hydrogel Microsphere Controlled-Releasing Curcumin for Photothermal Therapy against Endometriosis. *Adv. Funct. Mater.* **2024**, *34* (26), 2315907.
- (274) Zheng, L.; Yu, Q.; Li, Q.; Zheng, C. Targeted Local Anesthesia: A Novel Slow-Release Fe₃O₄-Lidocaine-PLGA Microsphere Endowed with a Magnetic Targeting Function. *J. Anesth.* **2024**, *38* (2), 232–243.
- (275) Liu, M.; An, Z.; Xu, J.; Deng, X.; Xiao, Y.; A, R.; Zhan, Y.; Yang, C.; Li, P.; Fan, Y. Netrin1-Carrying Magnetic Microspheres with Magnetic Field Activate Neurotrophin Factors to Guide Neuronal Outgrowth in Vitro and in Vivo. *Chem. Eng. J.* **2024**, *484*, 149687.
- (276) Guo, J.; Shu, X.; Yu, S.; Guo, C.; Shen, G.; Chen, L.; Zhou, J.; Xiao, J.; Guo, H.; Chen, Y.; Zeng, Z.; Wang, P. Injectable Hydrogel Microsphere-Bomb for MRSA-Infected Chronic Osteomyelitis. *J. Controlled Release* **2024**, *376*, 337–353.
- (277) Brzeziński, M.; Seiffert, S. Monodisperse Microspheres from Supramolecular Complexing Poly(lactides). *Mater. Lett.* **2015**, *161*, 471–475.
- (278) Sun, T.; Zhu, C.; Xu, J. Multiple Stimuli-Responsive Selenium-Functionalized Biodegradable Starch-Based Hydrogels. *Soft Matter* **2018**, *14* (6), 921–926.
- (279) Parvin, N.; Joo, S. W.; Mandal, T. K. Biodegradable and Stimuli-Responsive Nanomaterials for Targeted Drug Delivery in Autoimmune Diseases. *J. Funct. Biomater.* **2025**, *16* (1), 24.
- (280) Wu, S.; Gong, Y.; Liu, S.; Pei, Y.; Luo, X. Functionalized Phosphorylated Cellulose Microspheres: Design, Characterization and Ciprofloxacin Loading and Releasing Properties. *Carbohydr. Polym.* **2021**, *254*, 117421.
- (281) Smutzer, G.; Cherian, S.; Patel, D.; Lee, B. S.; Lee, K.; Sotelo, A. R.; Mitchell, K.-D. W. A Formulation for Suppressing Bitter Taste in the Human Oral Cavity. *Physiol. Behav.* **2020**, *226*, 113129.
- (282) Leite, A. C.; Pereira, R. N.; Rodrigues, R. M. Protein Aerogels as Food-Grade Delivery Systems—A Comprehensive Review. *Food Hydrocoll.* **2025**, *163*, 111138.
- (283) Anirudhan, T. S.; Rejeena, S. R. Poly(Acrylic Acid-Co-Acrylamide-Co-2-Acrylamido-2-Methyl-1-Propanesulfonic Acid)-Grafted Nanocellulose/Poly(Vinyl Alcohol) Composite for the in Vitro Gastrointestinal Release of Amoxicillin. *J. Appl. Polym. Sci.* **2014**, *131* (17), 40699.
- (284) Seo, S.; Lee, C.-S.; Jung, Y.-S.; Na, K. Thermo-Sensitivity and Triggered Drug Release of Polysaccharide Nanogels Derived from Pullulan-g-Poly(L-Lactide) Copolymers. *Carbohydr. Polym.* **2012**, *87* (2), 1105–1111.
- (285) Hou, Z.; Yan, W.; Li, T.; Wu, W.; Cui, Y.; Zhang, X.; Chen, Y.-P.; Yin, T.; Qiu, J.; Wang, G. Lactic Acid-Mediated Endothelial to Mesenchymal Transition through TGF- β 1 Contributes to in-Stent Stenosis in Poly-L-Lactic Acid Stent. *Int. J. Biol. Macromol.* **2020**, *155*, 1589–1598.
- (286) Pan, Q.; Su, W.; Yao, Y. Progress in Microsphere-Based Scaffolds in Bone/Cartilage Tissue Engineering. *Biomed. Mater.* **2023**, *18* (6), 062004.
- (287) Zhang, M.-L.; Cheng, J.; Xiao, Y.-C.; Yin, R.-F.; Feng, X. Raloxifene Microsphere-Embedded Collagen/Chitosan/ β -Tricalcium Phosphate Scaffold for Effective Bone Tissue Engineering. *Int. J. Pharm.* **2017**, *518* (1–2), 80–85.
- (288) Kamaraj, M.; Moghimi, N.; McCarthy, A.; Chen, J.; Cao, S.; Chethikkattuveli Salih, A. R.; Joshi, A.; Jucaud, V.; Panayi, A.; Shin, S. R.; Noshadi, I.; Khademhosseini, A.; Xie, J.; John, J. V. Granular Porous Nanofibrous Microspheres Enhance Cellular Infiltration for Diabetic Wound Healing. *ACS Nano* **2024**, *18* (41), 28335–28348.
- (289) Zhang, X.; Wang, M.; Cui, H.; Zhang, T.; Zhang, Z.; Li, J.; Zhou, J.; Jiang, X.; Liu, C.; Gao, J. Integrated Copper Nanomaterials-Decorated Microsphere Photothermal Platform for Comprehensive Melanoma Treatment. *Small Struct.* **2024**, *5* (6), 2400028.
- (290) Li, J.; Wu, Y.; Yuan, Q.; Li, L.; Qin, W.; Jia, J.; Chen, K.; Wu, D.; Yuan, X. Gelatin Microspheres Based on H8-Loaded Macrophage Membrane Vesicles to Promote Wound Healing in Diabetic Mice. *ACS Biomater. Sci. Eng.* **2024**, *10* (4), 2251–2269.
- (291) Xiao, Y.; Ding, T.; Fang, H.; Lin, J.; Chen, L.; Ma, D.; Zhang, T.; Cui, W.; Ma, J. Innovative Bio-Based Hydrogel Microspheres Micro-Cage for Neutrophil Extracellular Traps Scavenging in Diabetic Wound Healing. *Adv. Sci.* **2024**, *11* (21), 2401195.
- (292) Song, Q.; Wang, D.; Li, H.; Wang, Z.; Sun, S.; Wang, Z.; Liu, Y.; Lin, S.; Li, G.; Zhang, S.; Zhang, P. Dual-Response of Multi-Functional Microsphere System to Ultrasound and Microenvironment for Enhanced Bone Defect Treatment. *Bioact. Mater.* **2024**, *32*, 304–318.
- (293) Chen, S.; Han, X.; Cao, Y.; Yi, W.; Zhu, Y.; Ding, X.; Li, K.; Shen, J.; Cui, W.; Bai, D. Spatiotemporalized Hydrogel Microspheres Promote Vascularized Osteogenesis via Ultrasound Oxygen Delivery. *Adv. Funct. Mater.* **2024**, *34* (1), 2308205.
- (294) Wang, F.; Liu, M.; Liu, C.; Zhao, Q.; Wang, T.; Wang, Z.; Du, X. Light-Induced Charged Slippery Surfaces. *Sci. Adv.* **2022**, *8* (27), No. eabp9369.
- (295) Liu, C.; Wang, F.; Du, X. Self-Powered Electrostatic Tweezer for Adaptive Object Manipulation. *Device* **2024**, *2* (10), 100465.
- (296) Peng, M.; Zhao, Q.; Chai, A.; Wang, Y.; Wang, M.; Du, X. A Ferroelectric Living Interface for Fine-Tuned Exosome Secretion Toward Physiology-Mimetic Neurovascular Remodeling. *Matter* **2025**, *8* (2), 101901.
- (297) Zhu, X.; Wang, F.; Zhao, Q.; Du, X. Adaptive Interfacial Materials and Implants for Visual Restoration. *Adv. Funct. Mater.* **2024**, *34* (32), 2314575.
- (298) Wang, F.; Liu, M.; Liu, C.; Huang, C.; Zhang, L.; Cui, A.; Hu, Z.; Du, X. Light Control of Droplets on Photo-Induced Charged Surfaces. *Natl. Sci. Rev.* **2023**, *10* (1), nwac164.
- (299) Wang, F.; Liu, C.; Dai, Z.; Xu, W.; Ma, X.; Gao, Y.; Ge, X.; Zheng, W.; Du, X. Photopyroelectric Tweezers for Versatile Manipulation. *Innovation* **2025**, *6* (1), 100742.
- (300) McDonald, M. W.; Jeffers, M. S.; Filadelfi, M.; Vicencio, A.; Heidenreich, G.; Wu, J.; Silasi, G. Localizing Microemboli within the Rodent Brain through Block-Face Imaging and Atlas Registration. *ENeuro* **2021**, *8* (4), n/a.
- (301) Li, X.; Ji, X.; Chen, K.; Ullah, M. W.; Li, B.; Cao, J.; Xiao, L.; Xiao, J.; Yang, G. Immobilized Thrombin on X-Ray Radiopaque Polyvinyl Alcohol/Chitosan Embolic Microspheres for Precise Localization and Topical Blood Coagulation. *Bioact. Mater.* **2021**, *6* (7), 2105–2119.
- (302) Wu, Z.; Li, L.; Yang, Y.; Hu, P.; Li, Y.; Yang, S.-Y.; Wang, L. V.; Gao, W. A Microbotic System Guided by Photoacoustic Computed Tomography for Targeted Navigation in Intestines in Vivo. *Sci. Robot.* **2019**, *4* (32), No. eaax0613.
- (303) Zhang, H.; Li, Z.; Gao, C.; Fan, X.; Pang, Y.; Li, T.; Wu, Z.; Xie, H.; He, Q. Dual-Responsive Biohybrid Neurobots for Active Target Delivery. *Sci. Robot.* **2021**, *6* (52), No. eaaz9519.

- (304) Wei, C.; Wu, C.; Jin, X.; Yin, P.; Yu, X.; Wang, C.; Zhang, W. CT/MR Detectable Magnetic Microspheres for Self-Regulating Temperature Hyperthermia and Transcatheter Arterial Chemoembolization. *Acta Biomater.* **2022**, *153*, 453–464.
- (305) Nundy, S.; Mesloub, A.; Alsolami, B. M.; Ghosh, A. Electrically Actuated Visible and Near-Infrared Regulating Switchable Smart Window for Energy Positive Building: A Review. *J. Clean. Prod.* **2021**, *301*, 126854.
- (306) Kim, H.-N.; Yang, S. Responsive Smart Windows from Nanoparticle-Polymer Composites. *Adv. Funct. Mater.* **2020**, *30* (2), 1902597.
- (307) Torres-Pierna, H.; Ruiz-Molina, D.; Roscini, C. Highly Transparent Photochromic Films with a Tunable and Fast Solution-Like Response. *Mater. Horiz.* **2020**, *7* (10), 2749–2759.
- (308) Otaegui, J. R.; Ruiz-Molina, D.; Hernando, J.; Roscini, C. Multistimuli-Responsive Smart Windows Based on Paraffin-Polymer Composites. *Chem. Eng. J.* **2023**, *463*, 142390.
- (309) Tan, Y.; Chen, R.; Xiao, Y.; Wang, C.; Zhou, C.; Chen, D.; Li, S.; Wang, W. Temperature-Responsive ‘Cloud’ with Controllable Self-Assembled Particle Size for Smart Window Application. *Appl. Mater. Today* **2021**, *25*, 101248.
- (310) Li, X. H.; Liu, C.; Feng, S. P.; Fang, N. X. Broadband Light Management with Thermochromic Hydrogel Microparticles for Smart Windows. *Joule* **2019**, *3* (1), 290–302.
- (311) Song, Y. K.; Lee, T. H.; Kim, J. C.; Lee, K. C.; Lee, S.-H.; Noh, S. M.; Park, Y. I. Dual Monitoring of Cracking and Healing in Self-Healing Coatings Using Microcapsules Loaded with Two Fluorescent Dyes. *Molecules* **2019**, *24* (9), 1679.
- (312) Song, Y. K.; Lee, T. H.; Lee, K. C.; Choi, M. H.; Kim, J. C.; Lee, S.-H.; Noh, S. M.; Park, Y. I. Coating That Self-Reports Cracking and Healing Using Microcapsules Loaded with a Single AIE Fluorophore. *Appl. Surf. Sci.* **2020**, *511*, 145556.
- (313) Song, Y. K.; Kim, B.; Lee, T. H.; Kim, S. Y.; Kim, J. C.; Noh, S. M.; Park, Y. I. Monitoring Fluorescence Colors to Separately Identify Cracks and Healed Cracks in Microcapsule-Containing Self-Healing Coating. *Sens. Actuators B Chem.* **2018**, *257*, 1001–1008.
- (314) Zhang, Q.; Li, W.; Liu, X.; Ma, J.; Gu, Y.; Liu, R.; Luo, J. Polyaniline Microspheres with Corrosion Inhibition, Corrosion Sensing, and Photothermal Self-Healing Properties toward Intelligent Coating. *ACS Appl. Mater. Interfaces* **2024**, *16* (1), 1461–1473.
- (315) Ni, X.; Li, C.; Zhou, J.; Zhang, M.; You, B.; Wu, L.; Li, W.; Guo, J. Design of Chlorella-Inspired and Smart-Responsive Bio-Microspheres and Their Application in Eco-Friendly Anti-Biofouling Coatings. *Chem. Eng. J.* **2023**, *478*, 147426.
- (316) Song, Y. K.; Kim, B.; Lee, T. H.; Kim, J. C.; Nam, J. H.; Noh, S. M.; Park, Y. I. Fluorescence Detection of Microcapsule-Type Self-Healing Based on Aggregation-Induced Emission. *Macromol. Rapid Commun.* **2017**, *38* (6), 1600657.
- (317) Lu, X.; Li, W.; Sottos, N. R.; Moore, J. S. Autonomous Damage Detection in Multilayered Coatings via Integrated Aggregation-Induced Emission Luminogens. *ACS Appl. Mater. Interfaces* **2018**, *10* (47), 40361–40365.
- (318) Chen, S.; Han, T.; Liu, J.; Liang, X.; Yang, J.; Tang, B. Z. Visualization and Monitoring of Dynamic Damaging-Healing Processes of Polymers by Using AIEgen-Loaded Multifunctional Microcapsules. *J. Mater. Chem. A* **2022**, *10* (29), 15438–15448.
- (319) Yue, L.-L.; Xie, R.; Wei, J.; Ju, X.-J.; Wang, W.; Chu, L.-Y. Nano-Gel Containing Thermo-Responsive Microspheres with Fast Response Rate Owing to Hierarchical Phase-Transition Mechanism. *J. Colloid Interface Sci.* **2012**, *377* (1), 137–144.
- (320) Chen, Z.; Li, X.; Gong, B.; Scharnagl, N.; Zheludkevich, M. L.; Ying, H.; Yang, W. Double Stimuli-Responsive Conducting Polypyrrole Nanocapsules for Corrosion-Resistant Epoxy Coatings. *ACS Appl. Mater. Interfaces* **2023**, *15* (1), 2067–2076.
- (321) Zhou, C.; Qi, Y.; Zhang, S.; Niu, W.; Wu, S.; Ma, W.; Tang, B. Lotus Seedpod Inspiration: Particle-Nested Double-Inverse Opal Films with Fast and Reversible Structural Color Switching for Information Security. *ACS Appl. Mater. Interfaces* **2021**, *13* (22), 26384–26393.
- (322) Shi, N.; Ding, Y.; Wang, D.; Hu, X.; Li, L.; Dai, C.; Liu, D. Lignosulfonate/Diblock Copolymer Polyion Complexes with Aggregation-Enhanced and pH-Switchable Fluorescence for Information Storage and Encryption. *Int. J. Biol. Macromol.* **2021**, *187*, 722–731.
- (323) Alidaei-Sharif, H.; Roghani-Mamaqani, H.; Babazadeh-Mamaqani, M.; Sahandi-Zangabad, K.; Salami-Kalajahi, M. Photoluminescent Polymer Nanoparticles Based on Oxazolidine Derivatives for Authentication and Security Marking of Confidential Notes. *Langmuir* **2022**, *38* (45), 13782–13792.
- (324) Guo, Y.; Zhu, W.; Tao, M.; Wu, X.; Chen, J.; Peng, X.; Zheng, S.; Zhao, Z.; Cao, Z. Delicate and Independent Manipulation of Dynamic Fluorescence Behavior of Polymer Nanoparticles Based on a Core-Shell Strategy. *ACS Appl. Mater. Interfaces* **2022**, *14* (34), 39384–39395.
- (325) Abdollahi, A.; Rahmanidoust, M.; Hanaei, N.; Dashti, A. All-in-One Photoluminescent Janus Nanoparticles for Smart Technologies: Organic Light-Emitting Diodes, Anticounterfeiting, and Optical Sensors. *Eur. Polym. J.* **2023**, *186*, 111873.
- (326) Otaegui, J. R.; Ruiz-Molina, D.; Hernando, J.; Roscini, C. Multidimensional Data Encoding Based on Multicolor Microencapsulated Thermoresponsive Fluorescent Phase Change Materials. *Adv. Funct. Mater.* **2024**, *34* (34), 2402510.
- (327) Cai, L.; Wang, Y.; Xu, D.; Chen, H.; Zhao, Y. Bio-Inspired Pigment Particles with Dual-Variation Modes of Structural Colors and Fluorescence. *Chem. Eng. J.* **2023**, *461*, 142000.
- (328) Wang, M.; Jiang, K.; Gao, Y.; Liu, Y.; Zhang, Z.; Zhao, W.; Ji, H.; Zheng, T.; Feng, H. A Facile Fabrication of Conjugated Fluorescent Nanoparticles and Micro-Scale Patterned Encryption via High Resolution Inkjet Printing. *Nanoscale* **2021**, *13* (34), 14337–14345.
- (329) Abdollahi, A.; Roghani-Mamaqani, H.; Salami-Kalajahi, M.; Razavi, B.; Sahandi-Zangabad, K. Encryption and Optical Authentication of Confidential Cellulosic Papers by Ecofriendly Multi-Color Photoluminescent Inks. *Carbohydr. Polym.* **2020**, *245*, 116507.
- (330) Kazak, O.; Tor, A. In Situ Preparation of Magnetic Hydrochar by Co-Hydrothermal Treatment of Waste Vinasse with Red Mud and Its Adsorption Property for Pb(II) in Aqueous Solution. *J. Hazard. Mater.* **2020**, *393*, 122391.
- (331) Liu, X.; Wang, Y.; Wu, X.; Wang, Y.; Fan, G.; Huang, Y.; Zhang, L. Preparation of Magnetic DTPA-Modified Chitosan Composite Microspheres for Enhanced Adsorption of Pb(II) from Aqueous Solution. *Int. J. Biol. Macromol.* **2024**, *264*, 130410.
- (332) Zhou, S.; Jiao, Y.; Zou, J.; Zheng, Z.; Zhu, G.; Deng, R.; Wang, C.; Peng, Y.; Wang, J. Adsorption of Sb(III) from Solution by Immobilized *Microcystis aeruginosa* Microspheres Loaded with Magnetic Nano-Fe₃O₄. *Water* **2024**, *16* (5), 681.
- (333) Yang, K.; Xing, J.; Xu, P.; Chang, J.; Zhang, Q.; Usman, K. M. Activated Carbon Microsphere from Sodium Lignosulfonate for Cr(VI) Adsorption Evaluation in Wastewater Treatment. *Polymers* **2020**, *12* (1), 236.
- (334) Zuo, J.; Nan, X.; He, L.; Xu, Z.; Liu, Z.; Wang, T.; Bai, P. Preparation of Photo-Grafted Magnetic Nano-Silver Composites and Their Catalytic Studies on Organic Dyes. *Colloids Surf. A Physicochem. Eng. Asp.* **2024**, *684*, 133149.
- (335) Chen, B.; Chen, Y.; Chen, S.; Duan, X.; Gao, J.; Zhang, N.; He, L.; Wang, X.; Huang, J.; Chen, X.; Pan, X. Iron-Calcium Dual Crosslinked Graphene Oxide/Alginate Aerogel Microspheres for Extraordinary Elimination of Tetracycline in Complex Wastewater: Performance, Mechanism, and Applications. *Int. J. Biol. Macromol.* **2024**, *264*, 130554.
- (336) Deng, S.; Dai, Y.; Situ, Y.; Liu, D.; Huang, H. Preparation of Nanosheet-Based Spherical Ti/SnO₂-Sb Electrode by In-Situ Hydrothermal Method and Its Performance in the Degradation of Methylene Blue. *Electrochim. Acta* **2021**, *398*, 139335.
- (337) Dai, K.; Zhao, G.; Wang, Z.; Peng, X.; Wu, J.; Yang, P.; Li, M.; Tang, C.; Zhuang, W.; Ying, H. Novel Mesoporous Lignin-Calcium for Efficiently Scavenging Cationic Dyes from Dyestuff Effluent. *ACS Omega* **2020**, *6* (1), 816–826.

- (338) Xiao, P.; Xu, J.; Shi, H.; Du, F.; Du, H.; Li, G. Simultaneous Cr(VI) Reduction and Cr(III) Sequestration in a Wide pH Range by Using Magnetic Chitosan-Based Biopolymer. *Int. J. Biol. Macromol.* **2023**, *253*, 127398.
- (339) Pang, Y.; Lin, P.; Chen, Z.; Zhou, M.; Yang, D.; Lou, H.; Qiu, X. Preparation, Characterization, and Adsorption Performance of Porous Polyamine Lignin Microsphere. *Int. J. Biol. Macromol.* **2023**, *253*, 127026.
- (340) Wu, J.; Zhong, Y.; Hao, C.; Chen, J.; Gao, H.; Han, S.; Shen, Y.; Wang, X. Emulsion Synthesis of Cellulose/Lanthanum Alginate/La(III) Composite Microspheres for Efficient and Selective Adsorption of Phosphate. *Chem. Eng. J.* **2024**, *488*, 150949.
- (341) Wang, R.; Song, X.; Liu, L.; Zhou, C.; Wu, G. PAMAM Grafted Magnetic Chitosan Particles by EDTA Core for Efficient Removal of Cu(II). *J. Polym. Environ.* **2024**, *32* (7), 3326–3341.
- (342) Zeng, Q.; Li, J.; Dai, L.; Zhang, J.; Zeng, T.; Cheng, R.; Chen, J.; Zhou, M.; Hou, H. Synthesis of Hydrophilic Sulfur-Doped Carbon Aerogel Microspheres and Their Mechanism of Efficient Removal of Sb(III) from Aqueous Solution. *Sep. Purif. Technol.* **2024**, *329*, 125032.
- (343) Yang, L.; Sun, Y.; Yu, R.; Huang, P.; Zhou, Q.; Yang, H.; Lin, S.; Zeng, H. Urchin-like CO₂-Responsive Magnetic Microspheres for Highly Efficient Organic Dye Removal. *J. Hazard. Mater.* **2024**, *469*, 134101.
- (344) Ma, C.; Fan, W.; Qin, W.; Guo, Y.; Ma, L.; Belzile, N.; Deng, T. Zein-Enhanced Sodium Alginate/Thiostannate Microsphere Adsorbent Zein@SA/KBS for Efficient Removal of Cesium from Wastewater. *J. Hazard. Mater.* **2024**, *461*, 132600.
- (345) Yang, H.-R.; Li, S.-S.; An, Q.-D.; Zhai, S.-R.; Xiao, Z.-Y.; Zhang, L.-P. Facile Transformation of Carboxymethyl Cellulose Beads into Hollow Composites for Dye Adsorption. *Int. J. Biol. Macromol.* **2021**, *190*, 919–926.
- (346) Zhai, T.; Zheng, Q.; Cai, Z.; Xia, H.; Gong, S. Synthesis of Polyvinyl Alcohol/Cellulose Nanofibril Hybrid Aerogel Microspheres and Their Use as Oil/Solvent Superabsorbents. *Carbohydr. Polym.* **2016**, *148*, 300–308.
- (347) Wu, R.; Hu, C. Fabrication of Magnetic Cellulose Microspheres by Response Surface Methodology and Adsorption Study for Cu(II). *Cellulose* **2021**, *28* (3), 1499–1511.
- (348) Luo, X.; Zeng, J.; Liu, S.; Zhang, L. An Effective and Recyclable Adsorbent for the Removal of Heavy Metal Ions from Aqueous System: Magnetic Chitosan/Cellulose Microspheres. *Bioresour. Technol.* **2015**, *194*, 403–406.